NASA Technical Memorandum 104566, Vol. 39

SeaWiFS Technical Report Series

Stanford B. Hooker and Elaine R. Firestone, Editors

Volume 39, SeaWiFS Calibration Topics, Part 1

Robert A. Barnes, Eueng-nan Yeh, and Robert E. Eplee

October 1996

NASA Technical Memorandum 104566, Vol. 39

SeaWiFS Technical Report Series

Stanford B. Hooker, Editor
NASA Goddard Space Flight Center
Greenbelt, Maryland

Elaine R. Firestone, Technical Editor
General Sciences Corporation
Laurel, Maryland

Volume 39, SeaWiFS Calibration Topics, Part 1

Robert A. Barnes, Eueng-nan Yeh, and Robert E. Eplee
General Sciences Corporation
Laurel, Maryland

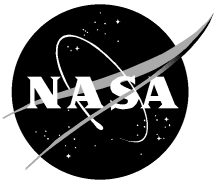

National Aeronautics and
Space Administration

Goddard Space Flight Center
Greenbelt, Maryland 20771

1996

Preface

The SeaWiFS Calibration and Validation Program consists of four primary components (see the Prologue of Volume 38), that is, the SeaWiFS Instrument, Field Program, SeaBASS, and Calibration and Validation Element Software. Several volumes of the *SeaWiFS Technical Report Series* provided detailed analyses of prelaunch SeaWiFS sensor performance data, e.g., Volumes 22 (prelaunch acceptance), 23 (prelaunch calibration) and 31 (stray light). This volume continues our efforts to identify and address issues associated with the SeaWiFS sensor calibration and characterization. The considerations described herein also apply to the calibration of other instruments with finite bandwidths including most *in situ* radiometers to be used in the vicarious calibration and algorithm development for SeaWiFS.

The chapters in this volume present discussions of:

a) Calculating an equivalent blackbody temperature for the GSFC sphere;

b) The effects of source spectral shape on SeaWiFS radiance measurements;

c) Comparing the spectral responses of SeaWiFS and the SeaWiFS Transfer Radiometer;

d) The SeaWiFS center wavelengths; and

e) The SeaWiFS solar difuser.

Greenbelt, Maryland —C.R.M.
Sept. 1996 Project Scientist

Table of Contents

Abstract

For Earth-observing satellite instruments, it was standard to consider each instrument band to have a spectral response that is infinitely narrow, i.e., to have a response from a single wavelength. The SeaWiFS bands, however, have nominal spectral bandwidths of 20 and 40 nm. These bandwidths affect the SeaWiFS measurements on orbit. The effects are also linked to the manner in which the instrument was calibrated and to the spectral shape of the radiance that SeaWiFS views. Currently, SeaWiFS is calibrated such that the digital counts from each instrument band are linked to the Earth-exiting radiance at an individual center wavelength. Before launch, SeaWiFS will be recalibrated so that the digital counts from each band will be linked to the Earth-exiting radiance integrated over the spectral response of that band. In this technical memorandum, the effects of the instrument calibration and the source spectral shape on SeaWiFS measurements, including the in-band and out-of-band responses, and the center wavelengths are discussed.

PROLOGUE

The Sea-viewing Wide Field-of-view Sensor (SeaWiFS) measures the Earth-exiting radiance at eight nominal center wavelengths (412, 443, 490, 510, 555, 670, 765, and 865 nm). It was the practice in the retrieval of ocean color measurements to assume that the measurements from the satellite instrument came from individual wavelengths and from individual wavelengths alone. The SeaWiFS bands, however, also have nominal spectral bandwidths (full-width at half-maximum response) of 20 and 40 nm. The incorporation of these broad spectral responses into the data reduction algorithms for SeaWiFS will lead to water-leaving radiances that are different from those based on the nominal center wavelengths alone.

For SeaWiFS, as for many other satellite sensors, the performance specification for the instrument defines the in-band and the out-of-band responses for each measurement band. The in-band response is defined as the response from the spectral region between the two 1% response points, that is, between the wavelengths at which the response of the band is 1% of the maximum response. Out-of-band is defined as the response from wavelengths outside of those 1% points. For SeaWiFS, the out-of-band specification allows up to 5% instrument response in the out-of-band wavelength regions for each band (Barnes et al. 1994a). The actual out-of-band responses for the eight SeaWiFS bands (to a source with the spectral shape of a 5,900 K blackbody) range from 0.3–3.7% of the total band responses (Barnes et al. 1994b). The out-of-band response on orbit, however, will be a function of the spectral shape of the Earth-exiting radiance that SeaWiFS actually views.

In addition, the laboratory calibration of SeaWiFS was performed using a spherical integrating source (SIS) that was, itself, calibrated at the nominal SeaWiFS center wavelengths. Thus, for SeaWiFS band 1, the counts from the instrument in the laboratory corresponded to a measured spectral radiance from the sphere at 412 nm. A similar pairing was made for the spectral radiances from the integrating sphere and the counts from the other SeaWiFS bands. Information from the instrument manufacturer, who performed the laboratory calibration, indicated that the spectral shape for the radiance from the integrating sphere approximated that for a 2,850 K blackbody. This type of calibration is consistent with the calibration of other Earth-observing satellite instruments, such as the Ocean Color and Temperature Scanner (OCTS).

As a result, it was necessary to devise a procedure for transferring the laboratory calibration of SeaWiFS to orbit. This was done by converting the SeaWiFS laboratory responses from those for a source with a 2,850 K spectral shape to those for a source with a 5,900 K spectral shape (Barnes et al. 1994b). The 5,900 K blackbody shape, which approximates the spectral shape of the solar irradiance, was the only spectral shape provided in the SeaWiFS performance specification (Barnes et al. 1994a).

The output of the SeaWiFS bands (in digital counts) is linked to spectral radiances at the nominal center wavelengths. This linkage leads to dependencies between the bands' output and the spectral shapes of the sources viewed. Those dependencies are a direct consequence of the manner in which SeaWiFS was calibrated in the laboratory. There is also a connection between the response of the instrument at wavelengths well away from the center wavelength (the out-of-band response) and the spectral shape of the sources that SeaWiFS views.

This technical memorandum contains chapters that address aspects of the dependence of the SeaWiFS bands—as they have been calibrated by the manufacturer—on the source spectral shape. In general, the sources in these studies are Planck function (blackbody) curves of different temperatures. For SeaWiFS, the spectral shape of the laboratory source approximated that for a 2,850 K blackbody. The shape of the solar output is that for a 5,900 K blackbody, and for the typical SeaWiFS radiances in the instrument performance specification (Barnes et al. 1994a) the spectral shape approximates that for a 12,000 K blackbody (Barnes et al. 1995a). For the source dependence studies in this document, the reference spectral shapes are

those for blackbodies with temperatures that range from 2,000 K to 30,000 K. Those studies are explained in Chapters 1 and 2.

The upwelling Earth radiance that SeaWiFS will view on orbit, however, does not have a spectral shape that changes smoothly with wavelength (see Fig. 3 of Hooker et al. 1992). There are absorption lines in that spectrum, particularly from water vapor and molecular oxygen. Oxygen A-band absorption can remove 10–15% of the in-band radiance viewed by SeaWiFS band 7 depending on pathlengths within the atmosphere (Ding and Gordon 1995 and Fraser 1995]. For SeaWiFS band 8, water vapor can remove up to 1% of the upwelling radiation in its out-of-band region for very long pathlengths within the atmosphere (Gordon 1995). It is possible to adapt the studies recounted in this document to account for these effects. The absorption spectra for molecular oxygen and for water vapor are available through the `LOWTRAN` and `MODTRAN` atmospheric models. The absorption spectra for these gasses are the kernels of the modeling studies of Ding and Gordon (1995), Fraser (1995), and Gordon (1995).

The `LOWTRAN` model for oxygen A-band absorption for two vertical passes through the atmosphere (an airmass of 2) is shown in Fig. 1. Other atmospheric transmission factors, such as absorption by water vapor and/or scattering by aerosols, are not shown. As this figure shows, oxygen A-band absorption occurs in the wavelength region within which SeaWiFS band 7 responds to light best.

A similar spectrum for water vapor, with a water column amount of $3.338\,\mathrm{g\,cm^{-2}}$ and an airmass of 2, is shown in Fig. 2. This figure includes the relative spectral response for SeaWiFS band 8. Atmospheric water vapor, both as a function of its column amount and the pathlength for solar radiation reflected from the ocean surface, causes a small, but significant, reduction of upwelling radiation in the spectral wings of band 8.

SeaWiFS bands 7 and 8 form the basis for the SeaWiFS atmospheric correction, a correction that is critical to the calculation of SeaWiFS water-leaving radiances. As shown in Figs. 1 and 2, oxygen and water vapor do not absorb at individual wavelengths, but over wavelength regions that extend from a few to more than 100 nm. Thus, based on the modelling results of Gordon (1995), it was decided by the Calibration Subgroup of the SeaWiFS Science Working Group that SeaWiFS should have a laboratory calibration which includes the response of each instrument band to upwelling Earth radiance over its full spectral range.

This response is known as the band-weighted spectral radiance (BSR). It is the spectral radiance of the source integrated over the spectral response of the band. To be useful for Earth observations, each BSR must be associated with a band-weighted center wavelength (BCW). The calibration of SeaWiFS for BSRs has not been performed as yet. This calibration awaits the final thermal-vacuum testing of SeaStar, the spacecraft that will carry SeaWiFS; the calibration is currently scheduled for the fourth quarter of 1996. It will be consistent with the calibration of other Earth-observing satellite instruments, such as the Moderate Resolution Imaging Spectroradiometer (MODIS).

Before the postthermal-vacuum calibration can occur, three things must be known: the spectral shape of the radiance from the laboratory source; the spectral response of the SeaWiFS bands; and the spectral shape of the bands in the reference radiometer. The spectral response of SeaWiFS is known (Barnes 1994). The spectral shape of the radiance from the GSFC sphere, which will be used as the source in the calibration, is described in Chapter 1. And, the spectral shape of the SeaWiFS Transfer Radiometer (SXR), which will be used as the reference radiometer in the calibration, is discussed in Chapter 3.

In addition to a calibration in terms of BSRs, the (future) postthermal-vacuum calibration of SeaWiFS can also be interpreted in the same manner as the original laboratory calibration of SeaWiFS by the manufacturer, that is, in terms of spectral radiances at the eight nominal SeaWiFS center wavelengths. So, before launch, SeaWiFS will be calibrated in two ways: in terms of the BSRs from each band, and in terms of the spectral radiances at the nominal center wavelengths for each band. For the BSRs, a corresponding center wavelength must be determined for each band. These center wavelengths are described in Chapter 4.

Finally, the effects of absorption by atmospheric water vapor and oxygen on SeaWiFS bands 7 and 8 can be calculated for measurements that use the original SeaWiFS calibration. For this type of calibration, in which the counts from the bands are linked to spectral radiances at the nominal center wavelengths for the bands, the absorption corrections require a nominal top-of-the-atmosphere spectral radiance curve, plus models for the spectral shapes and intensities of the molecular absorption lines. For water vapor, which absorbs in the wings of the band responses, `LOWTRAN` absorption values, with their relatively low wavelength resolution, are sufficient. For oxygen, which absorbs in the center of the response for band 7, `MODTRAN` spectra, interpolated to 0.1 nm intervals, are required. These data sets have been compiled, and the calculated results will be presented in a subsequent technical memorandum in this series. A short synopsis of each chapter in this volume is given below.

1. Calculation of an Equivalent Blackbody Temperature for the GSFC Sphere

The SeaWiFS radiometer shares a number of fundamental characteristics with other filter-based spectrometers. Among these characteristics is a dependence of the throughput of the interference filters on the spectral shape of the measured radiance. This dependence varies from band to band within the instrument and is based on the spectral response of each individual band. Here, the measured spectral response curves for the SeaWiFS bands and

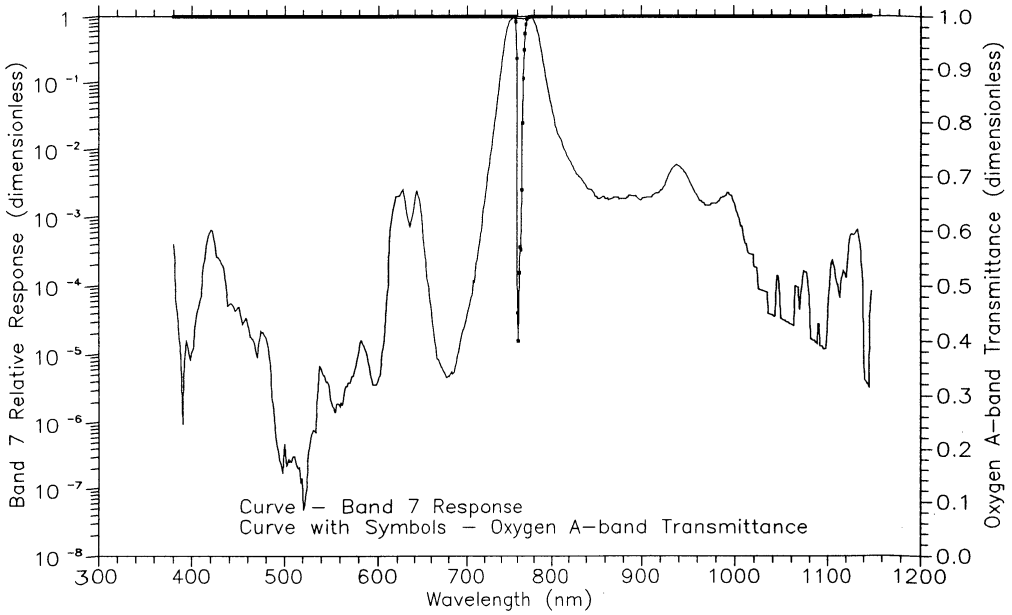

Fig. 1. Oxygen A-band transmittance and the spectral response for SeaWiFS band 7 are illustrated in this figure. The scale for oxygen transmittance, as given for the `LOWTRAN` atmospheric model, is on the right. The transmittance represents two vertical passes through the atmosphere, that is, an airmass of two. The scale for the band 7 relative spectral response is on the left.

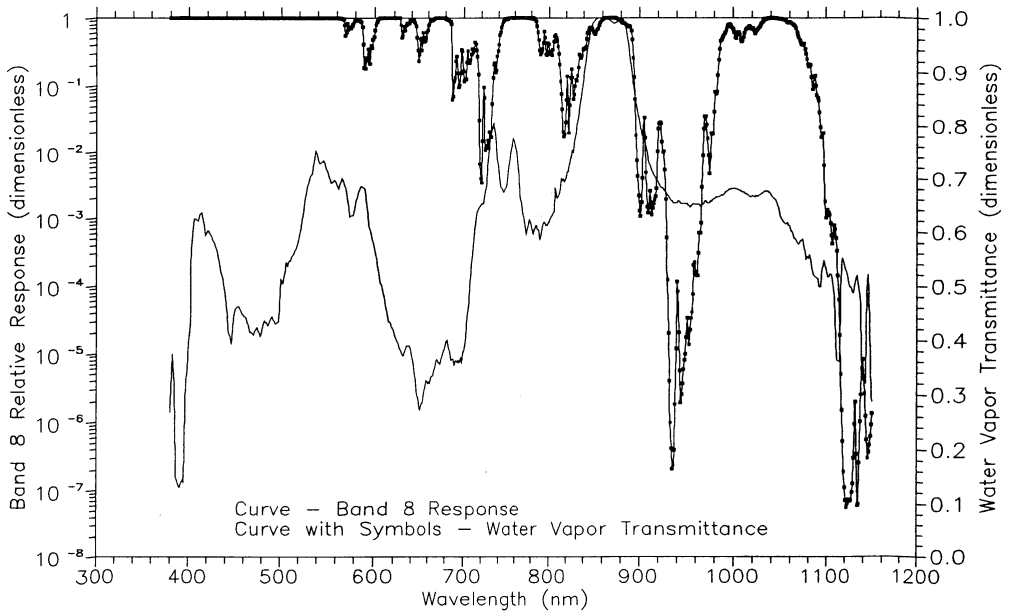

Fig. 2. The water vapor transmittance and the spectral response for SeaWiFS band 8 are shown. The scale for water vapor transmittance, as given for the `LOWTRAN` atmospheric model, is on the right. The transmittance represents two vertical passes through an atmosphere with a water vapor column amount of $3.338\,\mathrm{g\,cm^{-2}}$ (the amount in the `LOWTRAN` tropical model). The scale for the band 8 relative spectral response is on the left.

a set of radiance curves to provide a model for this dependence are used. The radiance curves are normalized at the nominal SeaWiFS center wavelengths, that is, at the wavelengths used in the laboratory calibration of the instrument. The model results show that, as far as the eight SeaWiFS bands are concerned, the radiance curves for the Goddard Space Flight Center (GSFC) SIS are equivalent to that for a 2,850 K blackbody. The model results also show that the output from the SeaWiFS bands will have differences of up to 5% on orbit, when compared with the radiometric calibration in the laboratory.

2. *Effects of Source Spectral Shape on SeaWiFS Radiance Measurements*

Two aspects of filter photometry on the radiances measured by SeaWiFS are examined: the dependence of the total band response, and the out-of-band response on source spectral shape. These effects are significant contributors to the SeaWiFS measurements on orbit. The corrections for out-of-band response range from about 0.5% to more than 5%, depending on the SeaWiFS band. The corrections for total band response range from near zero to about 5%. These corrections will be used to convert the laboratory calibration of SeaWiFS (in terms of total band response) to orbit (in terms of in-band response). The residual uncertainty in these corrections is estimated to be small, around 0.2%. With other significantly larger error sources in the SeaWiFS measurements, the contribution of these residual uncertainties to the propagation of error for SeaWiFS radiance measurements at the top of the atmosphere is also expected to be small. These corrections are prelaunch estimates and should be reexamined using flight data. In addition, these corrections have been tailored to SeaWiFS ocean measurements. The contributions to land measurements will be different.

3. *A Comparison of the Spectral Responses of SeaWiFS and the SeaWiFS Transfer Radiometer*

Both SeaWiFS and the SXR are filter radiometers with finite bandwidths. The use of these instruments requires a knowledge of the effects that finite bandwidths cause. These effects also depend on the source's spectral shape which the instruments measure. For the radiometric calibration of SeaWiFS, the source is the GSFC SIS. The BSRs and the effective center wavelengths (ECWs) for SeaWiFS and the SXR, when measuring the GSFC SIS, are presented here. They will be needed to convert the SXR measured spectral radiances to the SeaWiFS wavelengths.

4. *SeaWiFS Center Wavelengths*

With its 20 and 40 nm bandwidths, SeaWiFS does not make measurements at individual wavelengths. Rather, the output from each SeaWiFS band can be considered as an integral over a finite wavelength region of the source it measures. To make SeaWiFS measurements useful, it is important to relate the measured radiance from the instrument to a reference wavelength. That wavelength connects each SeaWiFS measurement to the spectral radiance from the source at that wavelength. For the initial calibration of SeaWiFS, the reference center wavelengths were those from the instrument's performance specifications. A set of BCWs for on-orbit use are presented here. The use of these new wavelengths will require a revision of the on-orbit radiometric calibration constants for the instrument.

5. *The SeaWiFS Solar Diffuser*

Measurements of the solar flux with an onboard solar diffuser will provide an important check of changes in the radiometric sensitivity of SeaWiFS over the duration of the instrument's on-orbit measurements of ocean color. Although diffuser measurements do not give an absolute determination of radiometric changes, they will identify any rapid changes that may occur in the instrument output. The diffuser was designed to produce radiance levels that approximate those for other SeaWiFS measurements. This design includes an attenuator to reduce the solar radiance levels on the diffuser, and hence, the effects of photolyzed organic compounds. The BRDF, which shows the output of the diffuser as a function of pitch and yaw angle, has been determined. This allows the removal of angular dependencies from the long-term radiometric sensitivity data. In addition, outdoor measurements have given the predicted output from SeaWiFS for initial on-orbit solar diffuser measurements.

Chapter 1

Calculation of an Equivalent Blackbody Temperature for the GSFC Sphere

Robert A. Barnes
General Sciences Corporation
Laurel, Maryland

Abstract

The SeaWiFS radiometer shares several fundamental characteristics with other filter-based spectrometers. Among these characteristics is a dependence of the throughput of the interference filters on the spectral shape of the measured radiance. This dependence varies from band to band within the instrument and is based on the spectral response of each individual band. Here, the measured spectral response curves for the SeaWiFS bands and a set of radiance curves to provide a model for this dependence are used. The radiance curves are normalized at the nominal SeaWiFS center wavelengths, that is, at the wavelengths used in the laboratory calibration of the instrument. The model results show that, as far as the eight SeaWiFS bands are concerned, the radiance curves for the GSFC SIS are equivalent to that for a 2,850 K blackbody. The model results also show that the output from the SeaWiFS bands will have differences of up to 5% on orbit, when compared with the radiometric calibration in the laboratory.

1.1 INTRODUCTION

The construction and calibration of SeaWiFS was completed in November 1993. The instrument was designed by the Santa Barbara Research Center (SBRC) to meet a set of performance specifications, including specifications for maximum ocean radiances and maximum cloud radiances (Barnes et al. 1994a). To determine the instrument output for these radiance levels, SBRC used a 100 cm SIS with a calibration traceable to the National Institute of Standards and Technology (NIST). The SBRC sphere used sets of 200 W, 45 W, and 5 W tungsten lamps. The spectral shape for the sphere output was assumed to be equivalent to a 2,850 K blackbody (Barnes et al. 1994b).

The output of the GSFC 106 cm SIS was characterized and calibrated by NIST in April 1995. The results of this characterization will be published as part of a future SeaWiFS technical memorandum. The absolute calibration of the sphere will change with time as the lamps and the reflective inner surface of the sphere age. The use of the sphere will require frequent recalibration using a transfer radiometer before it is viewed by the instruments under test. However, other characteristics of the sphere—the areal uniformity of the sphere's radiant output across its output aperture and the spectral shape of its output—need to be checked much less frequently. As part of the characterization of the sphere at NIST, its radiance was measured relative to a NIST-standard gold-point blackbody, using equipment and techniques described in Walker et al. (1987). For these measurements, the spectral response of the GSFC sphere has a maximum radiance at 890 nm (Fig. 3a). Using the Wein displacement law (Wyatt 1978) this wavelength corresponds to a Planck function (blackbody) temperature of 3,256 K.

The GSFC and SBRC integrating spheres were not designed to duplicate ideal flat-black radiators that emit at specific temperatures. This non-ideal spectral output for the GSFC sphere is shown in Fig. 3. The output from the sphere at 890 nm is less than 1 part in 10,000 of that from a 3,256 K blackbody, and normalization of the blackbody curve was required to create the figure. This gives the sphere an extremely small emissivity (ϵ), less than 0.0001. In addition, the GSFC sphere cannot be treated as a grey-body, since its emissivity changes with wavelength. This also can be seen in Fig. 3, where the sphere output does not follow the shape of the blackbody for wavelengths away from 890 nm.

The data from the characterization of the GSFC sphere are sufficient to calculate emissivity as a function of wavelength. These data can also be acquired for the SBRC sphere. Such characterizations of the integrating spheres, however, are not necessary. For the SeaWiFS Project, interest is limited to the manner in which the sphere output effects the eight SeaWiFS bands. Each SeaWiFS band has its own spectral response (Barnes et al. 1994b), and that spectral response interacts with the spectral shape of

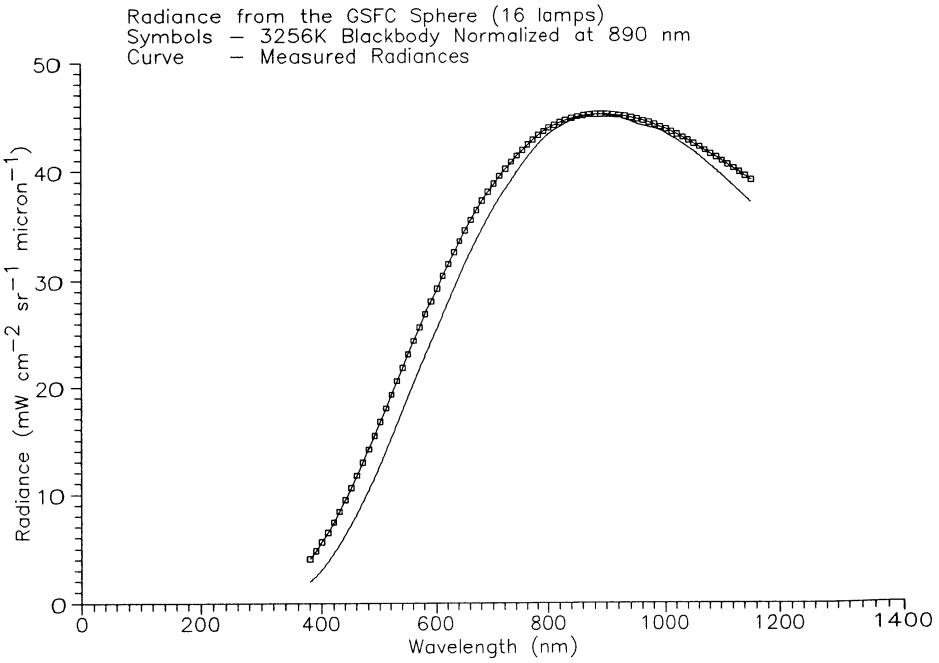

Fig. 3. Response of the GSFC sphere and a 3,256 K blackbody. Both responses have maximum radiances at 890 nm. The blackbody curve has been normalized to the sphere response at 890 nm.

the source that illuminates it. Such interactions, including those for the output from the GSFC sphere, are presented here. They are instrument dependent and are not readily extrapolated beyond SeaWiFS.

1.2 INSTRUMENT MODEL

On orbit, SeaWiFS will view, on a pixel by pixel basis, the upwelling Earth radiance. From a spectral viewpoint, the relative spectral response of each instrument band will be combined with the spectral shape of that upwelling radiance. The relative spectral responses of the SeaWiFS bands have been measured. For this study, the spectral shapes viewed by the instrument will be approximated by a set of Planck function curves. These models are used to give a zeroth order understanding of the instrument response on orbit.

1.2.1 Band Spectral Responses

This model for the response of SeaWiFS to source spectral shape is based on the spectral responses of the SeaWiFS bands. Those responses were described previously (Barnes et al. 1994b) for three different types of sources: a 2,850 K blackbody, a 5,900 K blackbody, and a spectrally flat source. The spectrally flat responses were calculated (on a nanometer by nanometer basis) using the spectral responses of the filters, lenses, and dichroics in each band's optical train. For each of these components, the response is dimensionless, that is, the response is the ratio of photons out to photons in (PO:PI). The silicon photodiode for each band also has a spectral dependence for its response, a response with the ratio of electrons out to photons in (EO:PI)—or milliamperes per milliwatt. Thus, at each nanometer interval from 380–1,150 nm, the output from the optical train for each band has units of mA mW^{-1}.

Here, as in Barnes et al. (1994b), the piece-part derived response ratios have been multiplied at each nanometer by 1 mW cm^{-2} sr^{-1} μm^{-1} to give the band's response-to-unit radiance. The output for SeaWiFS band 6 is shown in Fig. 4a. The output for this and the other SeaWiFS bands is the current from the photodiode. As shown in Fig. 4a for band 6 and a spectrally flat source, the current from the photodiode is the sum of the current at each nanometer interval; this integrated current is a few nanoamperes. This current can be used to determine the relative response of the instrument to sources with different spectral shapes; however, it cannot determine the output of the instrument on an absolute basis. There are other nonspectral factors that are part of the instrument's response, including the collecting power of the fore optics and the gains of the amplifiers in the electronics that follow the photodiodes.

1.2.2 Planck Function Curves

For an idealized blackbody radiator, the radiance can be given as a function of both temperature and wavelength

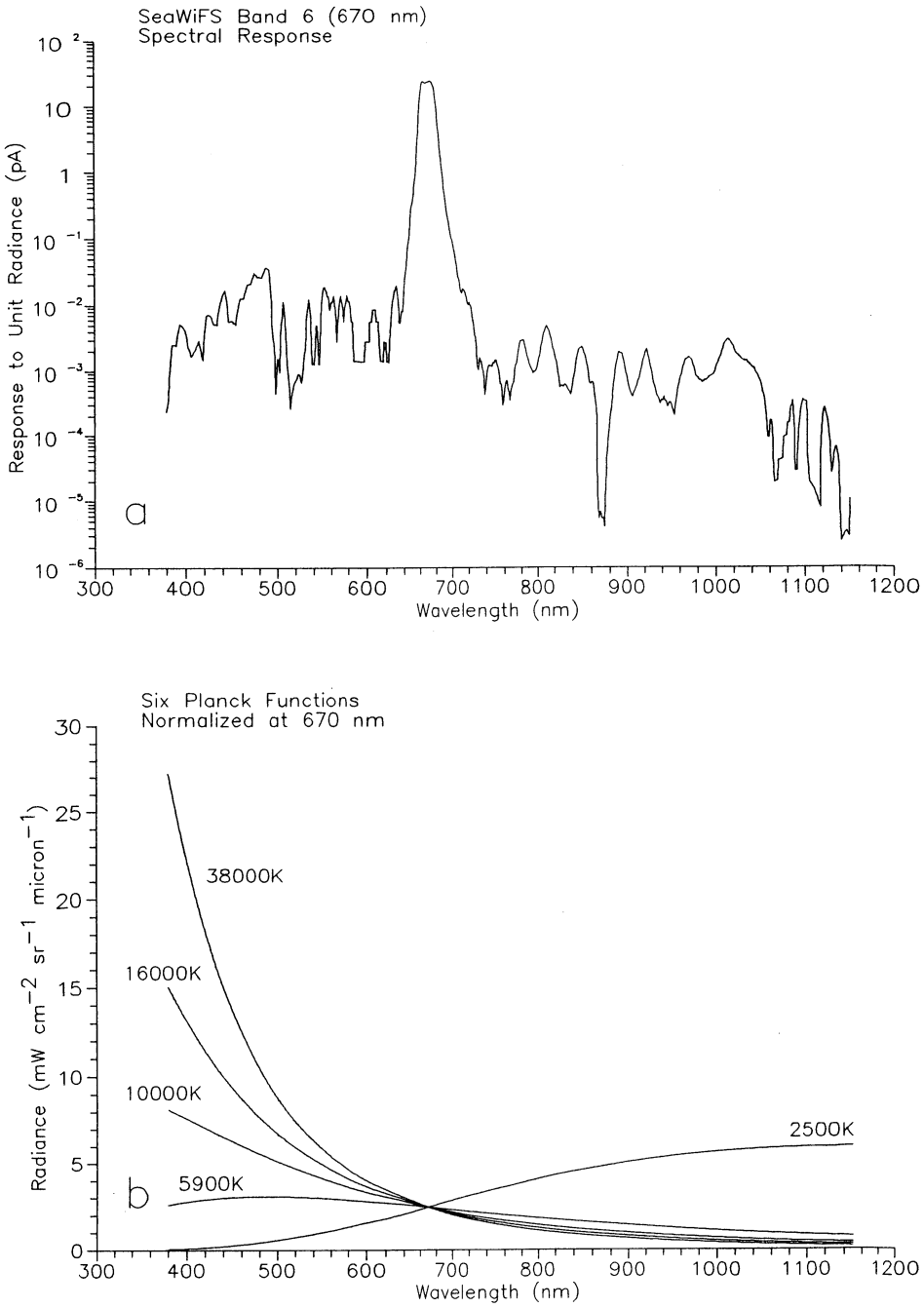

Fig. 4. Components in the Calculation of the Integrated Band Output. SeaWiFS band 6 (670 nm) is used as an example. The integrated band output is calculated as the sum of wavelength-by-wavelength products of the band spectral response and the radiance curve. **a)** Band 6 spectral response: this is the response to a source with unit radiance ($1\,\mathrm{mW\,cm^{-2}\,sr^{-1}\,\mu\,m^{-1}}$). **b)** A set of Planck function (blackbody) curves normalized at 670 nm, the nominal wavelength for SeaWiFS band 6.

(Wyatt 1978):

$$L(\lambda) = \frac{2hc^2}{\lambda^5\left(e^{hc/\lambda kT} - 1\right)}, \quad (1)$$

where L is the radiance (in $\mathrm{W\,m^{-3}\,sr^{-1}}$); λ is the wavelength (in meters); h is Planck's constant (in J sec); c is the velocity of light (in $\mathrm{m\,sec^{-1}}$); k is Boltzmann's constant (in $\mathrm{J\,K^{-1}}$); and T is the temperature (in K).

The radiance values from (1) can be converted directly into units of $\mathrm{mW\,cm^{-2}\,sr^{-1}\,\mu m^{-1}}$, the units for SeaWiFS measurements. As used in the model calculations below, these Planck function curves are normalized to the SeaWiFS typical radiances at the nominal wavelengths for the SeaWiFS bands, which are given in Table 1. These are the wavelengths at which SeaWiFS was calibrated in the laboratory. The wavelength for each band in Table 1 corresponds to the radiance for each band in Table 8 of Barnes et al. (1994b). The wavelengths in Table 1 are embedded in the radiometric calibration of SeaWiFS. For these fixed wavelengths, the output of the bands change with the spectral shapes of the sources. In an alternate approach to source spectral shape dependence, it is possible to keep the band output constant and let the reference wavelength vary as a function of the spectral shape of the source. However, the alternate approach lacks the security of well-defined, fixed reference wavelengths for the instrument.

Table 1. The center wavelengths are in nanometers and the typical (L_{typical}) radiances for the SeaWiFS bands are in units of $\mathrm{mW\,cm^{-2}\,sr^{-1}\,\mu m^{-1}}$. These values come from the performance specifications for the instrument (see Barnes et al. 1994a).

SeaWiFS Band	*Nominal Center Wavelength*	*Typical Radiance*
1	412	9.10
2	443	8.41
3	490	6.56
4	510	5.64
5	555	4.57
6	670	2.46
7	765	1.61
8	865	1.09

The radiance values from the Planck function increase at all wavelengths with increasing temperature, and the peak of the curve shifts toward shorter wavelengths with increasing temperature. The wavelength at which the maximum radiance occurs is given by the derivative of Planck's equation with respect to wavelength, also called Wein's displacement law:

$$\lambda_m = \frac{2898}{T}, \quad (2)$$

where λ_m is the wavelength for maximum radiance (in μ m). For a 2,850 K blackbody, the maximum radiance occurs at 1,017 nm; for a 5,900 K blackbody at 491 nm. These are within the wavelength range over which the spectral responses of the SeaWiFS bands have been measured (380–1,150 nm). Over the more restricted wavelength range of 394–908 nm, which covers the within-band responses for the eight SeaWiFS bands (Barnes et al. 1994b), Planck function curves with temperatures that are less than about 3,000 K have radiances that increase monotonically with wavelength. For blackbody temperatures that are greater than about 8,000 K, the radiances decrease monotonically over this range. A set of blackbody curves, normalized at 670 nm is shown in Fig. 3b.

For a combination of high temperatures and long wavelengths, Planck's law can be approximated by Rayleigh-Jeans' law:

$$L(\lambda) = \frac{2ckT}{\lambda^4}. \quad (3)$$

The wavelength dependence for radiance in the Rayleigh-Jeans' law is the same as that for light scattered by air molecules (Section 1.2.4). Fig. 5a shows the response of a 26,000 K blackbody and the Rayleigh-Jeans approximation, both normalized at the typical radiance for SeaWiFS band 8 ($1.09\,\mathrm{mW\,cm^{-2}\,sr^{-1}\,\mu m^{-1}}$) at 865 nm. Fig. 5b shows the difference between the blackbody curve and the power-law approximation from the Rayleigh-Jeans law, which appears as a straight line in log-log space.

1.2.3 GSFC Sphere Output

The radiances from the GSFC sphere were provided by B. Carol Johnson of NIST. The data are given for four lamp configurations: 1, 4, 8, and 16 lamps illuminated. These data, including the spectral responses of the Fastcal transfer radiometer (Walker et al. 1987) to a tungsten strip lamp and to the sphere, were taken at 10 nm intervals from 380–1,100 nm. Using reference values for the radiance from the tungsten strip lamp, the sphere radiances were calculated as ratios of the output from the transfer radiometer. As part of the preparation of the NIST-provided data for this study, the discontinuities in the responses of the Fastcal radiometer at 760 and 960 nm were smoothed using a power law interpolation, that is, an interpolation in log-log space.

Since the spectral response values for the SeaWiFS bands cover the range from 380–1,150 nm (Barnes et al. 1994b), the NIST data were extended from 1,100–1,150 nm using power law curve fits of the data from 1,000–1,100 nm. The region between 1,100–1,150 nm lies at the end of the out-of-band responses for each of the SeaWiFS bands, and the band responses at these wavelengths are 4–5 orders of magnitude below the peak responses (see Fig. 4a, for example). Errors of 20–30% in the radiances from the source in this region give negligible contributions to the model calculations. The extrapolations have been made with the

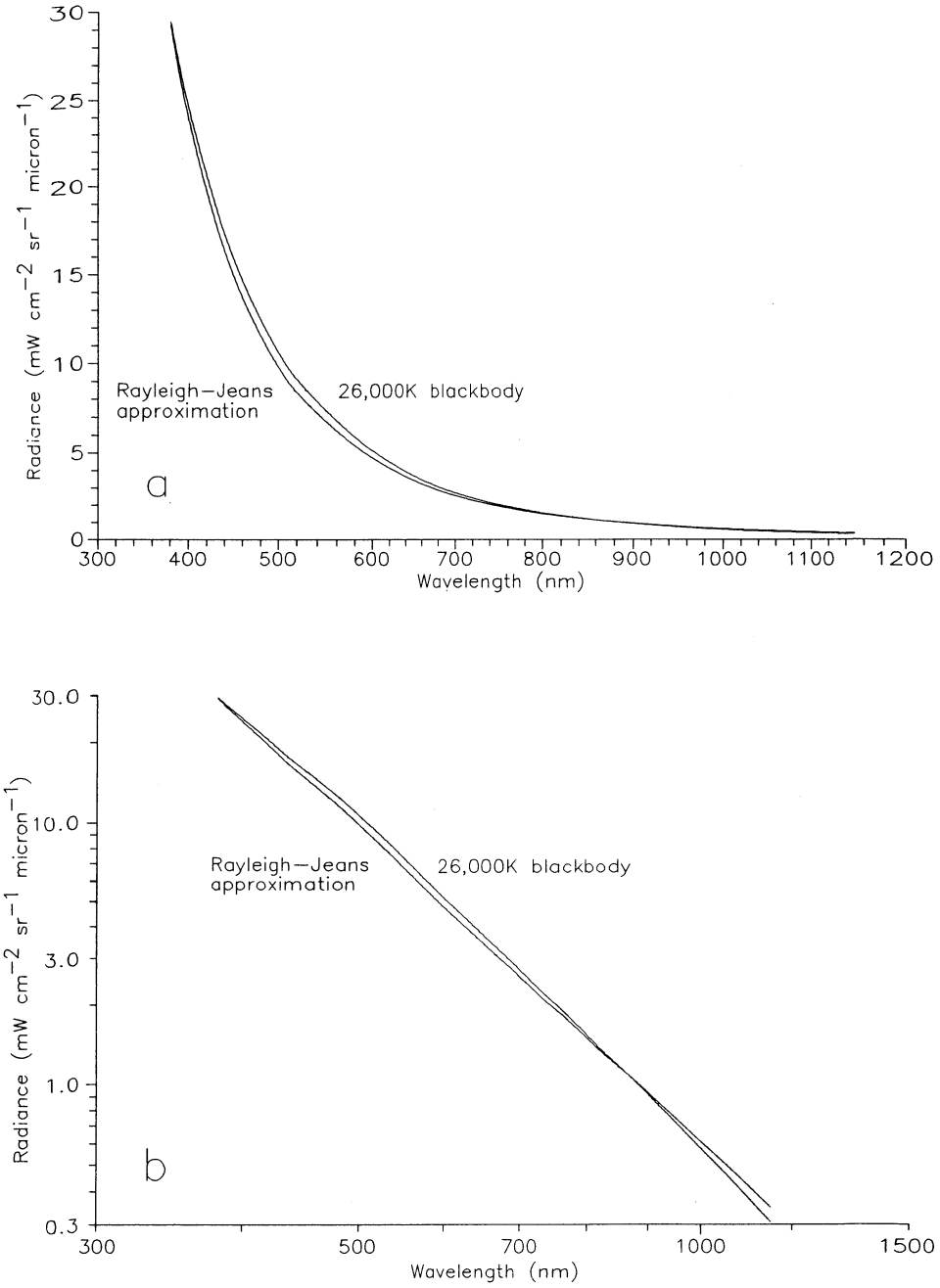

Fig. 5. Shown here is the spectral output of a 26,000 K blackbody and of the Rayleigh-Jeans approximation to the Planck function. Both curves have been normalized at 865 nm to the typical radiance for SeaWiFS band 8 ($1.09\,\mathrm{mW\,cm^{-2}\,sr^{-1}\,\mu\,m^{-1}}$). **b)** Radiances shown in linear coordinates. From 380–865 nm the radiance from the 26,000 K blackbody is greater than that for the approximation. **b)** Radiances shown in logarithmic coordinates. The Rayleigh-Jeans approximation appears as a straight line in these coordinates.

sole purpose of maintaining a uniform wavelength range for all components of the calculations.

Finally, because the SeaWiFS spectral response values are given at 1 nm intervals, the NIST-provided data have been interpolated between these 10 nm intervals, again using power-law interpolation, to provide data at those wavelengths. The use of linear interpolations of the NIST data was compared with that for power-law interpolations. Substituting one interpolation for the other caused changes of 0.05% or less in the results of the model calculations. This difference is sufficiently small that the results from the linear interpolations are not included here.

1.2.4 Solar Flux and Rayleigh Scattering

For wavelengths above 300 nm, the solar flux has a spectral shape that is approximated by a blackbody with a temperature of 900 K (Brasseur and Solomon 1987). As viewed by SeaWiFS during solar diffuser measurements (Woodward et al. 1993), the solar spectrum is essentially a continuum, and the 5,900 K spectral shape was used in several of the SeaWiFS performance specifications (Barnes et al. 1994a). The shape, however, is a poor approximation for the blue sky radiance—the upwelling Earth radiance seen by SeaWiFS on orbit. For SeaWiFS ocean measurements, the reflected light from the sea surface is a small fraction of the sky radiance. This radiance is dominated by scattering from air molecules.

Molecular, or Rayleigh, scattering of unpolarized light by anisotropic air molecules has a scattering coefficient with a dependence on wavelength (λ) which is approximated by the form λ^{-4} (Penndorf 1957).

$$\sigma = \frac{8\pi^3(n_s^2 - 1)^2 D}{3\lambda^4 N_s^2}, \tag{4}$$

where σ is the Rayleigh scattering cross section per molecule (cm^2); n_s is the refractive index of air (dimensionless); D is the depolarization factor which expresses the influence of the molecular anisotropy of air (dimensionless); and N_s is the number density of the scattering molecules (cm^{-3}).

There is an additional wavelength dependence in the Rayleigh scattering coefficient, since the coefficient also includes the refractive index of air, which has its own dependence on wavelength. Such a refinement is unnecessary here, since the additional wavelength dependence is small, and since the blue sky radiance is itself an approximation to the sky radiance. The actual upwelling Earth radiance seen by SeaWiFS also includes contributions from aerosol scattering, absorption and emission from gasses, and reflections from the surface of the Earth.

The model calculations presented here contain three special source spectral shapes: the measured shape for the spectral radiance from the GSFC integrating sphere; the spectral shape of a 5,900 K blackbody, which approximates the spectral shape of the solar flux; and a spectral shape with a wavelength dependence of λ^{-4}, which approximates the upwelling radiance from a molecular (or Rayleigh) atmosphere. The model calculations also include Planck functions with temperatures from 2,000–38,000 K. These Planck functions encompass the three special spectral shapes.

1.3 MODEL RESULTS

The integrated output for the eight SeaWiFS bands are listed in Table 2. The results are also shown in Fig. 6 (bands 1 and 2), Fig. 7 (bands 3 and 4), Fig. 8 (bands 5 and 6), and Fig. 9 (bands 7 and 8). For Figs. 6–9, the minimum values for the ordinates have not been set to zero. This was done to increase resolution for the relatively small changes in the output from the bands. To give some consistency to the vertical scales, however, the maximum values for the ordinates have been set to about 1.2–1.25 times the minimum values. The changes in the integrated band output are shown in Table 3, normalized to the output for a 5,900 K blackbody. For the prelaunch radiometric calibration of SeaWiFS (Barnes et al. 1994b), the coefficients for the calibration equations were calculated, based on a 5,900 K blackbody.

The equivalent blackbody temperatures for the GSFC sphere and the Rayleigh atmosphere are also shown in Figs. 6–9. These temperatures were determined by interpolation, using the band output for the blackbody radiances. The equivalent GSFC sphere temperatures are near 3,000 K and the equivalent Rayleigh atmosphere temperatures range from 25,000–35,000 K. This consistency was the basis for the selection of the equivalent temperature when two possible solutions were possible.

The NIST measurements include spectral responses for four configurations of the sphere: 1 lamp, 4 lamps, 8 lamps, and 16 lamps illuminated. The radiances from these output cover a range of radiance levels that is sufficient for the calibration of the SeaWiFS radiometer. The radiances from the NIST measurements, interpolated to the nominal SeaWiFS center wavelengths, are listed in Table 4.

The SeaWiFS integrated band output for the GSFC sphere radiances (Table 2) contain the average values for the four lamp settings. Table 5 gives the SeaWiFS integrated band output for each of the four NIST spectral curves. The mean values in Table 5 have small standard deviations. As a result, the results for the mean integrated band output are interchangeable with those for the individual lamp settings.

It should be stressed that *reality* for this discussion is based on the spectral response curves for the SeaWiFS bands. SeaWiFS radiance measurements from the GSFC sphere are not presented here, and, in fact, there are no SeaWiFS radiance measurements in this report. The results are based on model radiances only.

Table 2. The integrated band output is shown here in picoamperes. The output is given for several Planck functions (in kelvin) and for two special spectral shapes: the shape for the GSFC SIS output and for a Rayleigh scattering atmosphere.

Planck Function Temperature [K]	*Integrated Band Output* [pA]							
	Band 1	Band 2	Band 3	Band 4	Band 5	Band 6	Band 7	Band 8
2,000	2397.8	3570.3	4483.5	4690.5	4032.0	2059.8	2908.8	2254.2
2,500	2306.4	3514.9	4354.6	4636.5	3928.8	2065.5	2883.4	2249.1
2,850	2274.3	3492.9	4315.6	4623.7	3900.1	2069.4	2874.3	2249.0
3,000	2264.2	3485.7	4303.9	4620.5	3892.3	2071.0	2871.6	2249.4
3,500	2239.4	3468.0	4276.3	4614.3	3876.6	2075.9	2865.5	2252.2
4,000	2223.0	3456.4	4258.8	4611.9	3869.4	2080.1	2862.0	2256.3
5,000	2202.9	3442.2	4238.2	4611.3	3865.5	2087.2	2858.9	2266.0
5,900	2192.0	3434.9	4227.4	4612.4	3866.6	2092.3	2858.0	2275.3
8,000	2177.9	3425.8	4214.1	4616.0	3873.5	2101.2	2858.4	2295.5
0,000	2170.8	3421.6	4207.7	4619.1	3880.3	2107.3	2859.6	2311.9
12,000	2166.3	3419.1	4203.9	4621.5	3886.2	2111.9	2860.8	2325.6
14,000	2163.3	3417.5	4201.4	4623.5	3891.1	2115.5	2862.0	2337.0
16,000	2161.2	3416.4	4199.7	4625.1	3895.2	2118.3	2863.1	2346.7
18,000	2159.5	3415.6	4198.4	4626.5	3898.7	2120.7	2864.1	2354.9
20,000	2158.2	3415.0	4197.4	4627.6	3901.7	2122.7	2864.9	2361.9
22,000	2157.2	3414.6	4196.6	4628.5	3904.2	2124.4	2865.7	2368.1
24,000	2156.3	3414.2	4196.0	4629.3	3906.4	2125.8	2866.3	2373.4
26,000	2155.6	3413.9	4195.4	4630.0	3908.3	2127.1	2866.9	2378.1
28,000	2155.0	3413.6	4195.0	4630.6	3910.0	2128.2	2867.4	2382.3
30,000	2154.5	3413.4	4194.6	4631.1	3911.5	2129.1	2867.9	2386.1
32,000	2154.1	3413.2	4194.3	4631.6	3912.8	2130.0	2868.4	2389.4
34,000	2153.7	3413.1	4194.0	4632.0	3914.0	2130.8	2868.7	2392.4
36,000	2153.3	3412.9	4193.8	4632.4	3915.1	2131.5	2869.1	2395.2
38,000	2153.0	3412.8	4193.6	4632.8	3916.1	2132.1	2869.4	2397.7
Special Spectral Shapes								
GSFC SIS	2280.2	3490.4	4305.5	4618.3	3890.8	2069.8	2869.3	2248.2
Rayleigh Atmosphere	2153.9	3413.7	4195.5	4631.5	3911.9	2126.3	2867.1	2367.6

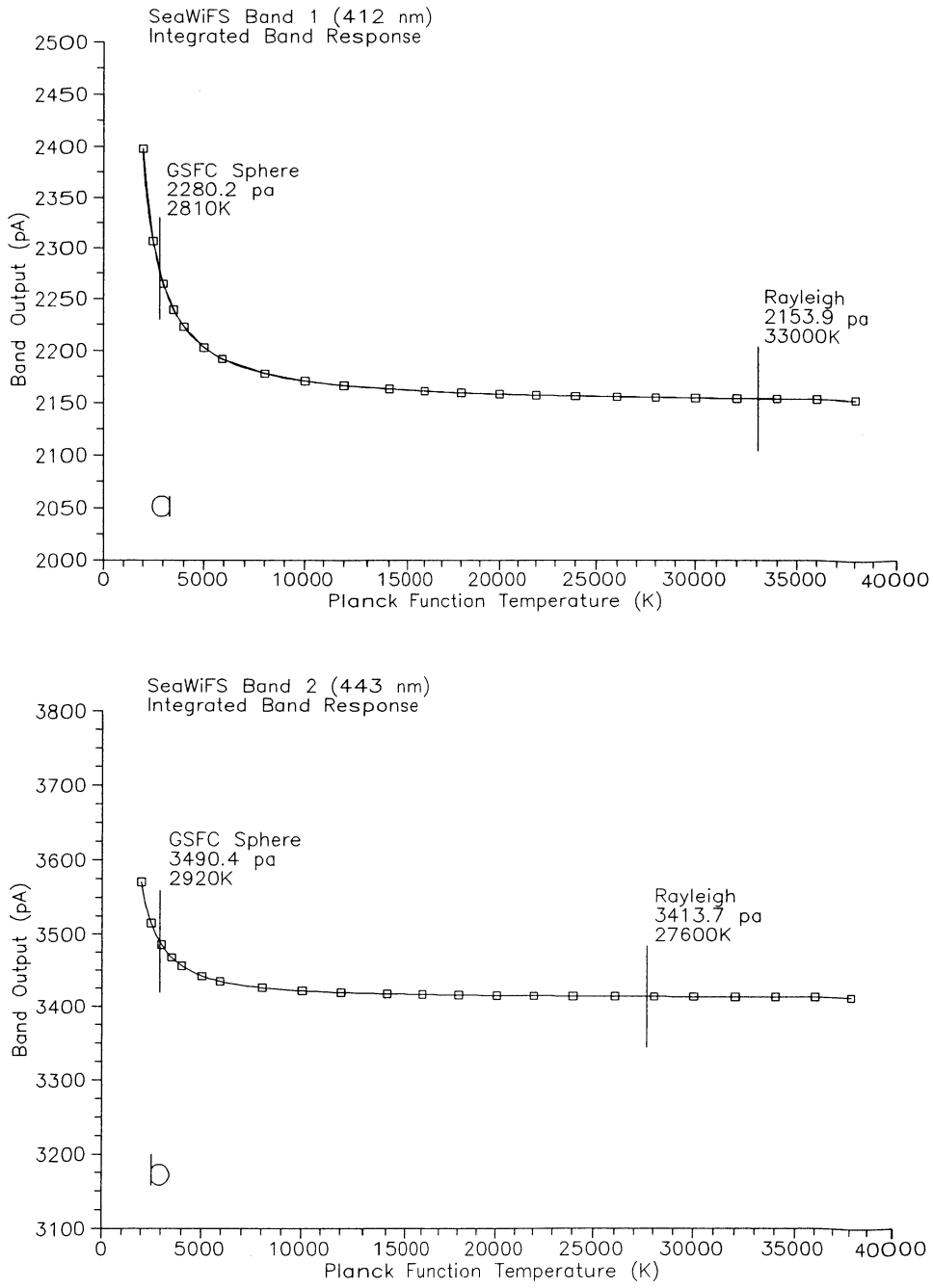

Fig. 6. Instrument responses to Planck function (blackbody) curves with temperatures from 2,000–38,000 K are shown. The vertical lines show the band responses to radiance spectra with the shape of the GSFC sphere and of a Rayleigh scattering atmosphere. **a)** Response of SeaWiFS band 1 (412 nm). **b)** Response of SeaWiFS band 2 (443 nm).

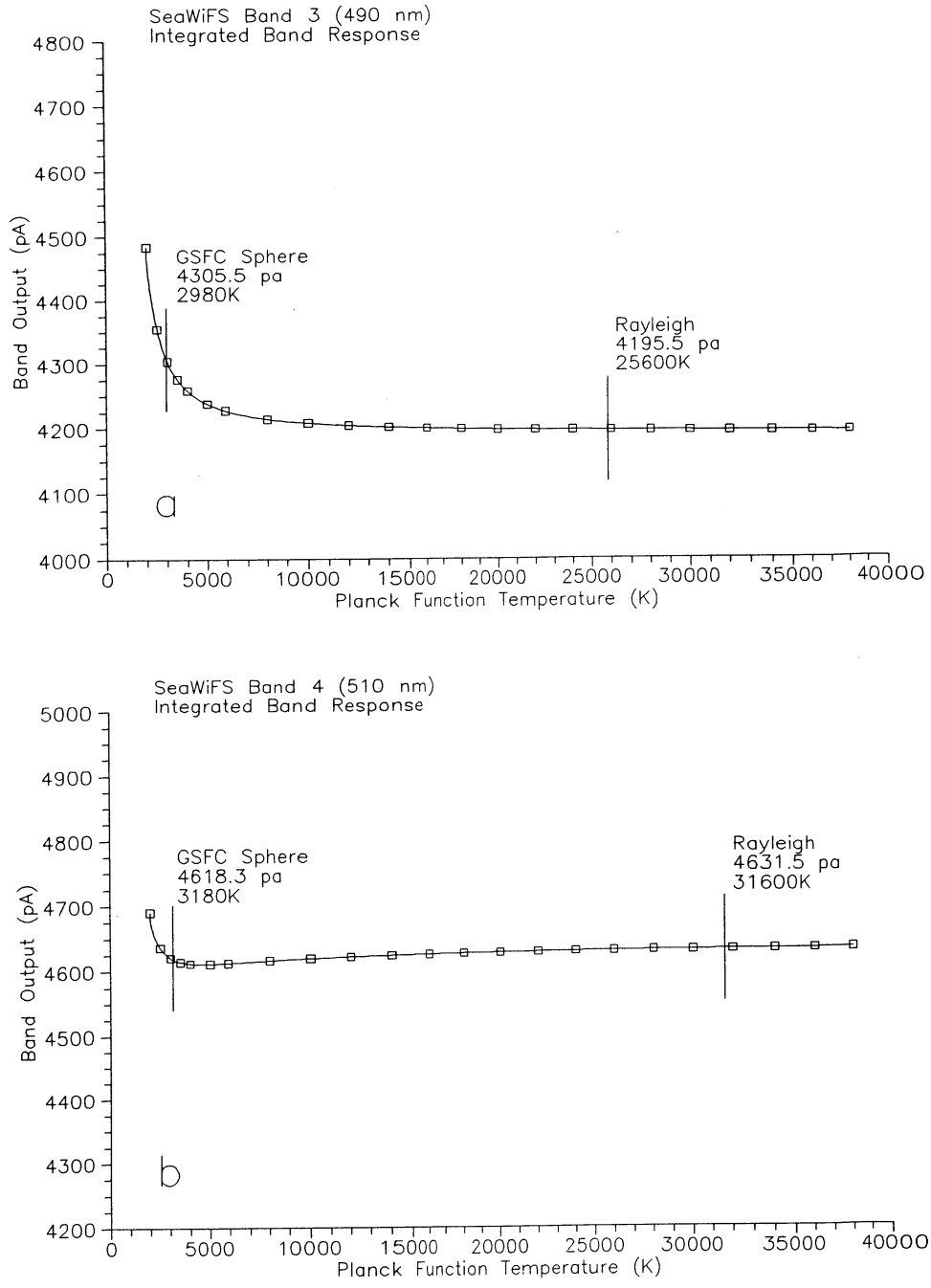

Fig. 7. Instrument responses to Planck function (blackbody) curves with temperatures from 2,000–38,000 K are shown. The vertical lines show the band responses to radiance spectra with the shape of the GSFC sphere and of a Rayleigh scattering atmosphere. **a)** Response of SeaWiFS band 3 (490 nm). **b)** Response of SeaWiFS band 4 (510 nm).

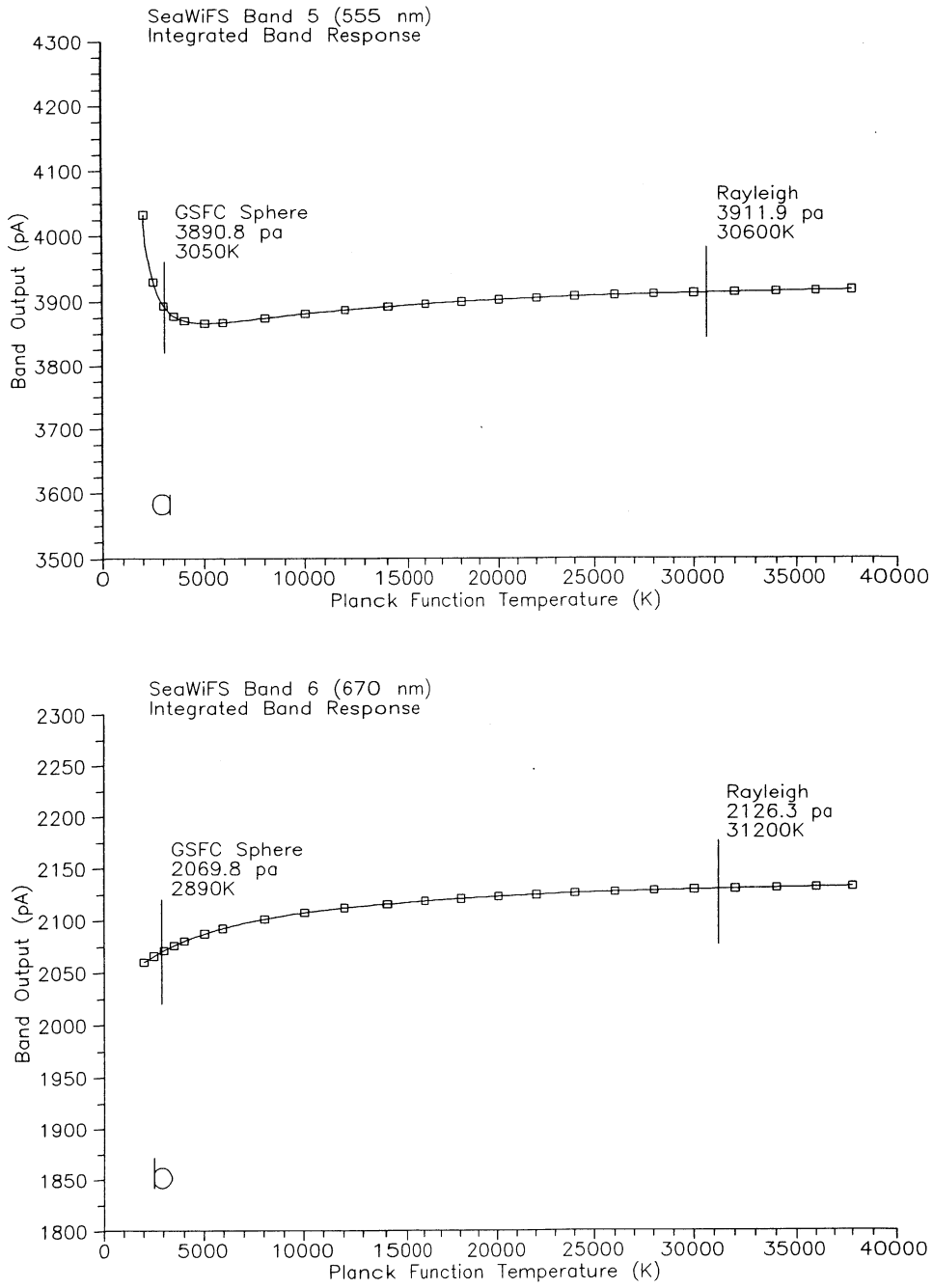

Fig. 8. Instrument responses to Planck function (blackbody) curves with temperatures from 2,000–38,000 K are shown. The vertical lines show the band responses to radiance spectra with the shape of the GSFC sphere and of a Rayleigh scattering atmosphere. **a)** Response of SeaWiFS band 5 (555 nm). **b)** Response of SeaWiFS band 6 (670 nm).

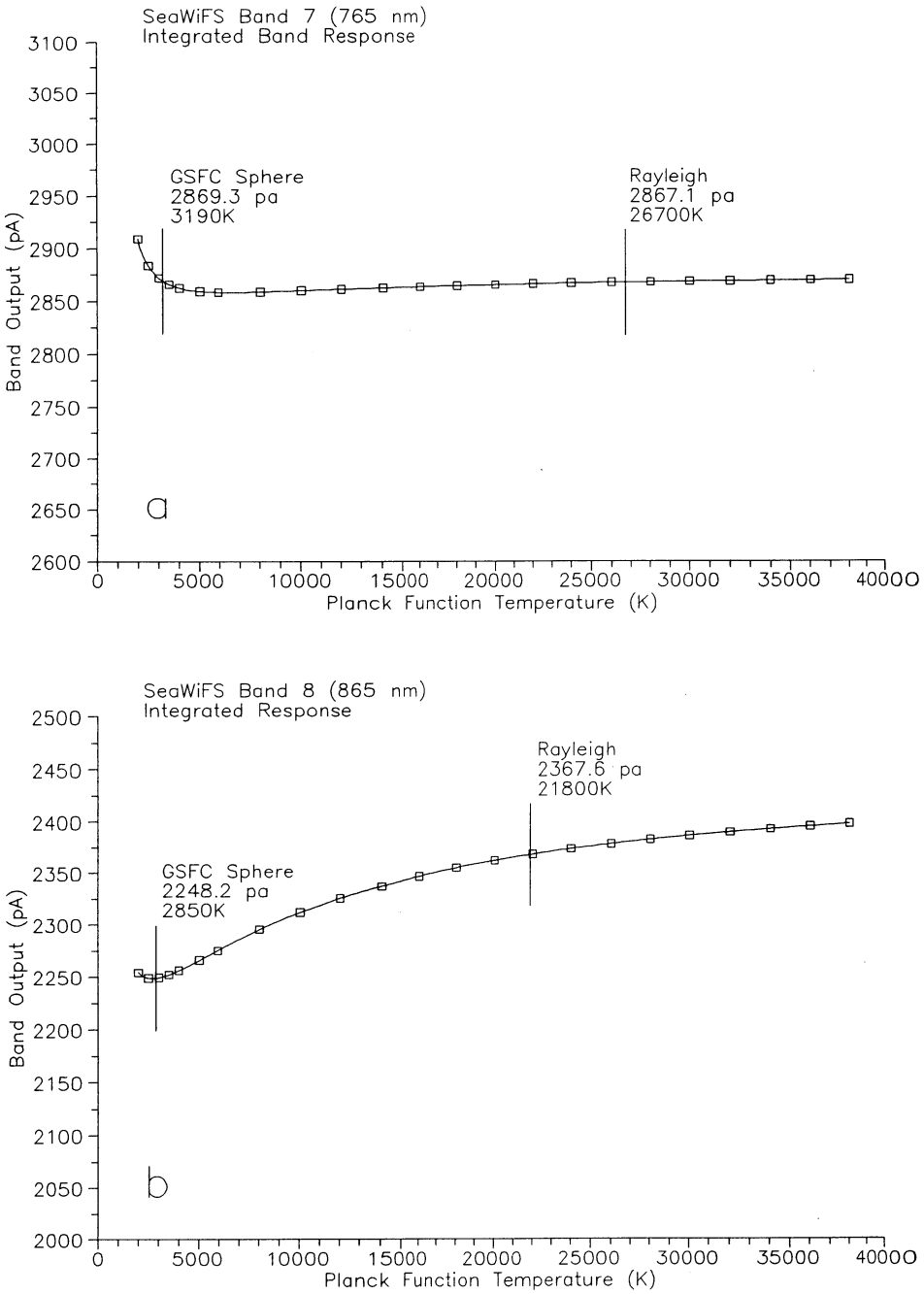

Fig. 9. Instrument responses to Planck function (blackbody) curves with temperatures from 2,000–38,000 K are shown. The vertical lines show the band responses to radiance spectra with the shape of the GSFC sphere and of a Rayleigh scattering atmosphere. **a)** Response of SeaWiFS band 7 (765 nm). **b)** Response of SeaWiFS band 8 (865 nm).

Table 3. The integrated band output relative to a 5,900 K Planck function is shown in this table. The output is given for several Planck functions and for two special spectral shapes: the shape for the GSFC SIS output and for a Rayleigh scattering atmosphere.

Planck Function Temperature [K]	*Integrated Band Output* [pA]							
	Band 1	Band 2	Band 3	Band 4	Band 5	Band 6	Band 7	Band 8
2,000	1.0938	1.0394	1.0606	1.0169	1.0428	0.9845	1.0178	0.9907
2,500	1.0522	1.0233	1.0301	1.0052	1.0161	0.9872	1.0089	0.9885
2,850	1.0375	1.0169	1.0209	1.0024	1.0087	0.9891	1.0057	0.9884
3,000	1.0329	1.0148	1.0181	1.0017	1.0066	0.9898	1.0047	0.9886
3,500	1.0216	1.0097	1.0115	1.0004	1.0026	0.9922	1.0026	0.9899
4,000	1.0141	1.0063	1.0074	0.9999	1.0007	0.9942	1.0014	0.9916
5,000	1.0050	1.0021	1.0025	0.9998	0.9997	0.9976	1.0003	0.9959
5,900	1.0000	1.0000	1.0000	1.0000	1.0000	1.0000	1.0000	1.0000
8,000	0.9935	0.9974	0.9968	1.0008	1.0018	1.0043	1.0001	1.0089
10,000	0.9903	0.9961	0.9953	1.0014	1.0035	1.0072	1.0005	1.0161
12,000	0.9883	0.9954	0.9944	1.0020	1.0051	1.0094	1.0010	1.0221
14,000	0.9869	0.9950	0.9938	1.0024	1.0063	1.0111	1.0014	1.0271
16,000	0.9859	0.9946	0.9934	1.0028	1.0074	1.0125	1.0018	1.0314
18,000	0.9852	0.9944	0.9931	1.0030	1.0083	1.0136	1.0021	1.0350
20,000	0.9846	0.9942	0.9929	1.0033	1.0091	1.0145	1.0024	1.0381
22,000	0.9841	0.9941	0.9927	1.0035	1.0097	1.0153	1.0027	1.0408
24,000	0.9837	0.9940	0.9926	1.0037	1.0103	1.0160	1.0029	1.0431
26,000	0.9834	0.9939	0.9924	1.0038	1.0108	1.0166	1.0031	1.0452
28,000	0.9831	0.9938	0.9923	1.0039	1.0112	1.0172	1.0033	1.0470
30,000	0.9829	0.9938	0.9922	1.0041	1.0116	1.0176	1.0035	1.0487
32,000	0.9827	0.9937	0.9922	1.0042	1.0120	1.0180	1.0036	1.0502
34,000	0.9825	0.9937	0.9921	1.0043	1.0123	1.0184	1.0037	1.0515
36,000	0.9824	0.9936	0.9920	1.0043	1.0125	1.0187	1.0039	1.0527
38,000	0.9822	0.9936	0.9920	1.0044	1.0128	1.0190	1.0040	1.0538
Special Spectral Shapes								
GSFC SIS	1.0402	1.0162	1.0185	1.0013	1.0063	0.9892	1.0040	0.9881
Rayleigh Atmosphere	0.9826	0.9938	0.9924	1.0041	1.0117	1.0163	1.0032	1.0406

Table 4. Radiances from the GSFC sphere. These are the radiances at the nominal SeaWiFS wavelengths at a distance of 1 m from the sphere aperture.

Wavelength [nm]	*Sphere Radiance*			
	16 lamps	8 lamps	4 lamps	1 lamp
412	3.907	1.8752	0.9311	0.2358
443	6.520	3.1410	1.5620	0.3977
490	11.521	5.5780	2.7800	0.7091
510	13.954	6.7670	3.3760	0.8609
555	19.770	9.6280	4.8060	1.2251
670	33.760	16.5450	8.2780	2.1060
765	41.580	20.4200	10.2260	2.5920
865	45.020	22.1800	11.1150	2.8080

Table 5. The integrated band output from the GSFC sphere is shown in picoamperes. The output is given for the individual lamp settings from the sphere, for the mean values, and the standard deviations.

Sphere Setting	*Integrated Band Output* [pA]							
(No. of Lamps)	Band 1	Band 2	Band 3	Band 4	Band 5	Band 6	Band 7	Band 8
16	2279.3	3489.7	4304.6	4618.0	3890.4	2069.9	2869.3	2248.3
8	2280.0	3490.3	4305.8	4618.5	3890.9	2069.8	2869.6	2248.2
4	2280.2	3490.6	4305.9	4618.1	3891.0	2069.7	2869.4	2248.2
1	2281.5	3491.0	4305.8	4618.4	3890.8	2069.8	2868.9	2248.1
Mean	2280.2	3490.4	4305.5	4618.3	3890.8	2069.8	2869.3	2248.2
Standard Deviation	0.8	0.4	0.5	0.2	0.2	0.1	0.2	0.0

On the average, the equivalent blackbody temperature for the eight SeaWiFS bands is 2,980 K, with a standard deviation of 140 K. The SeaWiFS band output, when viewing the GSFC sphere, are essentially the same as when viewing a 2,850 K blackbody. On the average, the integrated band output for the GSFC sphere is 0.07% lower than for a 2,850 K blackbody, with a 0.15% standard deviation. For individual bands, the differences between these two sources are 0.25% percent or less. Thus, for SeaWiFS, the GSFC sphere and a 2,850 K blackbody have equivalent spectral shapes.

For the radiance source used in SBRC's calibration of SeaWiFS, the spectral shape of the source was assumed to be 2,850 K, and no measurements of the source spectral shape were provided (Barnes et al. 1994b). Such a minimal dependence of the SeaWiFS output on spectral shape (between 2,800 and 3,000 K) shows that inaccuracies in the manufacturer's assumption contribute negligible error to the instrument's radiometric calibration.

1.4 CONCLUDING REMARKS

Filter photometers in general, and SeaWiFS in particular, have output that vary with the spectral shape of the source that they measure. For SeaWiFS, the transfer of the laboratory calibration to orbit requires source shape corrections for the eight bands that vary from near zero (for band 4) to more than 5% (for band 8). From Table 3, it is clear that the correction from a 2,850 K to a 5,900 K source (Barnes et al. 1994b) does not adequately account for the upwelling radiance that SeaWiFS will view on orbit. This said, there remain two additional factors that must be considered.

First, Rayleigh scattering does not completely account for the spectral shape of the Earth-exiting radiances that SeaWiFS will view on orbit. There are absorption and emission lines from atmospheric gasses within the wavelength region between 380 and 1,150 nm. The most important of these features are the oxygen absorption lines near 762 nm (McClain et al. 1994, Fraser 1995, and Ding and Gordon 1995) that lie within the bandpass for SeaWiFS band 7. These absorption lines create an *oxygen notch* within band 7, and they must be treated explicitly in the SeaWiFS data reduction algorithms.

In addition, scattered light from small atmospheric particles, i.e., Mie scattering, creates an additional source of Earth-exiting radiance. Since Rayleigh scattering decreases as a function of wavelength to the fourth power, Mie scattering becomes more important for wavelengths in the red and near-infrared. As the number of small particles in the atmosphere increases, the sky loses its blue color and turns white. Thus, the calculations presented in this chapter cover the color range of the Earth-exiting radiances viewed by SeaWiFS during ocean measurements. In addition, these results show the magnitude of the effects of source spectral shape on the integrated output from the SeaWiFS bands. This leads to the second factor that must be considered.

For SeaWiFS band 6 (Fig. 4), the region of greatest response, called the in-band response, occurs from 647–678 nm (Barnes et al. 1994a). It is the in-band response that is required from the on-orbit SeaWiFS measurements, but it is the total band response that is measured in the laboratory. The SeaWiFS in-band responses have source shape dependencies, as do the SeaWiFS out-of-band responses. Together they create the source shape dependency for the total band response. Both must be accounted for in order to convert the laboratory calibration of the instrument to the desired on-orbit values (Barnes and Yeh 1996).

Chapter 2

Effects of Source Spectral Shape on SeaWiFS Radiance Measurements

Robert A. Barnes
Eueng-nan Yeh
General Sciences Corporation, Laurel, Maryland

Abstract

Two aspects of filter photometry on the radiances measured by SeaWiFS are examined: the dependence of the total band response, and the out-of-band response on source spectral shape. These effects are significant contributors to the SeaWiFS measurements on orbit. The corrections for out-of-band response range from about 0.5% to more than 5%, depending on the SeaWiFS band. The corrections for total band response range from near zero to about 5%. These corrections will be used to convert the laboratory calibration of SeaWiFS (in terms of total band response) to orbit (in terms of in-band response). The residual uncertainty in these corrections is estimated to be small, around 0.2%. With other significantly larger error sources in the SeaWiFS measurements, the contribution of these residual uncertainties to the propagation of error for SeaWiFS radiance measurements at the top of the atmosphere is also expected to be small. These corrections are prelaunch estimates and should be reexamined using flight data. In addition, these corrections were tailored to SeaWiFS ocean measurements. The contributions to land measurements will be different.

2.1 INTRODUCTION

Barnes et al. (1994b) calculated the change in the responses of the SeaWiFS bands from those for a 2,850 K blackbody (the spectral shape of the radiance source for the SeaWiFS laboratory calibration) to those for a 5,900 K blackbody (the spectral shape of the sun). This conversion was used in the prelaunch radiometric calibration of SeaWiFS (Barnes et al. 1994b). An alternative conversion to a spectral shape of a 12,000 K blackbody is provided in this chapter. This spectral shape is consistent with the SeaWiFS typical radiances in the instrument specifications (Barnes et al. 1994a) and gives a better representation of the radiances to be found during on-orbit ocean measurements by SeaWiFS.

Barnes et al. (1995a) presented an out-of-band correction scheme for SeaWiFS that used a combination of the wavelength-dependent response of the instrument with the wavelength-dependent shape of the radiance measured by the instrument. The relative spectral responses for the eight SeaWiFS bands were tabulated at 1 nm intervals from 380–1,150 nm (Barnes et al. 1994b and Barnes 1994). As part of the calculations in Barnes et al. (1995a), the spectral radiances from the eight SeaWiFS bands were interpolated to 1 nm intervals and were used as the basis for the spectral shape of the radiance measured by the instrument. The radiances and spectral responses of the bands were integrated from 380–1,150 nm (for the total band output for each band) and from the lower extended band edge to the upper extended band edge (for the in-band response). With 771 points in the integration for each band, 8 bands per pixel, 1,285 pixels per scan line, and 6 scan lines per second in the on-orbit measurements, the out-of-band correction of Barnes et al. (1995a) provides a cumbersome and time-consuming algorithm for processing SeaWiFS data. In this chapter, the analysis method used in Barnes et al. (1995a) is used to create simplified out-of-band calculations which run significantly faster in the SeaWiFS data reduction.

2.2 BAND SPECIFICATIONS

The SeaWiFS specifications (Barnes et al. 1994a) define the in-band response region for each SeaWiFS band. It is the spectral region between the lower extended band edge (lower 1% response point) and the upper extended band edge (upper 1% response point). The band edges for the eight SeaWiFS bands, taken from Barnes et al. (1994b), are given in Table 6. With this information, it is possible to use the model of Barnes (1996a) to calculate the in-band response for each band, in addition to the total band response.

Table 6 also gives the nominal center wavelengths for each SeaWiFS band. These are the center wavelengths

Table 6. Band edges (half-maximum wavelengths) and extended band edges (1% response wavelengths) for the eight SeaWiFS bands. The edges are given for a radiance source with the shape of a 5,900 K blackbody. The center wavelength is calculated from the upper and lower band edges. The in-band response is the wavelength interval between the lower and upper extended band edges.

Band Number	*Nominal Band Edges* [nm]	*Lower Extended Band Edge* [nm]	*Lower Band Edge* [nm]	*Center Wavelength* [nm]	*Upper Band Edge* [nm]	*Upper Extended Band Edge* [nm]
1	402–422	395.2	403.4	413.4	423.4	433.6
2	433–453	424.1	434.2	444.0	453.8	463.7
3	480–500	470.7	480.8	491.1	501.4	511.7
4	500–520	488.1	498.9	510.1	521.2	530.7
5	545–565	536.3	545.4	554.6	563.8	577.2
6	660–680	646.7	658.3	668.2	678.1	692.5
7	745–785	727.3	744.4	764.6	784.9	813.4
8	845–885	826.4	845.5	866.1	886.7	907.5

from the specifications for the instrument (Barnes et al. 1994a). They are also the wavelengths at which SeaWiFS was calibrated in the laboratory. The radiances from the laboratory source [see Table 8 of Barnes et al. (1994b)] were themselves calibrated at the nominal center wavelengths in Table 6, using a reference source traceable to NIST. The selection of those wavelengths for the laboratory source embedded those wavelengths in the radiometric calibration of SeaWiFS. They are the wavelengths at which the radiances in the source shape curves are normalized, in the study described in this chapter.

As explained in Barnes (1996a), the model results presented here do not represent actual SeaWiFS measurements. The model examines only the spectral response of the optical components in the instrument, including the spectral response of the detectors. Since there are other nonspectral components in each SeaWiFS band that are not part of the model, the results can only be considered in relative terms. The SeaWiFS prelaunch radiometric calibration, which converts the instrument output into radiances, was given in Barnes et al. (1994b).

2.3 INSTRUMENT RESPONSE

As described in Barnes (1996a), the instrument relative spectral response uses the measured spectral response for each SeaWiFS band to a spectrally flat source and combines this response with a series of sources with different spectral shapes. The model uses a series of Planck functions with temperatures ranging from 2,000–38,000 K. These functions cover the source spectral shapes found in the laboratory and encompass the source spectral shapes to be found on orbit. The effects of sources with different color temperatures can be seen in Fig. 10.

Figure 10a shows several source spectral shapes normalized to the typical radiance for SeaWiFS band 1 (9.10 mW $cm^{-2}\,sr^{-1}\,\mu\,m^{-1}$ at 412 nm). For this band, a 2,850 K laboratory source provides orders of magnitude more radiance in the red and the near-infrared than do the higher temperature Planck functions. For SeaWiFS band 8, the effect is reversed, as can be seen in Fig. 10b. Higher temperature Planck functions produce more radiance in the blue and the near-ultraviolet. The convolution of these source shapes with the responses of the individual SeaWiFS bands produces dependencies on source spectral shape, both out-of-band and in-band, that differ from band to band.

The model results for the eight SeaWiFS bands are listed in Tables 7–10. They are given for Planck function temperatures from 2,000–38,000 K. These follow the temperature formats in Barnes (1996a) and include the special spectral shapes found there. Tables 7–10 also include the total band and the in-band responses. The in-band response is the integral between the 1% response points, also called the extended band edges. The band edges are listed in Table 6.

The out-of-band response is the difference between the in-band and the total band response normalized to the total band response. For data reduction, the desired quantity is the response of the band after the out-of-band has been removed. Those responses, in the form of a ratio, are also given in Tables 7–10.

The individual responses of the eight SeaWiFS bands are shown, as a function of blackbody temperature, in Figs. 11–18. For each of these figures, part a gives plots of the total band response and the in-band response in picoamperes. These correspond to the respective values in Tables 7–10. For Figs. 11–18, the minimum ordinate values have not been set to zero. This was done to increase the resolution for the relatively small changes in the output from the bands. To give some consistency to the vertical scales, however, the maximum values for the ordinates have been set to about 1.2–1.25 times the minimums.

Part c of Figs. 11–18 divides the total band response into three components. These components sum to unity at each Planck temperature. The components are: the *left side* out-of-band response, that is, the response for wavelengths less than the short wavelength 1% response point; the in-band response; and the *right side* out-of-band

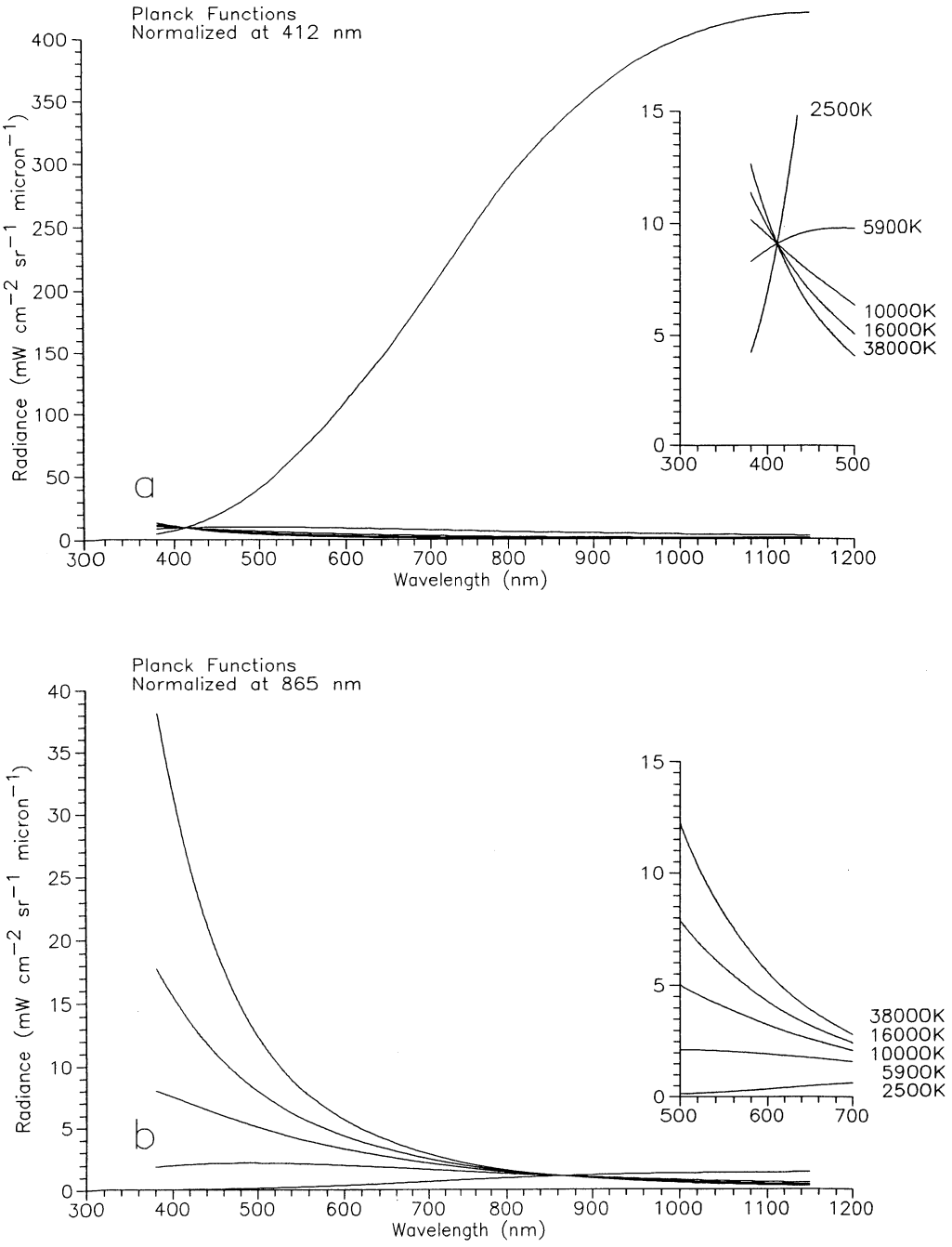

Fig. 10. Planck functions are normalized at 412 nm and 865 nm. **a)** Functions are normalized to 9.10 mW cm^{-2} sr^{-1} μ m^{-1} at 412 nm, the typical radiance (L_{typical}) and nominal center wavelength for SeaWiFS band 1. **b)** Functions are normalized to 1.09 mW cm^{-2} sr^{-1} μ m^{-1} at 865 nm, the typical radiance (L_{typical}) and nominal center wavelength for SeaWiFS band 8.

Table 7. The band responses in picoamperes for SeaWiFS bands 1 and 2 are listed here. The out-of-band response is the difference between the total response (R_T) and the in-band response (R_{IB}). The special spectral shapes, i.e., the GSFC SIS and the Rayleigh Atmosphere are shown at the bottom of the table.

Planck Function Temperature [K]	*Band 1 (412 nm)*			*Band 2 (443 nm)*		
	R_T	R_{IB}	R_{IB}/R_T	R_T	R_{IB}	R_{IB}/R_T
2,000	2397.752	2317.080	0.9664	3570.264	3542.373	0.9922
2,500	2306.404	2265.530	0.9823	3514.930	3494.853	0.9943
2,850	2274.303	2243.185	0.9863	3492.898	3474.751	0.9948
3,000	2264.153	2235.681	0.9874	3485.734	3468.086	0.9949
3,500	2239.354	2216.503	0.9898	3468.026	3451.334	0.9952
4,000	2223.022	2203.264	0.9911	3456.351	3440.047	0.9953
5,000	2202.907	2186.352	0.9925	3442.234	3426.076	0.9953
5,900	2192.031	2176.950	0.9931	3434.870	3418.588	0.9953
8,000	2177.883	2164.461	0.9938	3425.809	3409.077	0.9951
10,000	2170.768	2158.078	0.9942	3421.588	3404.459	0.9950
12,000	2166.343	2154.071	0.9943	3419.122	3401.671	0.9949
14,000	2163.334	2151.331	0.9945	3417.532	3399.823	0.9948
16,000	2161.158	2149.343	0.9945	3416.434	3398.511	0.9948
18,000	2159.514	2147.835	0.9946	3415.635	3397.539	0.9947
20,000	2158.228	2146.656	0.9946	3415.032	3396.789	0.9947
22,000	2157.196	2145.705	0.9947	3414.561	3396.194	0.9946
24,000	2156.349	2144.925	0.9947	3414.185	3395.714	0.9946
26,000	2155.642	2144.271	0.9947	3413.878	3395.313	0.9946
28,000	2155.043	2143.718	0.9947	3413.623	3394.982	0.9945
30,000	2154.529	2143.244	0.9948	3413.409	3394.697	0.9945
32,000	2154.083	2142.830	0.9948	3413.226	3394.450	0.9945
34,000	2153.693	2142.470	0.9948	3413.068	3394.235	0.9945
36,000	2153.348	2142.151	0.9948	3412.931	3394.047	0.9945
38,000	2153.041	2141.867	0.9948	3412.811	3393.883	0.9945
GSFC SIS	2280.169	2249.292	0.9865	3489.135	3471.437	0.9949
Rayleigh	2153.879	2142.609	0.9948	3413.669	3394.790	0.9945

Table 8. The band responses in picoamperes for SeaWiFS bands 3 and 4 are listed here. The out-of-band response is the difference between the total response (R_T) and the in-band response (R_{IB}). The special spectral shapes, i.e., the GSFC SIS and the Rayleigh Atmosphere are shown at the bottom of the table.

Planck Function Temperature [K]	*Band 3 (490 nm)*			*Band 4 (510 nm)*		
	R_T	R_{IB}	R_{IB}/R_T	R_T	R_{IB}	R_{IB}/R_T
2,000	4483.516	4316.599	0.9628	4690.465	4619.324	0.9848
2,500	4354.579	4270.518	0.9807	4636.462	4600.506	0.9922
2,850	4315.636	4250.698	0.9850	4623.705	4594.058	0.9936
3,000	4303.891	4244.067	0.9861	4620.456	4592.207	0.9939
3,500	4276.253	4227.234	0.9885	4614.326	4588.347	0.9944
4,000	4258.808	4215.722	0.9899	4611.929	4586.582	0.9945
5,000	4238.163	4201.202	0.9913	4611.322	4585.747	0.9945
5,900	4227.442	4193.247	0.9919	4612.427	4586.173	0.9943
8,000	4214.101	4182.874	0.9926	4616.010	4588.064	0.9939
10,000	4207.736	4177.680	0.9929	4619.067	4589.796	0.9937
12,000	4203.933	4174.467	0.9930	4621.536	4591.210	0.9934
14,000	4201.430	4172.297	0.9931	4623.518	4592.355	0.9933
16,000	4199.670	4170.738	0.9931	4625.126	4593.282	0.9931
18,000	4198.370	4169.565	0.9931	4626.450	4594.046	0.9930
20,000	4197.374	4168.655	0.9932	4627.557	4594.687	0.9929
22,000	4196.587	4167.920	0.9932	4628.494	4595.224	0.9928
24,000	4195.952	4167.323	0.9932	4629.297	4595.688	0.9927
26,000	4195.429	4166.828	0.9932	4629.992	4596.087	0.9927
28,000	4194.990	4166.406	0.9932	4630.600	4596.435	0.9926
30,000	4194.618	4166.049	0.9932	4631.135	4596.744	0.9926
32,000	4194.299	4165.736	0.9932	4631.610	4597.016	0.9925
34,000	4194.021	4165.464	0.9932	4632.034	4597.257	0.9925
36,000	4193.778	4165.223	0.9932	4632.416	4597.478	0.9925
38,000	4193.564	4165.010	0.9932	4632.760	4597.676	0.9924
GSFC SIS	4308.489	4248.162	0.9860	4620.657	4592.931	0.9940
Rayleigh	4195.469	4166.577	0.9931	4631.520	4596.954	0.9925

Table 9. The band responses in picoamperes for SeaWiFS bands 3 and 4 are listed here. The out-of-band response is the difference between the total response (R_T) and the in-band response (R_{IB}). The special spectral shapes, i.e., the GSFC SIS and the Rayleigh Atmosphere are shown at the bottom of the table.

Planck Function	*Band 5 (555 nm)*			*Band 6 (670 nm)*		
Temperature [K]	R_T	R_{IB}	R_{IB}/R_T	R_T	R_{IB}	R_{IB}/R_T
2,000	4031.971	3784.638	0.9387	2059.801	2041.659	0.9912
2,500	3928.768	3778.835	0.9618	2065.459	2049.506	0.9923
2,850	3900.117	3777.220	0.9685	2069.400	2053.747	0.9924
3,000	3892.322	3776.840	0.9703	2070.996	2055.322	0.9924
3,500	3876.564	3776.336	0.9741	2075.873	2059.768	0.9922
4,000	3869.381	3776.453	0.9760	2080.127	2063.262	0.9919
5,000	3865.481	3777.344	0.9772	2087.168	2068.382	0.9910
5,900	3866.629	3778.296	0.9772	2092.267	2071.637	0.9901
8,000	3873.456	3780.249	0.9759	2101.209	2076.568	0.9883
10,000	3880.281	3781.637	0.9746	2107.277	2079.433	0.9868
12,000	3886.181	3782.680	0.9734	2111.863	2081.382	0.9856
14,000	3891.117	3783.481	0.9723	2115.452	2082.791	0.9846
16,000	3895.242	3784.114	0.9715	2118.338	2083.860	0.9837
18,000	3898.714	3784.622	0.9707	2120.709	2084.695	0.9830
20,000	3901.665	3785.044	0.9701	2122.691	2085.370	0.9824
22,000	3904.199	3785.394	0.9696	2124.373	2085.921	0.9819
24,000	3906.394	3785.694	0.9691	2125.817	2086.385	0.9815
26,000	3908.312	3785.947	0.9687	2127.071	2086.778	0.9811
28,000	3910.002	3786.172	0.9683	2128.170	2087.115	0.9807
30,000	3911.501	3786.364	0.9680	2129.141	2087.408	0.9804
32,000	3912.840	3786.537	0.9677	2130.005	2087.665	0.9801
34,000	3914.042	3786.690	0.9675	2130.779	2087.893	0.9799
36,000	3915.127	3786.828	0.9672	2131.476	2088.096	0.9796
38,000	3916.111	3786.950	0.9670	2132.107	2088.277	0.9794
GSFC SIS	3890.195	3776.410	0.9708	2069.907	2054.460	0.9925
Rayleigh	3911.922	3786.190	0.9679	2126.325	2085.906	0.9810

Table 10. The band responses in picoamperes for SeaWiFS bands 7 and 8 are listed here. The out-of-band response is the difference between the total response (R_T) and the in-band response (R_{IB}). The special spectral shapes, i.e., the GSFC SIS and the Rayleigh Atmosphere are shown at the bottom of the table.

Planck Function Temperature [K]	*Band 7 (765 nm)*			*Band 8 (865 nm)*		
	R_T	R_{IB}	R_{IB}/R_T	R_T	R_{IB}	R_{IB}/R_T
2,000	2908.806	2831.298	0.9734	2254.213	2207.528	0.9793
2,500	2883.359	2823.812	0.9793	2249.117	2200.968	0.9786
2,850	2874.331	2821.321	0.9816	2248.979	2198.295	0.9775
3,000	2871.607	2820.621	0.9822	2249.414	2197.430	0.9769
3,500	2865.465	2819.219	0.9839	2252.214	2195.310	0.9747
4,000	2862.032	2818.650	0.9848	2256.286	2193.943	0.9724
5,000	2858.921	2818.539	0.9859	2266.044	2192.347	0.9675
5,900	2858.048	2818.864	0.9863	2275.286	2191.558	0.9632
8,000	2858.373	2819.874	0.9865	2295.514	2190.655	0.9543
10,000	2859.558	2820.723	0.9864	2311.900	2190.276	0.9474
12,000	2860.844	2821.398	0.9862	2325.586	2190.074	0.9417
14,000	2862.046	2821.938	0.9860	2337.030	2189.956	0.9371
16,000	2863.125	2822.371	0.9858	2346.676	2189.880	0.9332
18,000	2864.080	2822.725	0.9856	2354.884	2189.831	0.9299
20,000	2864.922	2823.020	0.9854	2361.939	2189.796	0.9271
22,000	2865.667	2823.270	0.9852	2368.057	2189.770	0.9247
24,000	2866.329	2823.480	0.9851	2373.408	2189.751	0.9226
26,000	2866.918	2823.665	0.9849	2378.124	2189.736	0.9208
28,000	2867.446	2823.824	0.9848	2382.311	2189.727	0.9192
30,000	2867.922	2823.965	0.9847	2386.050	2189.719	0.9177
32,000	2868.351	2824.087	0.9846	2389.410	2189.710	0.9164
34,000	2868.742	2824.199	0.9845	2392.444	2189.706	0.9153
36,000	2869.097	2824.299	0.9844	2395.197	2189.701	0.9142
38,000	2869.423	2824.387	0.9843	2397.707	2189.698	0.9132
GSFC SIS	2869.275	2820.374	0.9830	2248.207	2196.183	0.9769
Rayleigh	2867.115	2823.305	0.9847	2367.631	2190.131	0.9250

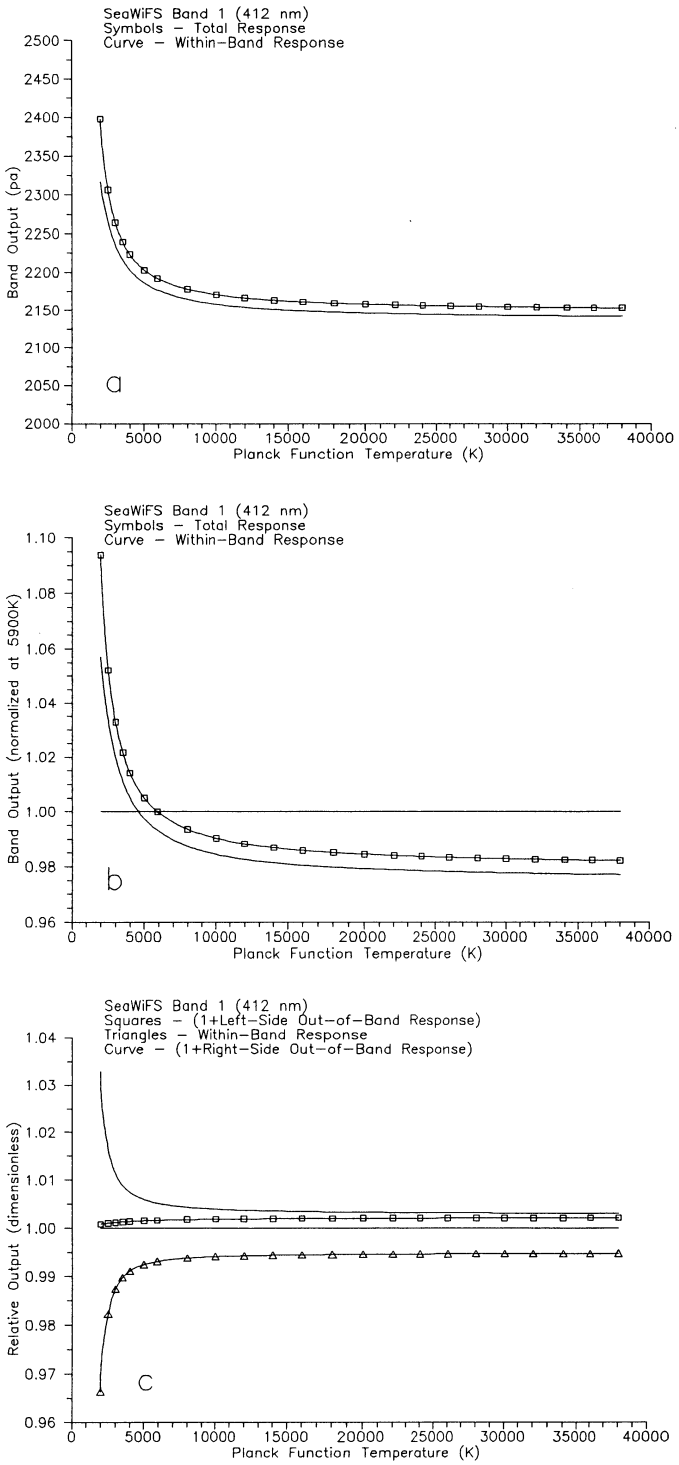

Fig. 11. Instrument responses for SeaWiFS band 1 to Planck functions with temperatures from 2,500–38,000 K. The Planck functions are normalized at 412 nm, the nominal center wavelength for the band. **a)** The total band response and the in-band response are given for band 1. The in-band wavelength range is given in Table 6. **b)** The total band response and the in-band response are given for band 1. The responses are normalized to the total band response at 5,900 K to show response changes from the band in relative terms. **c)** The components of the band response are given in relative terms. The out-of-band responses have been added to unity to place all three components on the same graph. The left side out-of-band response includes all wavelengths that are shorter than the in-band and the right side out-of-band includes all wavelengths that are longer.

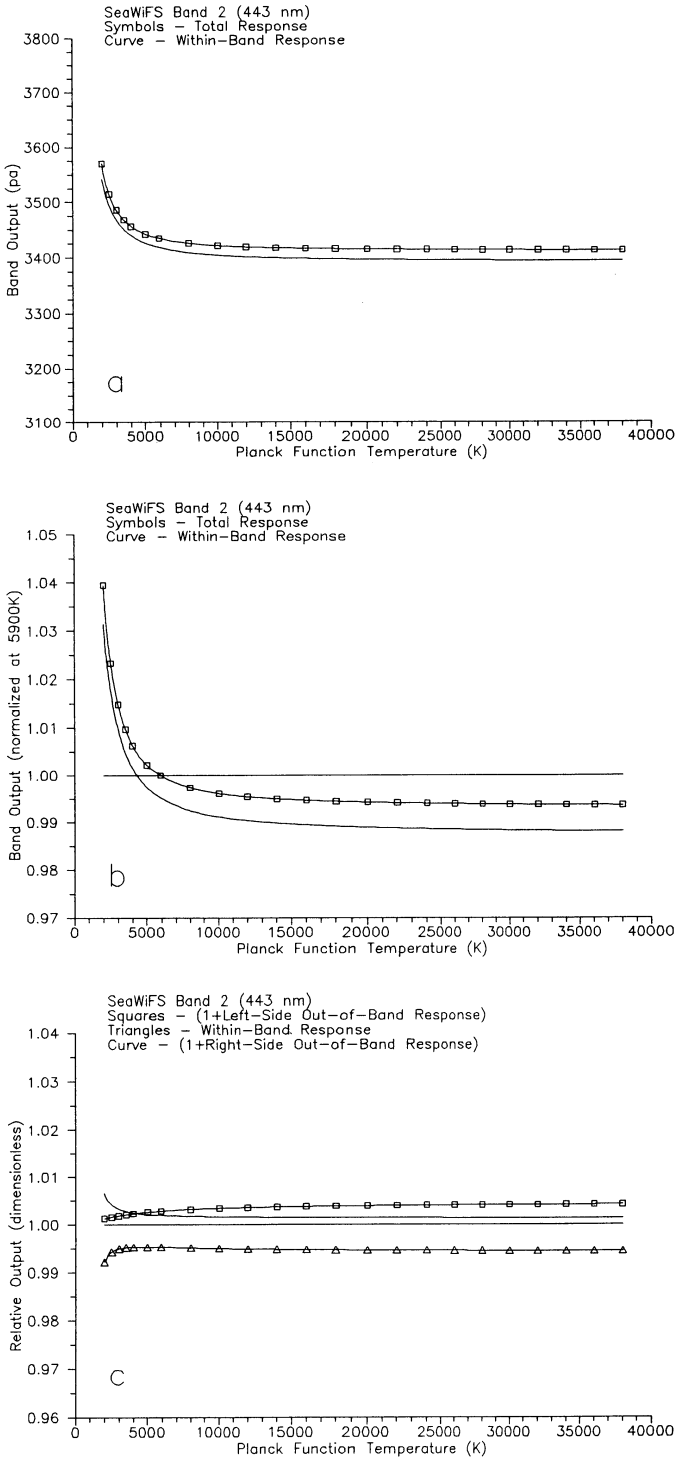

Fig. 12. Instrument responses for SeaWiFS band 2 to Planck functions with temperatures from 2,500–38,000 K. The Planck functions are normalized at 412 nm, the nominal center wavelength for the band. **a)** The total band response and the in-band response are given for band 2. The in-band wavelength range is given in Table 6. **b)** The total band response and the in-band response are given for band 2. The responses are normalized to the total band response at 5,900 K to show response changes from the band in relative terms. **c)** The components of the band response are given in relative terms. The out-of-band responses have been added to unity to place all three components on the same graph. The left side out-of-band response includes all wavelengths that are shorter than the in-band and the right side out-of-band includes all wavelengths that are longer.

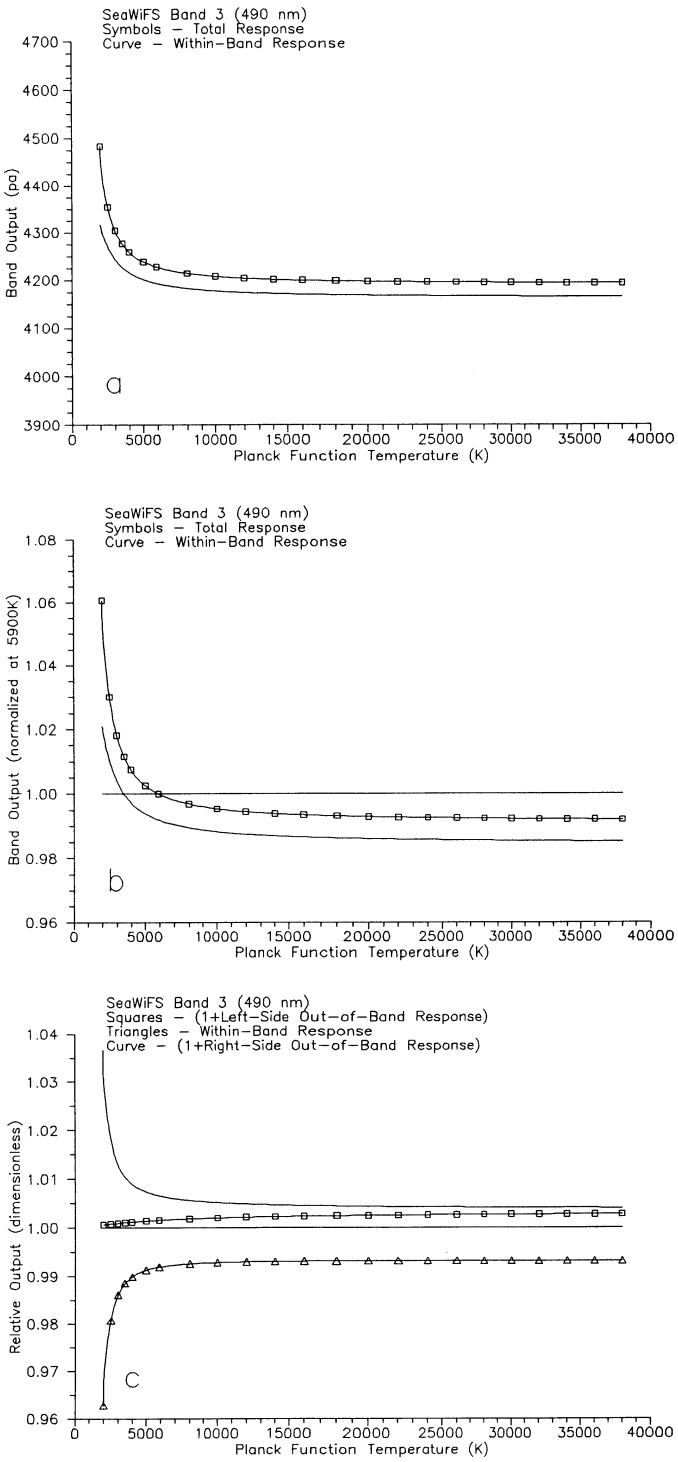

Fig. 13. Instrument responses for SeaWiFS band 3 to Planck functions with temperatures from 2,500–38,000 K. The Planck functions are normalized at 412 nm, the nominal center wavelength for the band. **a)** The total band response and the in-band response are given for band 3. The in-band wavelength range is given in Table 6. **b)** The total band response and the in-band response are given for band 3. The responses are normalized to the total band response at 5,900 K to show response changes from the band in relative terms. **c)** The components of the band response are given in relative terms. The out-of-band responses have been added to unity to place all three components on the same graph. The left side out-of-band response includes all wavelengths that are shorter than the in-band and the right side out-of-band includes all wavelengths that are longer.

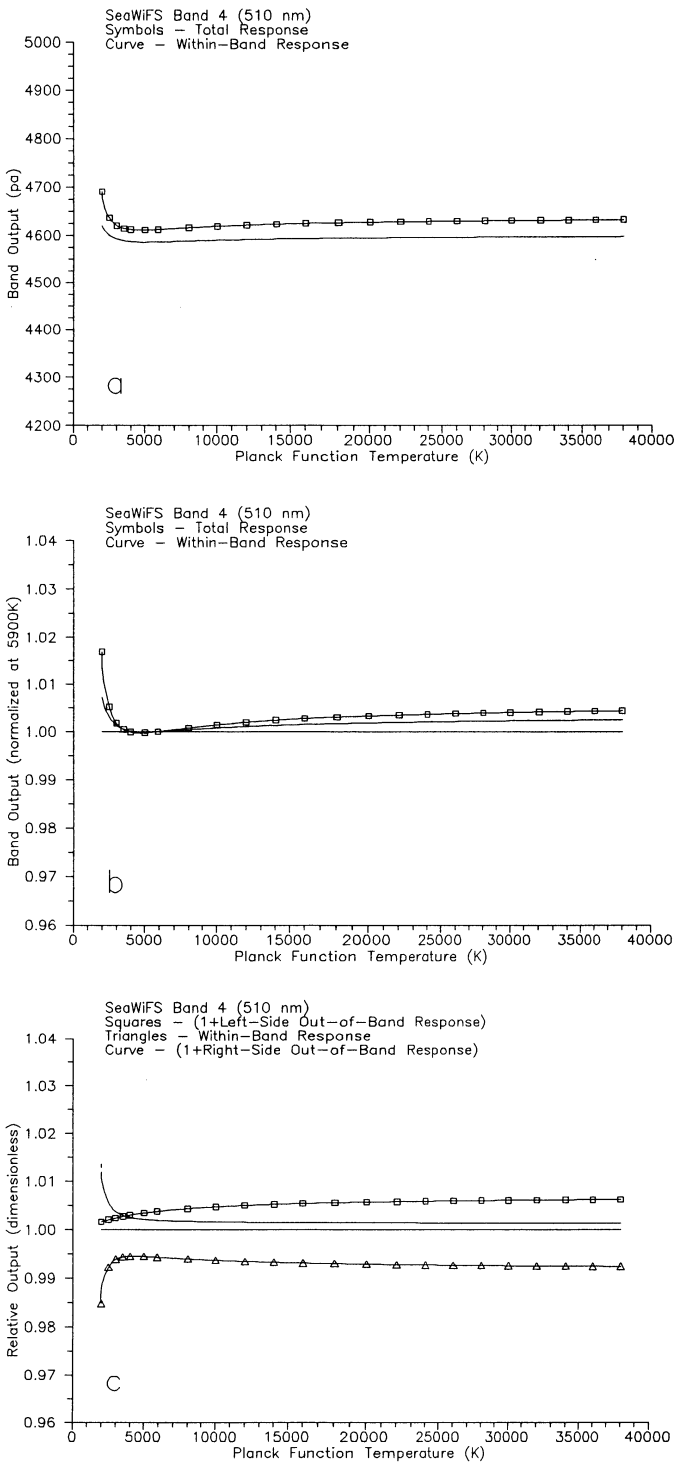

Fig. 14. Instrument responses for SeaWiFS band 4 to Planck functions with temperatures from 2,500–38,000 K. The Planck functions are normalized at 412 nm, the nominal center wavelength for the band. **a)** The total band response and the in-band response are given for band 4. The in-band wavelength range is given in Table 6. **b)** The total band response and the in-band response are given for band 4. The responses are normalized to the total band response at 5,900 K to show response changes from the band in relative terms. **c)** The components of the band response are given in relative terms. The out-of-band responses have been added to unity to place all three components on the same graph. The left side out-of-band response includes all wavelengths that are shorter than the in-band and the right side out-of-band includes all wavelengths that are longer.

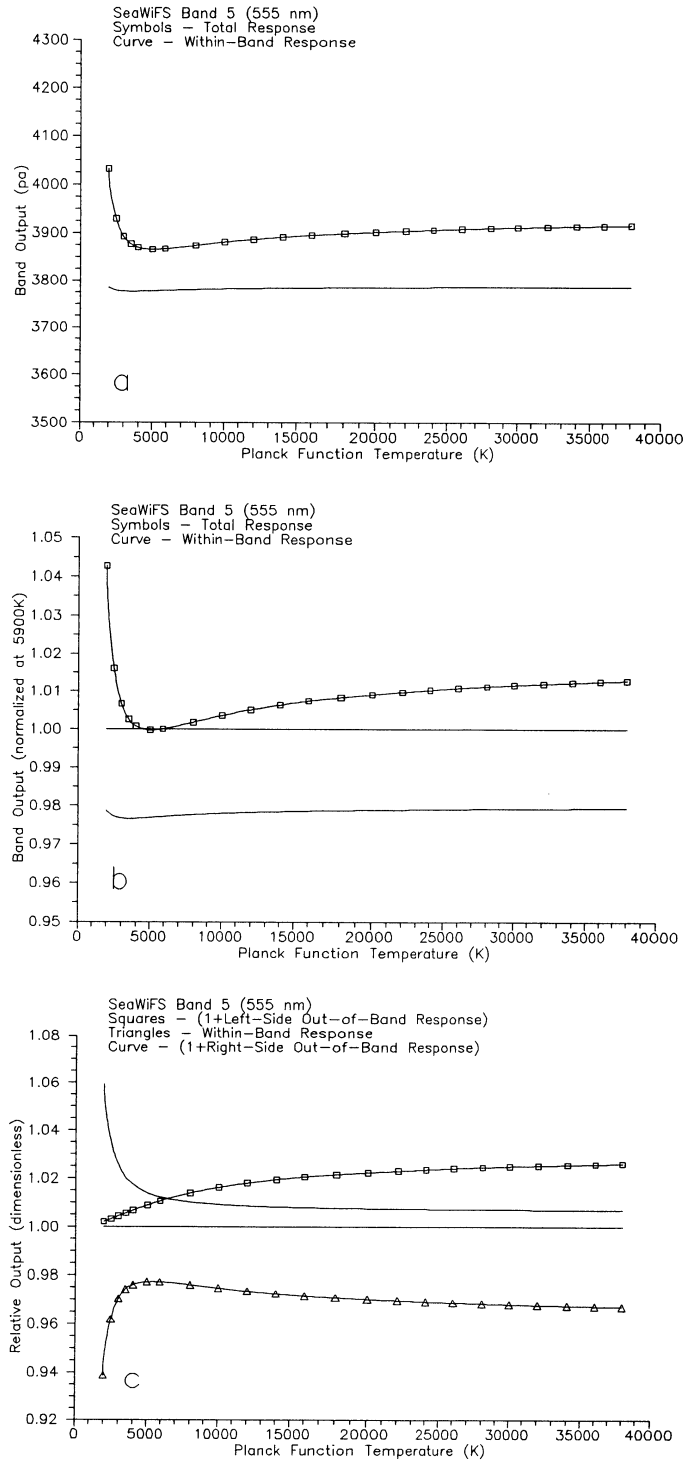

Fig. 15. Instrument responses for SeaWiFS band 5 to Planck functions with temperatures from 2,500–38,000 K. The Planck functions are normalized at 412 nm, the nominal center wavelength for the band. **a)** The total band response and the in-band response are given for band 5. The in-band wavelength range is given in Table 6. **b)** The total band response and the in-band response are given for band 5. The responses are normalized to the total band response at 5,900 K to show response changes from the band in relative terms. **c)** The components of the band response are given in relative terms. The out-of-band responses have been added to unity to place all three components on the same graph. The left side out-of-band response includes all wavelengths that are shorter than the in-band and the right side out-of-band includes all wavelengths that are longer.

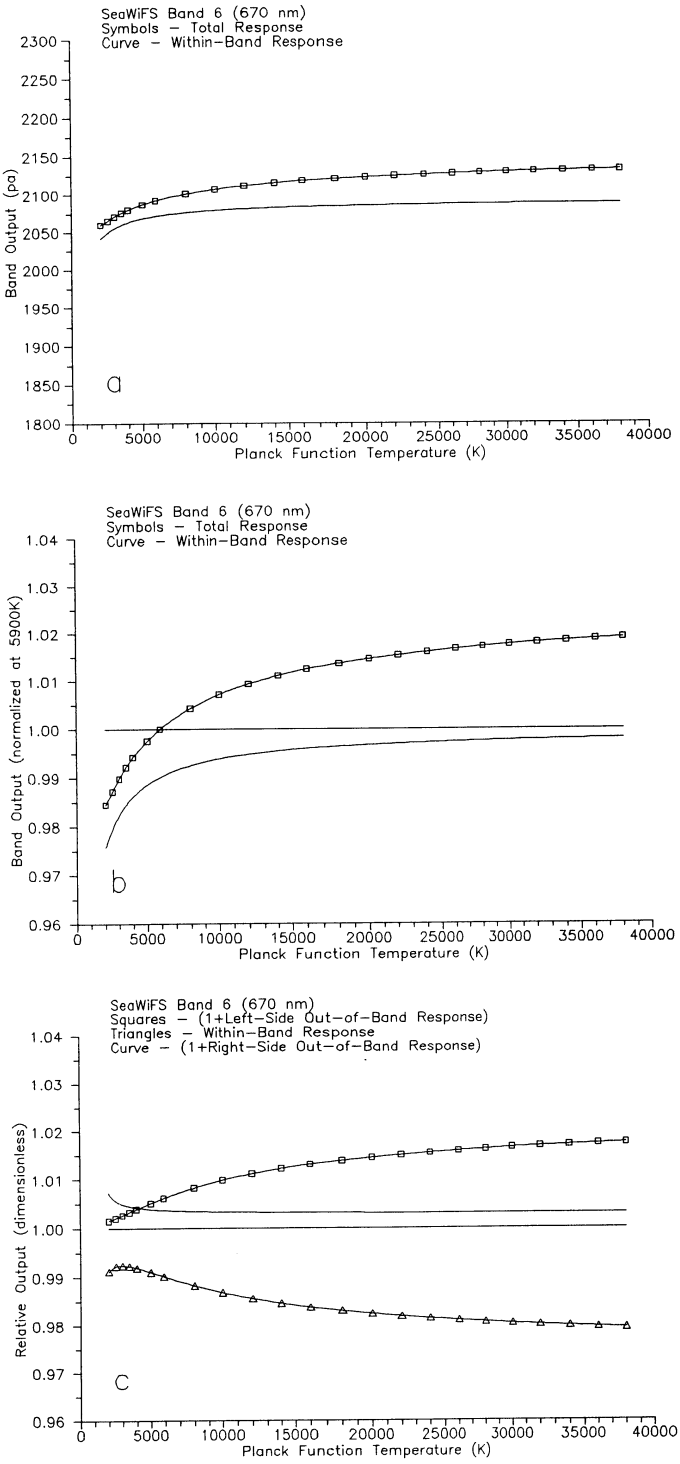

Fig. 16. Instrument responses for SeaWiFS band 6 to Planck functions with temperatures from 2,500–38,000 K. The Planck functions are normalized at 412 nm, the nominal center wavelength for the band. **a)** The total band response and the in-band response are given for band 6. The in-band wavelength range is given in Table 6. **b)** The total band response and the in-band response are given for band 6. The responses are normalized to the total band response at 5,900 K to show response changes from the band in relative terms. **c)** The components of the band response are given in relative terms. The out-of-band responses have been added to unity to place all three components on the same graph. The left side out-of-band response includes all wavelengths that are shorter than the in-band and the right side out-of-band includes all wavelengths that are longer.

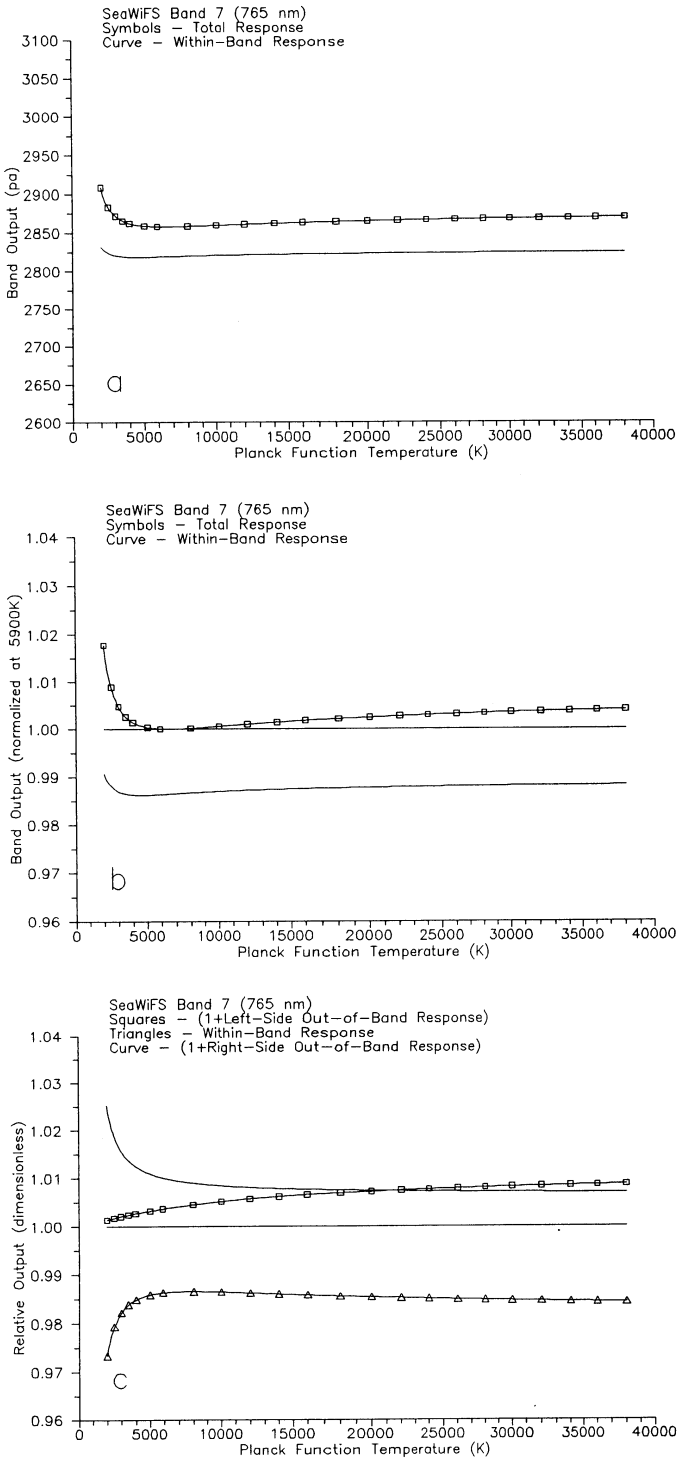

Fig. 17. Instrument responses for SeaWiFS band 7 to Planck functions with temperatures from 2,500–38,000 K. The Planck functions are normalized at 412 nm, the nominal center wavelength for the band. **a)** The total band response and the in-band response are given for band 7. The in-band wavelength range is given in Table 6. **b)** The total band response and the in-band response are given for band 7. The responses are normalized to the total band response at 5,900 K to show response changes from the band in relative terms. **c)** The components of the band response are given in relative terms. The out-of-band responses have been added to unity to place all three components on the same graph. The left side out-of-band response includes all wavelengths that are shorter than the in-band and the right side out-of-band includes all wavelengths that are longer.

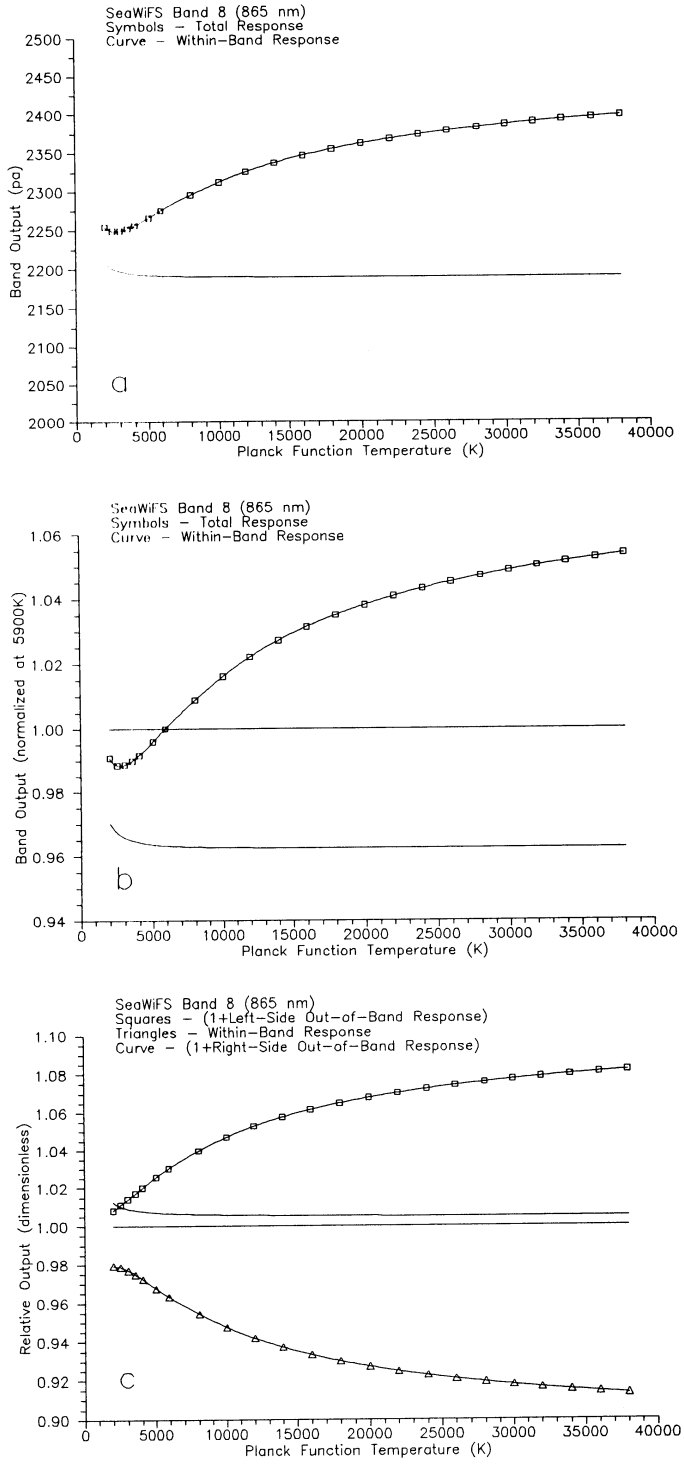

Fig. 18. Instrument responses for SeaWiFS band 8 to Planck functions with temperatures from 2,500–38,000 K. The Planck functions are normalized at 412 nm, the nominal center wavelength for the band. **a)** The total band response and the in-band response are given for band 8. The in-band wavelength range is given in Table 6. **b)** The total band response and the in-band response are given for band 8. The responses are normalized to the total band response at 5,900 K to show response changes from the band in relative terms. **c)** The components of the band response are given in relative terms. The out-of-band responses have been added to unity to place all three components on the same graph. The left side out-of-band response includes all wavelengths that are shorter than the in-band and the right side out-of-band includes all wavelengths that are longer.

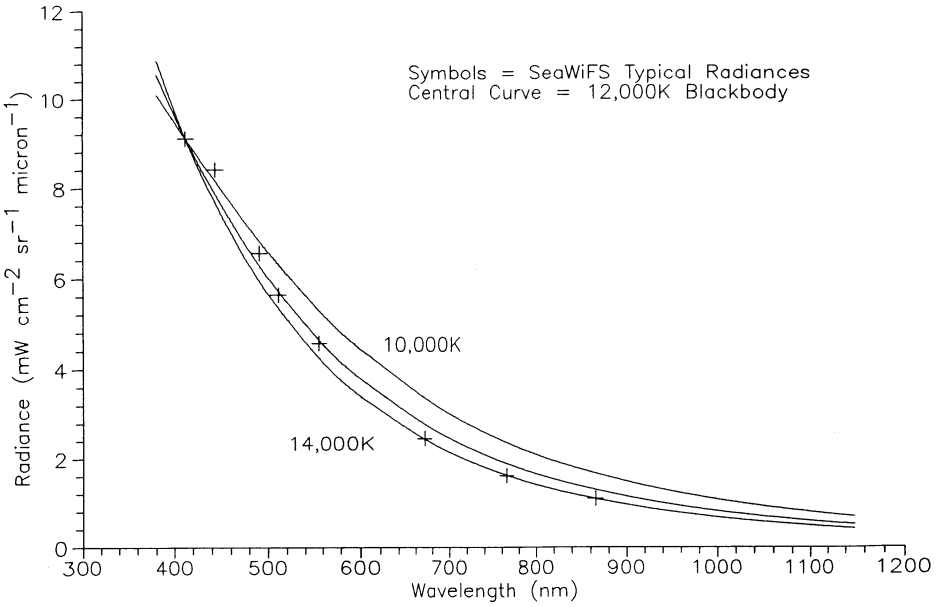

Fig. 19. Typical input radiances from SeaWiFS plotted with three blackbody radiance curves.

response, that is, the response for wavelengths greater than the long wavelength 1% response point. The terms "left side" and "right side" refer to locations on a plot of the band spectral response [see Fig. 2a of Barnes (1996a), for example]. In that type of plot, wavelength increases from left to right along the abscissa. Part c gives the out-of-band components after they have been added to unity. This allows the presentation of each of the three components on the same plot with the same vertical resolution. Thus, Fig. 11c shows the right-side out-of-band response for band 1 to be 1.033 at a Planck temperature of 2,000 K. With the subtraction of unity, the right-side out-of-band response for band 1 is about 3.3% of the total response at 2,000 K. At this blackbody temperature, the in-band response is 0.966.

For SeaWiFS bands 1, 2, 3, 4, and 7, Figs. 11c, 12c, 13c, 14c, and 17c, respectively, show that for Planck temperatures from 10,000–38,000 K, the in-band response is a constant fraction of the total response. For these bands and for these blackbody temperature ranges, changes in the left-side and right-side out-of-band responses are small, equal in magnitude, and opposite in sign, creating a summation for out-of-band that is a constant fraction of the total band response. For on-orbit SeaWiFS measurements, the out-of-band responses for bands 1, 2, 3, 4, and 7 can be considered as constant fractions of the total band responses.

For SeaWiFS bands 5, 6, and 8, Figs. 15c, 16c, and 18c show less constancy for the in-band output for Planck function temperatures from 10,000–38,000 K. For band 5, the fractional in-band decrease is 0.7% from 10,000–38,000 K; for band 6, 0.7%; and for band 8, 3.4%. For comparisons of Figs. 15c (band 5), 16c (band 6), and 18c (band 8), it should be noted that the ordinates for these figures range from 0.92–1.08, 0.96–1.04, and 0.90–1.10, respectively. With significant band-to-band differences in the band responses, it was not practical to place all of the plots on the same vertical scales.

Band 8 is the keystone for the SeaWiFS atmospheric correction (Gordon and Wang 1994). As a result, an accurate and well-defined out-of-band correction for this band is crucial for SeaWiFS data reduction. Band 8 also shows the greatest change in the size of its out-of-band with source spectral shape. The out-of-band correction for band 8 cannot be based on Planck function curves alone, but must be based on the spectrum of the on-orbit radiance viewed by SeaWiFS.

2.4 ON-ORBIT SPECTRAL SHAPE

For SeaWiFS ocean measurements, the spectral shape of the upwelling radiances will resemble that for the typical (L_{typical}) radiances from the SeaWiFS specifications (Barnes et al. 1994a). Those L_{typical} are shown in Fig. 19,

Table 11. The initial out-of-band correction factors are listed here. For bands 1–4 and band 7, these are also the final correction factors. The calculation of the final correction factors for bands 5, 6, and 8 uses these initial values as input data.

Band Number	*Nominal Center Wavelength [nm]*	$k(\mathrm{b})$	*Comments*
1	412	0.9943	Final value, also taken from Table 7, 12,000 K
2	443	0.9949	Final value, also taken from Table 7, 12,000 K
3	490	0.9930	Final value, also taken from Table 8, 12,000 K
4	510	0.9934	Final value, also taken from Table 8, 12,000 K
5	555	0.9734	Final value calculated using (9)
6	670	0.9856	Final value calculated using (12)
7	765	0.9844	Final value, also taken from Table 10, 12,000 K and corrected for oxygen absorption (Section 2.5.2, below)
8	865	0.9417	Final value calculated using (14)

along with a set of three Planck function curves. Although not a perfect fit, the L_{typical} radiances are approximated by a 12,000 K blackbody. As shown in Tables 7–10, the responses of the SeaWiFS bands are nearly identical for Planck function curves of 10,000 K; 12,000 K; and 14,000 K. For the purposes here, it is assumed that the typical SeaWiFS radiances for ocean measurements have the spectral shape of a 12,000 K blackbody.

2.5 OUT-OF-BAND CORRECTION

2.5.1 Bands 1–4

Tables 7 and 8 show the ratios of the in-band to the total-band responses (for bands 1–4) to be about 0.990–0.995 for blackbody spectral curves between 12,000 K and 38,000 K. For each of these bands, the change in the out-of-band correction factor is negligible—between 12,000 K and 38,000 K; thus, for bands 1–4 the 12,000 K correction factor is used in the simplified correction scheme proposed here (Table 11). As shown for band 1 (412 nm), the out-of-band correction is applied using the formula:

$$L_o(412) = k_{\mathrm{b}}(412) L_i(412), \tag{5}$$

where $L_i(412)$ is the input radiance to the correction scheme for band 1 (412 nm); $k_{\mathrm{b}}(412)$ is the out-of-band correction factor for band 1 (412 nm); and $L_o(412)$ is the output radiance from the correction scheme for band 1 (412 nm). It is the k_{b} correction factor for each SeaWiFS band that this simplified calculation scheme provides. For bands 1–4, k_{b} is a constant value, listed in Table 11.

For the SeaWiFS Project, there is a naming convention for the radiances from the eight bands. In this convention, the bands are not described in terms of their number (1 through 8) but in terms of their nominal center wavelength (412, 443, 490, 510, 555, 670, 765, and 865 nm). This convention is also applied in the equations used here.

2.5.2 Band 7

For SeaWiFS band 7 (the 765 nm band), there is an atmospheric oxygen absorption feature in the center of the pass band response (McClain et al. 1994, Fraser 1995, and Ding and Gordon 1995). This oxygen A-band absorption does not effect the out-of-band response for the 765 nm band. Using the same technique, McClain et al. (1994) and Fraser (1995) both estimated the reduction in the output of band 7 from this absorption feature to be 12% for an air mass of 2, and 13% for an air mass of 3. Ding and Gordon (1995) used a separate calculation to estimate the reduction in Rayleigh scattered light at the top of the atmosphere from oxygen absorption to be 7% for an air mass of 2, and 11% for an air mass of 5. Because the out-of-band contribution to the output of band 7 is close to zero (about 1.5%), the error in the calculated effect of oxygen absorption on the out-of-band correction is also small. For the calculations here, oxygen absorption is assumed to decrease the in-band response of SeaWiFS band 7 by 12%.

The modification of band 7's correction factor, $k_{\mathrm{b}}(765)$, is shown in Table 12. In this table, the total band, the in-band, and the out-of-band responses (for a 12,000 K blackbody) were taken from Table 10. The effect of oxygen absorption was calculated by removing 12% from the in-band response (338.568 pA) and by removing the same number of picoamperes from the total band response. The out-of-band response remains constant. The revised out-of-band correction factor is calculated as the ratio of the revised in-band response to the revised total response. That ratio is 0.9844, and this value is given in Table 11 for the band 7 correction, $k_{\mathrm{b}}(765)$. Thus, the out-of-band correction for band 7 is:

$$L_o(765) = k_{\mathrm{b}}(765) L_i(765), \tag{6}$$

where $L_o(765)$ is the output from this correction scheme for band 7. The correction to this band for oxygen A-band absorption is applied as part of the atmospheric correction algorithms in the SeaWiFS data reduction process.

$L_o(765)$ provides the input to that process for band 7. However, for use with the band 8 (865 nm) out-of-band correction below, the oxygen notch is replaced, using the equation

$$L_c(765) = 1.12\Big[L_o(765)\Big] \tag{7}$$

where $L_c(765)$ is the band 7 spectral radiance corrected for oxygen A-band absorption.

Table 12. The band 7 out-of-band correction factor, modified for the out-of-band response is presented. The effect of this modification is minimal. The total band response values are taken from Table 10. The units are in picoamperes [pA]. In the second row, 338.658 pA are removed from the R_T and R_{IB} to account for oxygen absorption.

R_T *Values*	R_{IB} *Values*	R_{OB} *Values*	$k_{\rm b}(765)$
2860.844	2821.398	39.446	0.9862
2522.296	2482.830	39.446	0.9844

2.5.3 Band 8

The simplified, out-of-band calculation for SeaWiFS band 8 uses the relative spectral response of the band divided into six components (Fig. 20). Each component gives the output of the band for a spectrally flat source over a wavelength subset of the band's relative spectral response. Component S_5 gives the in-band response for the 865 nm band, covering the wavelength range from 827–907 nm (Table 13). For a spectrally flat source, the out-of-band correction for band 8 is the response of component (S_5) divided by the summed response for all six components (S_1 through S_6). For on-orbit calculations, the measured radiances from the SeaWiFS bands are included in the band 8 out-of-band correction. In addition, an estimate of the radiance to be paired with component S_6 is obtained before the correction can be calculated.

In these calculations, each component of the band 8 spectral response is associated with the radiance from a SeaWiFS band: component S_1 with band 1, $L_o(412)$; component S_2 with band 4, $L_o(510)$; component S_3 with band 5, $L_o(555)$; component S_4 with band 7, $L_o(765)$; component S_5 with band 8, $L_o(865)$; and component S_6 with an estimate for the radiance at 965 nm, $L_o(965)$.

The calculation scheme starts with initial output radiances for the SeaWiFS bands, $L_o(412)$ through $L_o(865)$, calculated using the form of (5). For band 7, $L_c(765)$ is used. Finally, the radiance at 965 nm is calculated using an extrapolation based on the radiances at 765 nm and 865 nm as in,

$$L_o(965) = 2\Big[L_o(865)\Big] - L_o(765). \tag{8}$$

The selection of 965 nm for the radiance associated with component S_6 was made to correspond with the 100 nm spacing between bands 7 and 8. This selection is arbitrary and is based on the judgement of the authors.

With these values, it is possible to calculate the revised out-of-band correction factor, which is the in-band response divided by the sum of the responses for all six components. The new $k_{\rm b}(865)$ replaces the initial $k_{\rm b}(865)$ from Table 11,

$$k_{\rm b}(865) = \frac{L_o(865)S_5}{W} \tag{9}$$

where W represents the denominator to (9),

$$\begin{aligned} W &= L_o(412)S_1 + L_o(510)S_2 + L_o(555)S_3 \\ &+ L_c(765)S_4 + L_o(865)S_5 + L_o(965)S_6 \end{aligned}, \tag{10}$$

and a new output radiance is calculated for band 8

$$L_o(865) = k_{\rm b}(865)L_i(865). \tag{11}$$

2.5.4 Bands 5–6

The correction calculations for bands 5 and 6 (555 nm and 670 nm) are simplified versions of that for band 8. For these bands, the corrections are calculated, using only three components. Those components are listed in Tables 14 and 15. For bands 5 and 6, the out-of-band correction factors vary by less than 1% for blackbody curves between 12,000 K and 38,000 K. This is less than a third of the change in the correction factor for band 8. In addition, the relative magnitudes of the out-of-band responses for these bands are one-third to one-half those for band 8.

For bands 5 and 6, the relative spectral response is divided into a short wavelength (left-side) out-of-band, an in-band, and a long wavelength (right-side) out-of-band response. Figures 11 and 12 show the right-side out-of-band to contribute a nearly constant fraction of the band response for these bands for Planck function temperatures from 12,000–38,000 K. The variability in the out-of-band correction comes from the left-side, or shorter wavelength, contribution.

For band 6, the spectral response is shown in Fig. 23 of Barnes et al. (1994b), and the tabulated values are given in Barnes (1994). The three components of the band 6 spectral response are separated at the extended band edges (Table 6). The components for this band (Table 14) are associated with three SeaWiFS bands: component S_7 with band 3, $L_o(490)$; component S_8 with band 6, $L_o(670)$; and component S_9 with band 8, $L_o(865)$. The calculation of the out-of-band correction for band 6 provides a new $k_{\rm b}(670)$ to replace the initial value from Table 11:

$$k_{\rm b}(670) = \frac{L_o(670)S_8}{L_o(490)S_7 + L_o(670)S_8 + L_o(865)S_9} \tag{12}$$

and the calculation of a new output radiance for the band.

$$L_o(670) = k_{\rm b}(670)L_i(670). \tag{13}$$

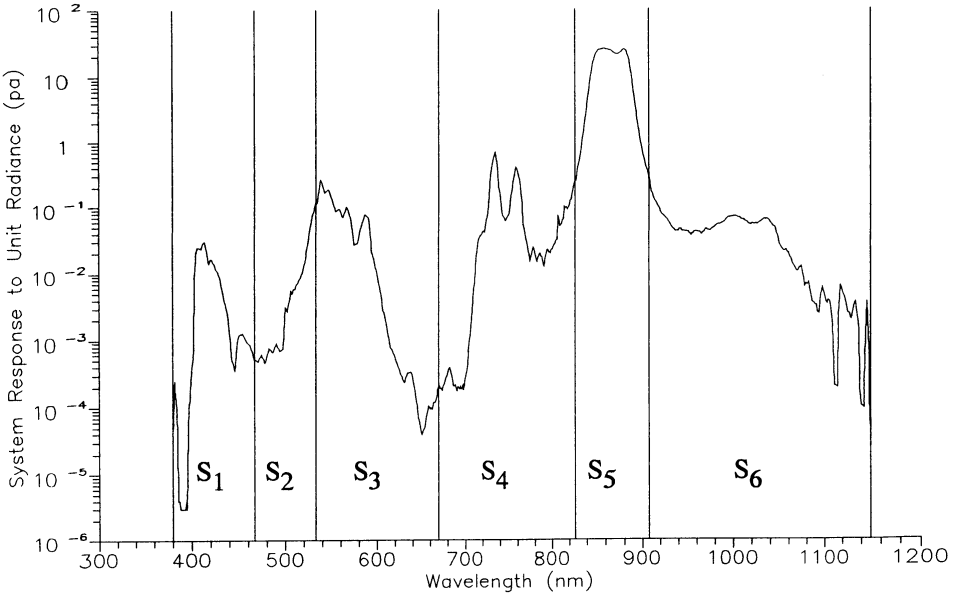

Fig. 20. Six components of the spectral response for SeaWiFS band 8 are shown. The component S_5 contains the in-band response.

Table 13. The spectral response of band 8 is divided into six components. The spectral responses are given for a spectrally flat source, that is, a source with a radiance of $1\,\mathrm{mW\,cm^{-2}\,sr^{-1}\mu\,m^{-1}}$.

Symbol	*Value*	*Description*
S_1	0.583	Out-of-band spectral response (380–466 nm)
S_2	0.829	Out-of-band spectral response (467–532 nm)
S_3	6.251	Out-of-band spectral response (533–669 nm)
S_4	13.533	Out-of-band spectral response (670–826 nm)
S_5	1013.592	In-band spectral response (827–907 nm)
S_6	9.374	Out-of-band spectral response (908–1,150 nm)

Table 14. The spectral response of band 6 is divided into three components. The spectral responses are given for a spectrally flat source, that is, a source with a radiance of $1\,\mathrm{mW\,cm^{-2}\,sr^{-1}\mu\,m^{-1}}$.

Symbol	*Value*	*Description*
S_{10}	2.592	Out-of-band spectral response (380–646 nm)
S_{11}	491.802	In-band spectral response (647–692 nm)
S_{12}	2.112	Out-of-band spectral response (693–1,150 nm)

Table 15. The spectral response of band 5 is divided into three components. The spectral responses are given for a spectrally flat source, that is, a source with a radiance of $1\,\mathrm{mW\,cm^{-2}\,sr^{-1}\mu\,m^{-1}}$.

Symbol	*Value*	*Description*
S_7	5.261	Out-of-band spectral response (380–536 nm)
S_8	488.215	In-band spectral response (537–577 nm)
S_9	7.475	Out-of-band spectral response (578–1,150 nm)

The calculation of the out-of-band correction for band 5 follows the pattern for band 6. For band 5, the spectral response is also shown in Fig. 23 of Barnes et al. (1994b), and the tabulated values are also given in Barnes (1994). The three components of the band 5 spectral response are also separated at the extended band edges (Table 6), and the components for this band (Table 15) are associated with three SeaWiFS bands: component S_{10} with band 2, $L_o(443)$; component S_{11} with band 5, $L_o(555)$; and component S_{12} with band 6, $L_o(670)$. The calculation of the out-of-band correction for band 5 provides a new $k_{\rm b}(555)$ to replace the initial value from Table 11:

$$k_{\rm b}(555) = \frac{L_o(555)S_{11}}{L_o(443)S_{10} + L_o(555)S_{11} + L_o(670)S_{12}}, \quad (14)$$

and the calculation of a new output radiance for the band.

$$L_o(555) = k_{\rm b}(555)L_i(555). \quad (15)$$

2.6 COMPARISON OF RESULTS

For comparison, out-of-band corrections were calculated using the SeaWiFS typical radiances. The calculations were done in two ways: using the method of Barnes et al. (1995a) and using the simplified method presented here. The results of the two sets of calculations are presented in Table 16. The two sets of corrections should be nearly identical, since they are based on the same set of radiances. The agreement in the comparison is good, with corrections for seven of the eight bands that agree within 0.1%.

For band 1, the difference is 0.2%. This is due, in part, to the estimate of the spectral source shape for the wavelength range from 380–412 nm in the two calculations. This difference can be seen in Figs. 8 and 9 of Barnes et al. (1995a). The method of Barnes et al. (1995a) assumes a constant source radiance for wavelengths shorter than 412 nm. The simplified method assumes a source radiance that increases with decreasing wavelength below 412 nm. This tends to give the simplified method slightly more out-of-band response from the left side (shorter wavelengths). For such a small difference, the authors feel it is appropriate to split the difference and use an out-of-band correction for band 1, i.e., 0.9953, for the simplified technique.

For band 7, the calculations using the method of Barnes et al. (1995a) do not include oxygen A-band absorption. Such an atmospheric effect was not a consideration in that paper; thus, the comparison in Table 16 uses the result from the simplified method without the correction for oxygen absorption. The difference is small; however, it is recommended that when using the correction technique of Barnes et al. (1995a), a correction of 0.0018 should be added to the result for band 7.

Table 16. Out-of-band corrections for the SeaWiFS typical using the method of Barnes et al. (1995a) and those using the simplified method presented here. Note that the corrections for band 7 have been applied without the oxygen absorption notch.

Band Number	*Barnes et al. (1995a)*	*Simplified Method*
1	0.9963	0.9943
2	0.9946	0.9949
3	0.9928	0.9930
4	0.9928	0.9934
5	0.9729	0.9721
6	0.9843	0.9842
7	0.9863†	0.9862†
8	0.9414	0.9418

† Calculated without oxygen absorption.

The two recommendations in this section are small and of little consequence; however, they are easy to apply and take very little time in the data reduction. Overall, the simplified calculation method reduces computation time by more than two orders of magnitude, compared to the method of Barnes et al. (1995a).

2.7 TOTAL BAND RESPONSES

The SeaWiFS prelaunch radiometric calibration (see Barnes et al. 1994b) provided an adjustment to the laboratory calculation of the instrument. In the laboratory, SeaWiFS was calibrated using a source with the spectral shape of a 2,850 K blackbody, while measurements on orbit will have a spectral shape that is much more blue. The adjustment in Barnes et al. (1994b) was based on a 5,900 K blackbody, the only spectral shape given in the SeaWiFS specifications (Barnes et al. 1994a).

Figure 19 shows the on-orbit spectral shape to be close to that for a 12,000 K blackbody. It is the adjustment for this spectral shape that should be included in the SeaWiFS radiometric calibration. The appropriate adjustments for total band response are given in Table 17. For band 1, the adjustment in Table 17 differs from that in Barnes et al. (1994b) by 1%. For the other bands, the differences in the adjustments are less. A 1% factor is significant, if the calibrations of the SeaWiFS bands are to be made consistent at the 2% level.

2.8 CONCLUDING REMARKS

For SeaWiFS, the conversion of the spectral shape dependence in the SeaWiFS laboratory calibration to orbit is done in two steps. First, the total band responses are converted to those for a source spectral shape representative of the Earth-exiting radiances viewed during ocean measurements on orbit. Second, the residual in-band response is calculated after the removal of the out-of-band response.

The first step is described in Section 2.7, and the second step in Section 2.5. Both conversions are done in relative terms. There are no absolute values in the spectral shape dependencies calculated here.

Table 17. Shown here are the model results of the band responses to a 2,850 K blackbody and a 12,000 K blackbody (in picoamperes) for the SeaWiFS bands. The ratio gives the total band output on orbit relative to that in the laboratory. Thus, on orbit, SeaWiFS band 1 will produce fewer counts per unit radiance than it will in the laboratory.

Band Number	*2,850 K Blackbody*	*12,000 K Blackbody*	*Ratio*
1	2274.303	2166.343	0.9525
2	3492.898	3419.122	0.9789
3	4315.636	4203.993	0.9741
4	4623.705	4621.536	0.9995
5	3900.117	3886.181	0.9964
6	2069.400	2111.836	1.0205
7	2874.331	2860.844	0.9953
8	2248.979	2325.586	1.0341

The calculations presented here use the actual spectral responses of the SeaWiFS bands and Planck functions as simplified models of the Earth-exiting radiances to be viewed on orbit. For example, the Planck functions do not include the absorption and emission lines from atmospheric gasses, including the oxygen A-band absorption lines at 761 and 763 nm. The effect of this absorption feature on the out-of-band response of band 8 was examined, since band 8 has the greatest out-of-band response of the SeaWiFS bands and since the oxygen absorption lines occur in a region of maximum out-of-band response for band 8 (Fig. 20). For air masses of five or less, the fractional decrease in the response of band 8 is 0.1% or less. For the other SeaWiFS bands, the effects of atmospheric oxygen A-band absorption are much smaller. Atmospheric absorption and emission features do not expand the residual uncertainties in the corrections presented here. They remain at about 0.2%, both for total and out-of-band response.

Studies of atmospheric effects on ocean color imagery, e.g., Ding and Gordon (1995), used detailed models of the atmospheric and oceanic contributors to the top-of-the-atmosphere radiances, but used a simplified model of the response of the instrument. For Ding and Gordon (1995), SeaWiFS band 7 was assumed to have a square wave response with wavelength, with the band response outside of the band edges (the 50% response points) set to zero and the response inside the band edges set to a constant value.

It is now possible to combine the actual response of the SeaWiFS instrument with detailed models of the atmosphere and ocean, since ocean color imagery from SeaWiFS is an amalgam of the top-of-the-atmosphere radiances and the instrument. In the concept of Evans and Gordon (1994), however, the imagery derives from the ocean atmosphere instrument system.

Chapter 3

A Comparison of the Spectral Responses of SeaWiFS and the SeaWiFS Transfer Radiometer

Robert A. Barnes
General Sciences Corporation
Laurel, Maryland

Abstract

Both SeaWiFS and the SXR are filter radiometers with finite bandwidths. The use of these instruments requires a knowledge of the effects that finite bandwidths cause. These effects also depend on the source's spectral shape, which the instruments measure. For the radiometric calibration of SeaWiFS, the source is the GSFC SIS. The BSRs and the ECWs for SeaWiFS and the SXR, when measuring the GSFC SIS, are presented here. They will be needed to convert the SXR measured spectral radiances to the SeaWiFS wavelengths.

3.1 INSTRUMENT MODELS

Six of the SeaWiFS bands have bandwidths (full-width at half-maximum) of 20 nm; the other two have bandwidths of 40 nm (Barnes et al. 1994a). These bandwidths are sufficiently wide to cause the output from SeaWiFS to be dependent on the spectral shape of the source it measures. On orbit, the measurements from each SeaWiFS band involve a range of wavelengths:

$$L_e = \int_0^\infty L_e(\lambda) R(\lambda) d\lambda, \tag{16}$$

where $L_e(\lambda)$ is the Earth-exiting spectral radiance at wavelength λ, and $R(\lambda)$ is the spectral response of the band at wavelength λ. By this definition, L_e is the Earth-exiting spectral radiance *integrated* over the SeaWiFS spectral response.

For the SeaWiFS Project, spectral radiance is expressed in $\mathrm{mW\,cm^{-2}\,sr^{-1}\,\mu\,m^{-1}}$. For SeaWiFS measurements on orbit, the spectral shape of the Earth-exiting radiance is never known exactly. The calibration of the instrument is forced to use approximations to that on-orbit spectral radiance. A study of several spectral approximations can be found in Barnes and Yeh (1996).

The output from each SeaWiFS band is the solution of the integral in (16), plus the inclusion of several multiplicative constants that have no spectral dependence. For the SeaWiFS Project, radiance, i.e., the solution to (16), is expressed in $\mathrm{mW\,cm^{-2}\,sr^{-1}}$. For most uses of the SeaWiFS measurements, the radiance for each band must be expressed in a form that represents the spectral radiance from the source at a given wavelength. This representation will be discussed below.

The spectral response of each band is given in terms of milliamperes of current from the photodiode in the detector per unit of spectral radiance. The photodiode performs the integration for the instrument. It converts the integral in (15) into an electric current. The electronics within the instrument convert this current into volts and then into digital counts. These conversions are multiplicative with no spectral dependence.

There are practical limits to the wavelength ranges of the spectral responses of the SeaWiFS bands. Outside of those wavelength limits, the responses of the bands are next to zero. For example, there is a limited wavelength range over which the silicon photodiodes respond to incoming flux (see Fig. 11 of Barnes et al. 1994b). In the laboratory characterization of SeaWiFS, the wavelength interval over which the band spectral responses have been determined extends from 380–1,150 nm. For most of this interval, the responses of the individual bands are effectively zero (Barnes et al. 1994b).

For the laboratory calibration of SeaWiFS, the spectral shape of the radiance from the source, i.e., from the GSFC SIS, is known (Barnes 1996a). In the laboratory, therefore, the measurement of the sphere radiance by a SeaWiFS band can be expressed as

$$L_s = \int_{380}^{1150} L_s(\lambda) R(\lambda) d\lambda, \tag{17}$$

where $L_s(\lambda)$ is the spectral radiance from the integrating sphere at wavelength λ. As used here, $L_s(\lambda)$ and $R(\lambda)$ are normalized values—normalized to unity at their maximum values. L_s is the sphere spectral radiance *integrated* over the SeaWiFS spectral response.

For SeaWiFS and for several other satellite instruments managed at GSFC, there is a distinction made between in-band and out-of-band response from the instrument. The in-band response is defined as the integrated response between the 1% transmission points for each band (Barnes et al. 1994a). Since the spectral shape of the source and the spectral response of the individual SeaWiFS bands are known, it is possible to calculate the fraction of the instrument response that comes from outside of the 1% transmission points. In this manner, it is possible, for a given source spectral shape, to calculate the fraction of the total response for a given band that is in-band and the fraction that is out-of-band (see for example, Barnes and Yeh 1996). The in-band and out-of-band distinction is made here. With the removal of the out-of-band response, that is, with the removal of a few percent of the total band response, the measurement of the integrating sphere by SeaWiFS is given by:

$$L_s = \int_{\lambda_1}^{\lambda_2} L_s(\lambda) R(\lambda) d\lambda, \tag{18}$$

where λ_1 and λ_2 are the lower and upper 1% transmission points for the band, respectively.

Using (18), it is possible to calculate the BSR, using $R(\lambda)$ as the weighting function:

$$L_{\mathrm{B}}(\lambda_{\mathrm{B}}) = \frac{\int_{\lambda_1}^{\lambda_2} L_s(\lambda) R(\lambda) d\lambda}{\int_{\lambda_1}^{\lambda_2} R(\lambda) d\lambda}, \tag{19}$$

where $L_{\mathrm{B}}(\lambda_{\mathrm{B}})$ is the BSR for the band.

In a similar manner, the BCW associated with this spectral radiance can be calculated, using $L_s(\lambda)R(\lambda)$ as the weighting function.

$$\lambda_{\mathrm{B}} = \frac{\int_{\lambda_1}^{\lambda_2} \lambda L_s(\lambda) R(\lambda) d\lambda}{\int_{\lambda_1}^{\lambda_2} L_s(\lambda) R(\lambda) d\lambda}, \tag{20}$$

where λ_{B} is the BCW.

Alternately, it is possible to define an ECW for each band, λ_{eff}, which is the wavelength where $L_s(\lambda)$ equals $L_{\mathrm{B}}(\lambda_{\mathrm{B}})$. The ECW can be applied to sources that are *well behaved* spectrally, that is, to sources whose spectral radiance increases or decreases monotonically between the 1% response points for each band. In this regard, the GSFC sphere is a well behaved source.

For an instrument that measures with infinitely narrow bandwidths, λ_{B} and λ_{eff} are the same; however, for SeaWiFS and the SXR, the spectral bandwidths are finite. The calculated center wavelengths are different for the two methods. For the SXR, the differences are very small. The results from both calculation methods are given below.

The comparisons presented here will use the relative spectral response (RSR) for the SXR, the RSR for SeaWiFS, and the relative source spectral shape for the GSFC SIS. Each of these will be described briefly in the sections that follow.

3.2 SXR AND SEAWIFS RSRS

The relative spectral responses of the six SXR bands are also shown in Fig. 21. The responses were provided by B. Carol Johnson at NIST. These are system level responses, measured using a source with a bandwidth of less than 0.5 nm. The technique for the measurement of the system level response of the SXR is similar to that used for the system level response measurement of SeaWiFS (see Sect. 10 of Barnes et al. (1994b). The SXR responses were normalized by NIST to a maximum of unity.

The spectral responses of the eight SeaWiFS bands are shown in Fig. 21. The curves for SeaWiFS were previously compiled at 1 nm intervals from 380–1,150 nm (Barnes et al. 1994b and Barnes 1994). For the comparisons presented here, the spectral responses were also normalized to a maximum of unity.

3.3 SPHERE SPECTRAL SHAPE

The radiance curves for the GSFC sphere were provided by NIST. The complete characterization of the sphere by NIST will be described in a future SeaWiFS technical memorandum. The spectral shape of the sphere output is described in Barnes (1996a). For the comparison here, the output of the sphere has been normalized to unity at its maximum radiance level. There are no actual radiance measurements in this comparison—the radiance measurements will come later. The spectral shape comparison presented here was performed to allow the conversion of the SXR measurements to the wavelengths which SeaWiFS measures.

The normalized response curve for the GSFC sphere is shown in Fig. 22. This curve shows the shape of the output when the full complement of 16 lamps are lit. For the radiometric calibration of SeaWiFS, the sphere will be operated in four configurations with 16, 8, 4, and 1 lamp illuminated. The spectral response curves for these lamp configurations are not identical to the curve in Fig. 22, but they are very close duplicates. For the comparisons presented here and for the recalibration of SeaWiFS, the spectral curve for each lamp configuration is treated independently. The differences between lamp configurations, although slight, can be seen in the results below.

Changes in the spectral shapes of the sphere radiances do occur over time. The changes are most evident in the *blue* wavelengths from the sphere, that is, in the spectral radiances near 412 nm in this comparison. These changes result from the aging of the lamps and of the reflective surface on the interior of the sphere. These changes are greatest for new lamps and for a fresh coating on the sphere's interior. Over time, the rate at which these changes occur approaches zero. For the GSFC sphere, the output in the blue appears to have been stable during the most recent SeaWiFS Intercomparison Round-Robin Experiment (SIRREX) comparison (Johnson et al. 1996). Although

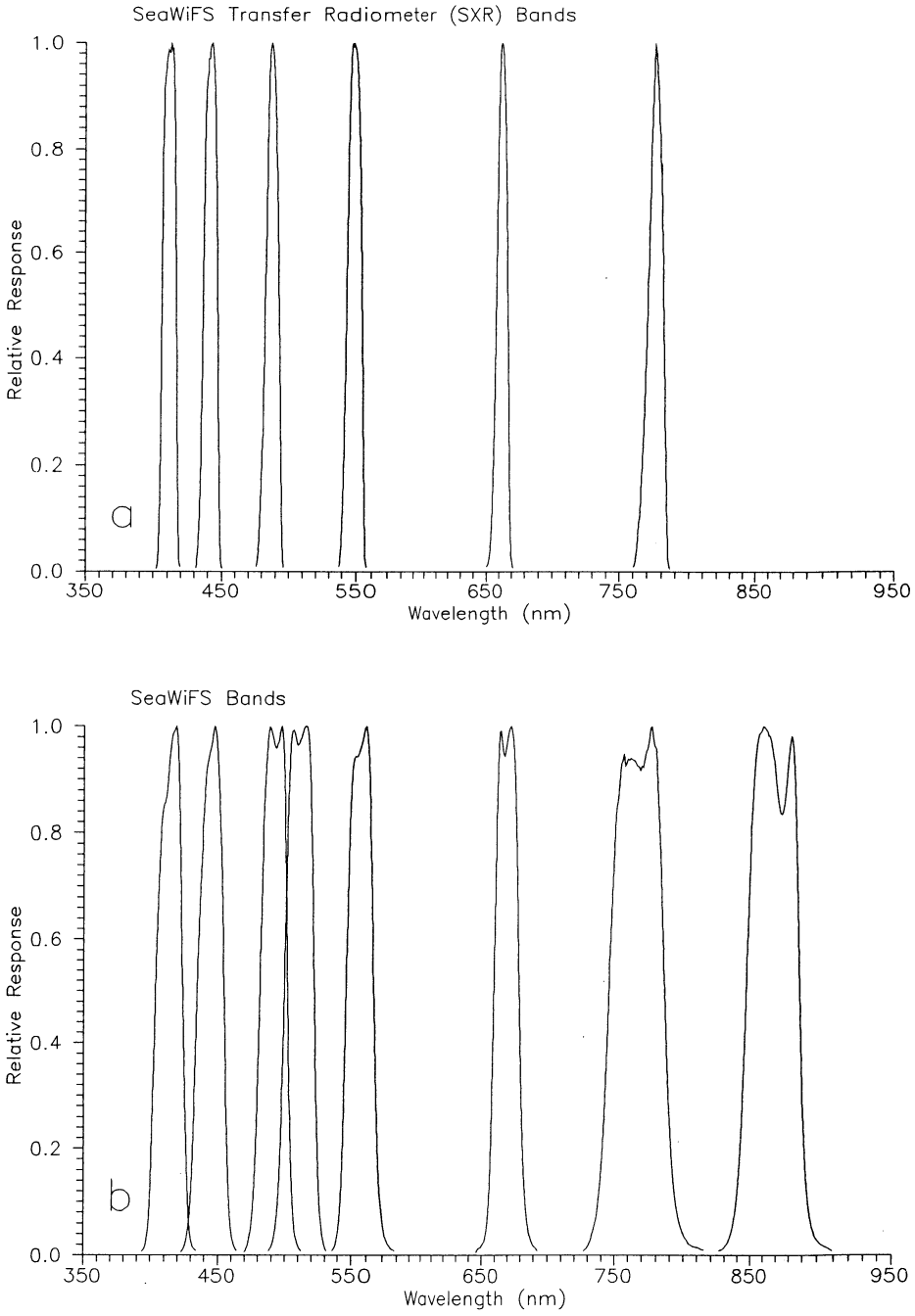

Fig. 21. The RSRs are shown for the bands in the comparison. The responses are normalized to a maximum of unity. For each band, responses that are less than 1% of the maximum have been eliminated; the out-of-band responses are not shown. **a)** Responses of the SXR. **b)** Responses of the SeaWiFS instrument.

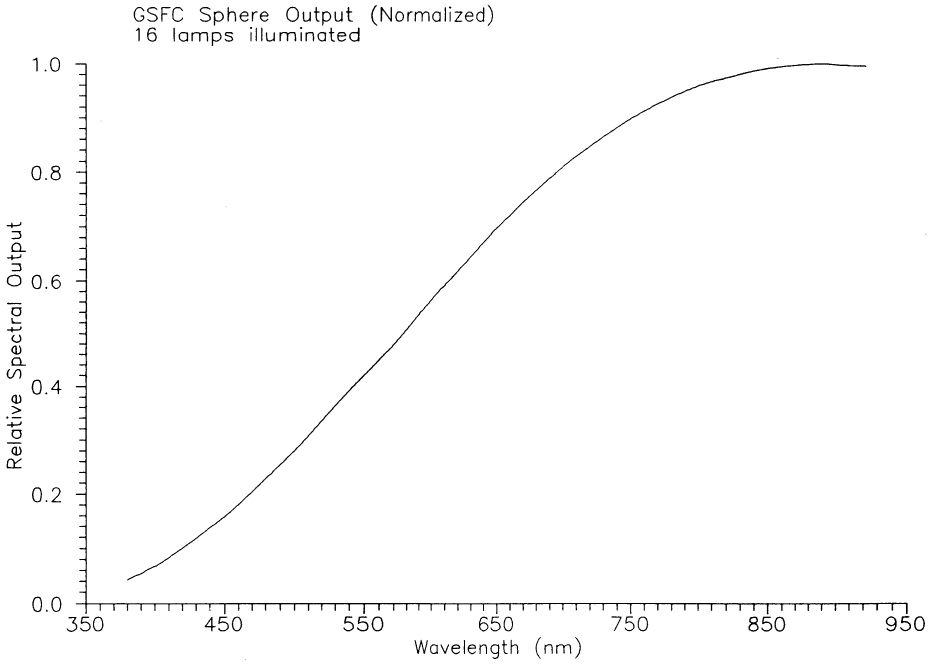

Fig. 22. The relative spectral output from the GSFC sphere is shown in this figure. The response is shown for the full complement of lamps (16 lamps) illuminated. The relative spectral output for other lamp configurations are very similar.

changes from the source spectral shapes presented here are not expected for the SeaWiFS recalibration, changes, if they do occur, could require a revision of these results before they are applied to the laboratory measurements.

3.4 OUT-OF-BAND REMOVAL

For SeaWiFS and for several other satellite instruments managed at GSFC, there is a distinction made between the in-band and out-of-band responses from the instrument. The in-band response is defined as the integrated response between the 1% transmission points (Barnes et al. 1994a). The remaining response is out-of-band. The out-of-band responses for SeaWIFS and the SXR, given as percentages of the total band responses, are listed in Table 18. The in- and out-of-band responses are calculated from the products of the GSFC sphere output and the band response, that is, for $L_s(\lambda)R(\lambda)$ in (17), over the wavelength intervals for the spectral characterization of the instruments. For SeaWiFS, the spectral characterization was made over the wavelength interval from 380–1,150 nm. The wavelengths for the 1% response points for each band in both instruments are listed in Table 19.

The out-of-band responses for the SeaWiFS instrument in Table 18 are very close to those previously calculated for a 2,850 K blackbody (Barnes et al. 1994b and Barnes and Yeh 1996). This is not surprising, since the GSFC sphere, as viewed by SeaWiFS, has an equivalent blackbody temperature of 2,980 K (Barnes 1996a). For the same reason, the out-of-band responses for the SXR in Table 18 should also be very close to those for a 2,850 K blackbody.

3.5 IN-BAND RADIANCES

The band-weighted responses for the SeaWiFS and SXR bands are listed in Table 18. The responses were calculated using output from the GSFC SIS normalized to unity at 890 nm. For SeaWiFS band 8, which has a center wavelength near 865 nm, the BSR is within 0.5% of unity.

The BSRs were calculated, using a set of summations that approximate (19). The calculation of the spectral radiance for SXR channel 1, viewing the GSFC sphere output with 16 lamps illuminated, can be found in Table 20. The contributors to the summations are listed at 0.5 nm intervals from 402.0–419.5 nm. The band responses at the end wavelengths are just below 1% of the maximum response.

The spectral radiances for each band in Table 18 are accompanied by an ECW (λ_{eff}). This wavelength has been calculated for the 16 lamp sphere configuration. A sample calculation of λ_{eff} for SXR band 1 is given in Table 20 and illustrated in Fig. 23. As shown below, the ECWs for the other lamp configurations very closely agree with those in Table 18.

3.6 CENTER WAVELENGTHS

The ECW, λ_{eff}, ties the BSR from the band to the spectral radiance from the sphere. At λ_{eff}, both spectral

Table 18. The ECWs and BSRs [$L_B(\lambda_B)$] from the GSFC sphere for SeaWiFS and the SXR are shown here. For each band, the weighting is made over the wavelength range between the band's 1% response points. The GSFC sphere radiances have been normalized to unity at the maximum spectral radiance (i.e., the spectral radiance at 890 nm). The center wavelengths are calculated for the sphere output with 16 lamps illuminated.

Band Number	*ECW* λ_{eff} [nm]	*BSRs* $L_B(\lambda_B)$				*Out-of-Band Response* [%]
		16 Lamps	8 Lamps	4 Lamps	1 Lamp	
SXR 1	411.26	0.085180	0.082925	0.082125	0.082334	0.50
2	441.42	0.141042	0.137828	0.136701	0.137806	0.19
3	486.97	0.247171	0.242745	0.241247	0.243699	0.42
4	547.88	0.416733	0.411506	0.409644	0.413591	0.38
5	661.63	0.727251	0.722906	0.721130	0.726807	1.48
6	774.70	0.932858	0.929945	0.928896	0.932218	0.70
SeaWiFS 1	413.78	0.089553	0.087212	0.086381	0.086612	1.37
2	444.09	0.146546	0.143257	0.142106	0.143294	0.52
3	491.19	0.258126	0.253620	0.252091	0.254651	1.50
4	510.10	0.309091	0.304265	0.302594	0.305630	0.64
5	554.91	0.437253	0.432014	0.430128	0.434211	3.15
6	668.33	0.743251	0.739068	0.737314	0.742960	0.76
7	764.85	0.919969	0.916657	0.915525	0.918936	1.84
8	862.74	0.995819	0.995166	0.994892	0.995347	2.25

Table 19. In this table, the center wavelengths for measurements of the GSFC sphere by SeaWiFS and the SXR are shown. The upper and lower integration wavelengths are the 1% response points for the bands.

Band Number	*ECW* λ_{eff} [nm]	*BCW* λ_B [nm]	*Lower Integration Wavelength* λ_1 [nm]	*Upper Integration Wavelength* λ_2 [nm]
SXR 1	411.26	411.39	402.0	419.5
2	441.42	441.55	431.5	450.0
3	486.97	487.09	476.0	496.0
4	547.88	547.96	538.0	556.5
5	661.63	661.67	650.0	671.0
6	774.70	774.80	760.5	786.0
SeaWiFS 1	413.78	414.48	394.0	433.0
2	444.09	444.62	423.0	464.0
3	491.19	491.59	470.0	512.0
4	510.10	510.51	488.0	531.0
5	554.91	555.19	536.0	578.0
6	668.33	668.69	646.0	693.0
7	764.85	765.76	727.0	815.0
8	862.74	866.29	826.0	909.0

radiances are the same. The calculation of the effective wavelength for SXR band 1 is shown in Table 20. The wavelength for $L_s(\lambda)$ is obtained using interpolation between the sphere spectral radiances that bracket the BSR, $L_B(\lambda_B)$, for the band. The sphere output at 411.26 nm is the same as the BSR for SXR band 1. As shown in Fig. 23, the spectral radiance from the sphere increases monotonically with wavelength over the in-band response range of the band.

The BCW, λ_B, is calculated in the same manner as the BSR, as in (20). A sample calculation of λ_B is given in Table 21. This calculation is made for the sphere output with 16 lamps illuminated. Clearly, $L_B(\lambda_B)$ and λ_B are also tied together uniquely. For an instrument with infinitely narrow bandwidths, λ_B and λ_{eff} will be identical. For SeaWiFS, and to a much lesser extent for the SXR, the two types of calculated center wavelengths are different. The two types of center wavelengths for all SeaWiFS and SXR bands are listed in Table 19, along with the upper and lower integration limits for the calculations.

Table 22 shows the spectral radiances from the sphere at the effective and BCWs for the SeaWIFS and SXR bands. It shows the differences in spectral radiance that correspond to the differences in wavelength. For the SXR,

Table 20. Shown is the calculation of the BSR [$L_{\mathrm{B}}(\lambda_{\mathrm{B}}) = 0.085180$] for SXR band 1 when measuring the output of the GSFC sphere with 16 lamps illuminated. $L_{\mathrm{B}}(\lambda_{\mathrm{B}})$ is calculated by the summation of $L_s(\lambda)R(\lambda) = 1.805337$ [which approximates the integral in (18)] divided by the summation of $R(\lambda) = 21.194483$. The ECW, which equals 411.26, is calculated by interpolation. It is the wavelength at which $L_s(\lambda) = L_{\mathrm{B}}(\lambda_{\mathrm{B}})$. The calculated spectral radiances and ECWs for each of the SeaWiFS and SXR bands can be found in Table 18.

λ [nm]	*Normalized Band Response* $R(\lambda)$	*Normalized Sphere Response* $L_s(\lambda)$	*Product* $L_s(\lambda)R(\lambda)$
402.0	0.006211	0.070502	0.000438
402.5	0.010747	0.071283	0.000766
403.0	0.020770	0.072065	0.001497
403.5	0.042285	0.072846	0.003080
404.0	0.098298	0.073628	0.007237
404.5	0.145084	0.074409	0.010796
405.0	0.259889	0.075191	0.019541
405.5	0.390215	0.075972	0.029646
406.0	0.536661	0.076754	0.041191
406.5	0.704143	0.077535	0.054596
407.0	0.814871	0.078317	0.063818
407.5	0.904308	0.079098	0.071529
408.0	0.935774	0.079880	0.074749
408.5	0.938132	0.080661	0.075671
409.0	0.958579	0.081443	0.078069
409.5	0.972649	0.082224	0.079976
410.0	0.979553	0.083006	0.081309
410.5	0.987429	0.083872	0.082817
411.0	0.985067	0.084737	0.083472
411.5	0.980620	0.085603	0.083944
412.0	0.984612	0.086468	0.085138
412.5	1.000000	0.087334	0.087334
413.0	0.993836	0.088200	0.087656
413.5	0.983767	0.089065	0.087620
414.0	0.989480	0.089931	0.088985
414.5	0.942185	0.090797	0.085547
415.0	0.895148	0.091662	0.082051
415.5	0.816659	0.092528	0.075564
416.0	0.667959	0.093393	0.062383
416.5	0.544351	0.094259	0.051310
417.0	0.345317	0.095125	0.032848
417.5	0.200552	0.095990	0.019251
418.0	0.105112	0.096856	0.010181
418.5	0.031104	0.097722	0.003040
419.0	0.013452	0.098587	0.001326
419.5	0.009666	0.099453	0.000961
Totals	21.194483		1.805337

Table 21. The calculation of the BCW ($\lambda_B = 411.39$) is given for the SXR band 1. The summations approximate the integral in (21) and are arrived at by taking the summation of $\lambda L_s(\lambda)R(\lambda)$ (equals 742.693515) divided by the summation of $L_s(\lambda)R(\lambda)$ (equals 1.805337). The calculations are made for the sphere output with 16 lamps illuminated.

λ [nm]	*Normalized Band Response* $R(\lambda)$	*Normalized Sphere Response* $L_s(\lambda)$	*Product* $L_s(\lambda)R(\lambda)$	*Product* $\lambda L_s(\lambda)R(\lambda)$
402.0	0.006211	0.070502	0.000438	0.176041
402.5	0.010747	0.071283	0.000766	0.308355
403.0	0.020770	0.072065	0.001497	0.603209
403.5	0.042285	0.072846	0.003080	1.242906
404.0	0.098298	0.073628	0.007237	2.923942
404.5	0.145084	0.074409	0.010796	4.366813
405.0	0.259889	0.075191	0.019541	7.914198
405.5	0.390215	0.075972	0.029646	12.021256
406.0	0.536661	0.076754	0.041191	16.723439
406.5	0.704143	0.077535	0.054596	22.193241
407.0	0.814871	0.078317	0.063818	25.973972
407.5	0.904308	0.079098	0.071529	29.148187
408.0	0.935774	0.079880	0.074749	30.497788
408.5	0.938132	0.080661	0.075671	30.911619
409.0	0.958579	0.081443	0.078069	31.930407
409.5	0.972649	0.082224	0.079976	32.749987
410.0	0.979553	0.083006	0.081309	33.336591
410.5	0.987429	0.083872	0.082817	33.996470
411.0	0.985067	0.084737	0.083472	34.306926
411.5	0.980620	0.085603	0.083944	34.542898
412.0	0.984612	0.086468	0.085138	35.076814
412.5	1.000000	0.087334	0.087334	36.025319
413.0	0.993836	0.088200	0.087656	36.201945
413.5	0.983767	0.089065	0.087620	36.230671
414.0	0.989480	0.089931	0.088985	36.839731
414.5	0.942185	0.090797	0.085547	35.459323
415.0	0.895148	0.091662	0.082051	34.051282
415.5	0.816659	0.092528	0.075564	31.396705
416.0	0.667959	0.093393	0.062383	25.951327
416.5	0.544351	0.094259	0.051310	21.370620
417.0	0.345317	0.095125	0.032848	13.697699
417.5	0.200552	0.095990	0.019251	8.037327
418.0	0.105112	0.096856	0.010181	4.255551
418.5	0.031104	0.097722	0.003040	1.272032
419.0	0.013452	0.098587	0.001326	0.555676
419.5	0.009666	0.099453	0.000961	0.403249
Totals			1.805337	742.693515

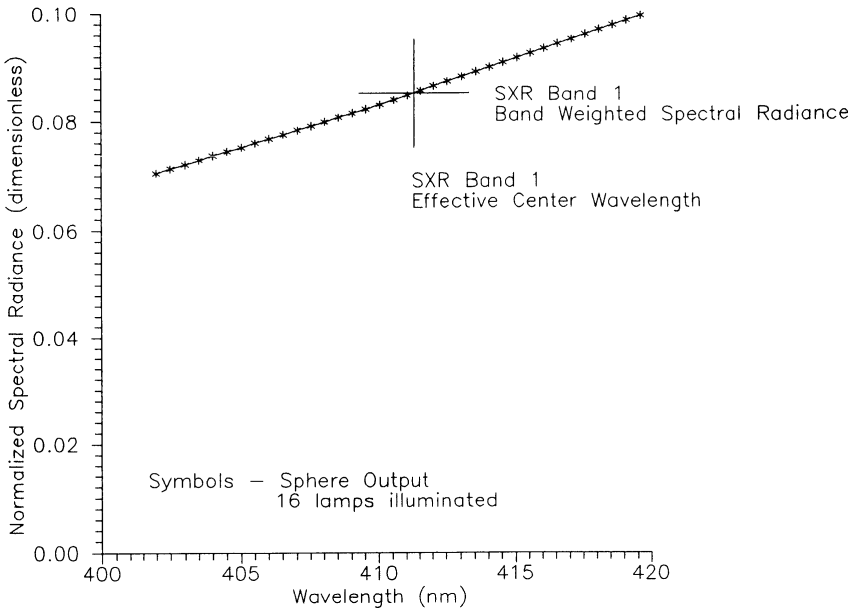

Fig. 23. The BSR and ECW for SXR band 1 are shown here. These factors are tied together by the spectral radiance from the source. In this case, the source is the GSFC sphere with 16 lamps illuminated. The data for this figure come from Table 20.

Table 22. The sphere spectral radiances at the ECWs $[L_s(\lambda_{\text{eff}})]$, and BCWs $[L_s(\lambda_{\text{B}})]$, are shown in this table for the SeaWiFS and SXR bands. The calculations are made for the sphere output with 16 lamps illuminated. The ratio gives $L_s(\lambda_{\text{B}})/L_s(\lambda_{\text{eff}})$.

Band Number	λ_{eff} [nm]	*Sphere Spectral Radiance* $L_s(\lambda_{\text{eff}})$	λ_{B} [nm]	*Sphere Spectral Radiance* $L_s(\lambda_{\text{B}})$	*Ratio*
SXR 1	411.26	0.085180	411.39	0.085409	1.0003
2	441.42	0.141042	441.55	0.141302	1.0003
3	486.97	0.247171	487.10	0.247495	1.0003
4	547.88	0.416733	547.96	0.416972	1.0002
5	661.63	0.727251	661.67	0.727339	1.0001
6	774.70	0.932858	774.80	0.932977	1.0001
SeaWiFS 1	413.77	0.089553	414.48	0.090763	1.0135
2	444.09	0.146546	444.62	0.147627	1.0074
3	491.19	0.258126	491.59	0.259192	1.0041
4	510.10	0.309091	510.51	0.313017	1.0127
5	554.91	0.437253	555.19	0.438068	1.0019
6	668.33	0.743251	668.69	0.744111	1.0012
7	764.85	0.919969	765.76	0.921223	1.0014
8	862.74	0.995819	866.29	0.996629	1.0008

Table 23. The ECWs (λ_{eff}) for the SeaWiFS and SXR bands are shown for all lamp configurations (16, 8, 4, and 1) for the GSFC sphere. All units are in nanometers [nm].

Band	*Sphere*				*Average*	*Standard*
Number	16 Lamps	8 Lamps	4 Lamps	1 Lamp		*Deviation*
SXR 1	411.2555	411.2541	411.2523	411.2517	411.2534	0.0015
2	441.4250	441.4258	441.4266	441.4262	441.4259	0.0006
3	486.9690	486.9700	486.9694	486.9695	486.9695	0.0004
4	547.8817	547.8814	547.8816	547.8815	547.8816	0.0001
5	661.6315	661.6309	661.6298	661.6314	661.6309	0.0007
6	774.7044	774.6911	774.6846	774.6675	774.6869	0.0133
SeaWiFS 1	413.7820	413.7813	413.7800	413.7439	413.7718	0.0186
2	444.0919	444.0938	444.0960	444.0943	444.0940	0.0017
3	491.1895	491.1952	491.1920	491.1921	491.1922	0.0023
4	510.1038	510.1121	510.1034	510.1124	510.1079	0.0050
5	544.9090	544.9086	544.9074	544.9089	544.9085	0.0007
6	668.3344	668.3443	668.3355	668.3392	668.3384	0.0045
7	764.8503	764.8856	764.8420	764.7767	764.8386	0.0454
8	862.7743	863.0759	863.1742	862.9470	862.9854	0.1857

with its narrow bandwidths, the spectral radiance differences are very small, 0.03% or less. For SeaWiFS, the radiance differences are greater, particularly with the shorter wavelength bands. Thus, the choice of the appropriate center wavelength for the SeaWiFS bands becomes important, when the SXR is used as a calibration standard for SeaWiFS with both instruments viewing the GSFC sphere. For that comparison, λ_{eff} has been chosen, since $L_{\text{B}}(\lambda_{\text{B}})$ and $L_s(\lambda_{\text{eff}})$ are identical by definition.

Table 23 shows the ECWs for each SeaWiFS and SXR band for each sphere configuration. The center wavelength differences are essentially insignificant. For example, Table 22 shows that a 0.7 nm difference in center wavelength causes a 1.35% difference in the sphere spectral radiance for SeaWiFS band 1. This corresponds to a 0.2% difference per 0.1 nm. The 0.04 nm range in the ECWs for SeaWiFS band 1 in Table 23 would cause a difference of less than 0.1% in sphere spectral radiance. For SeaWiFS band 8, a 3.5 nm change in center wavelength causes only an 0.08% change in sphere output (Table 23). Thus, the 0.3 nm range in ECWs for SeaWIFS band 8 in Table 23 causes a negligible difference in sphere spectral radiance.

Barnes (1996b) made a similar comparison, using the shape of a 12,000 K blackbody to approximate the spectrum of the Earth-exiting radiance that SeaWiFS will view on orbit. Those results show that, on orbit, the differences in the source radiances at λ_{eff} and λ_{B} will be 0.12% or less for each of the SeaWiFS bands.

3.7 RADIANCE CONVERSION

For measurements of the GSFC sphere, the BSRs for the SeaWiFS bands can be calculated directly from the BSRs measured by the SXR. These calculations, using band pairs, require no information about the center wavelengths for the bands. The steps in this calculation are simple. They start with a measured radiance from an SXR band of the sphere output.

1. Remove the out-of-band response from the SXR measured radiance. The percent out-of-band response for each SXR band is given in Table 18.
2. Convert the SXR in-band radiance to the SeaWiFS in-band response using the ratios of the BSRs in Table 18. The conversion factors for measurements of the GSFC sphere with 16 lamps illuminated is given in Table 24. A similar use of the conversion factors from Table 18 can be made for the other sphere configurations.
3. Restore the out-of-band response to the SeaWiFS band to calculate the total band response. Depending on the use for the results, this step may not be necessary. The percent out-of-band response for each SeaWiFS band is listed in Table 18.

There are other conversion techniques that can use the set of SXR BSRs to calculate the spectral radiances from the sphere at the SeaWiFS wavelengths. These techniques require a clear and consistent understanding of the center wavelengths for the bands. For example, by using the spectral radiance from each SXR band and the values in Table 18, it is possible to calculate the sphere output at 890 nm, that is, at the wavelength where the sphere output is normalized to unity. From the six resulting values for the spectral radiance at 890 nm, a best value for the radiance at that wavelength can be determined. This combination uses the entire set of SXR measurements so that effects in measurement errors by any one band will be minimized.

Table 24. The factors for converting the SXR spectral radiances to SeaWiFS are given in this table. These values (dimensionless) are for measurements of the GSFC sphere with 16 lamps illuminated; these factors are derived from values in Table 18. Spectral radiances are given as $\mathrm{mW\,cm^{-2}\,sr^{-1}\,\mu m^{-1}}$. There are no SXR bands that correspond to SeaWiFS band 4 (510 nm); conversions for SeaWiFS band 4, however, can be made using SXR bands 3 and 4.

SeaWiFS		*SXR*		*SeaWiFS*	*SXR*	*Conversion*
Band Number	λ_{eff} [nm]	*Band Number*	λ_{eff} [nm]	*Spectral Radiance*	*Spectral Radiance*	*Factor*
1	413.77	1	411.25	0.089553	0.085180	1.0513
2	444.10	2	441.43	0.146546	0.141042	1.0390
3	491.21	3	486.97	0.258126	0.247171	1.0443
4	510.10	3	486.97	0.309091	0.247171	1.2505
4	510.10	4	547.88	0.309091	0.416733	0.7417
5	554.91	4	547.88	0.437253	0.416733	1.0492
6	668.38	5	661.63	0.743251	0.727251	1.0220
7	764.91	6	774.69	0.919969	0.932858	0.9862
8	862.95	6	774.69	0.995819	0.932858	1.0675

Using the sphere output at 890 nm and the SeaWiFS factors in listed in Table 18 (which are based on the knowledge of the wavelength dependence of the spectral radiance from the sphere), the radiances at the SeaWiFS center wavelengths can be calculated. If the spectral shape of the sphere output is very well determined, then using the technique, such as the one outlined in this chapter, should reduce the scatter in the spectral radiances at the SeaWiFS wavelengths, compared to those calculated from the SeaWiFS–SXR band pairs. This should reduce the relative, or band-to-band, differences in the calibration of SeaWiFS.

Chapter 4

SeaWiFS Center Wavelengths

Robert A. Barnes
General Sciences Corporation, Laurel, Maryland

Abstract

With its 20 and 40 nm bandwidths, SeaWiFS does not make measurements at individual wavelengths. Rather, the output from each SeaWiFS band can be considered as an integral over a finite wavelength region of the source it measures. To make SeaWiFS measurements useful, it is important to relate the measured radiance from the instrument to a reference wavelength. That wavelength connects each SeaWiFS measurement to the spectral radiance from the source at that wavelength. For the initial calibration of SeaWiFS, the reference center wavelengths were those from the instrument's performance specifications. A set of BCWs for on-orbit use are presented here. The use of these new wavelengths will require a revision of the on-orbit radiometric calibration constants for the instrument.

4.1 INTRODUCTION

For the development of the initial SeaWiFS calibration equations (Barnes et al. 1994b), the instrument was assumed to have a set of eight fixed center wavelengths, one for each band. For SeaWiFS bands 1–8, these wavelengths are 412, 443, 490, 510, 555, 670, 765, and 865 nm, respectively. These wavelengths come from the instrument specifications (Barnes et al. 1994a), and they are the wavelengths at which the laboratory source for the SeaWiFS radiometric calibration was itself calibrated. These center wavelengths are embedded in the radiometric calibration of SeaWiFS. For the current calibration of the instrument, they are the de facto center wavelengths for the instrument. Since the development of the original SeaWiFS calibration equations, studies were performed to investigate the effects of different source spectral shapes on the output of the SeaWiFS bands (Barnes 1996a, and Barnes and Yeh 1996). In addition, these studies used the de facto center wavelengths for each band and calculated changes in the output from the bands for different source spectral shapes normalized at those wavelengths. Those studies were particularly instructive in developing an approach for calculating the out-of-band responses of the SeaWiFS bands for different source spectral shapes.

It is also possible, however, to examine the effects of source spectral shape in terms of fixed radiometric output from the SeaWiFS bands, accompanied by changes in their center wavelengths with changes in source spectral shape. The groundwork for this approach was presented in a comparison of the spectral responses of SeaWiFS and the SeaWiFS Transfer Radiometer (SXR) (Barnes 1996c). That comparison centered on the in-band responses of the two instruments for the spectral shape of the GSFC sphere—the source to be used in the recalibration of SeaWiFS.

In spectral terms, the output from the GSFC sphere varies smoothly with wavelength over the extended bandpasses of the SeaWiFS bands (Barnes 1996a). This allows the calculation of the wavelength at which the spectral radiance from the sphere equals the BSR from each instrument band. The same smooth changes with wavelength are found in the Planck function curves that were used as approximations to the spectral shapes of the Earth-exiting spectral radiance which SeaWiFS will view on orbit (Barnes 1996a and Barnes and Yeh 1996). Eventually, these approximations to the Earth-exiting spectral radiances may be replaced with spectral shapes based on atmospheric radiometric transfer models. The adoption of these *more realistic* spectral shapes will require a modification of the results presented here.

4.2 INSTRUMENT RESPONSE

As part of a comparison of the spectral responses of SeaWiFS and the SXR, Barnes (1996c) examined the effects of the finite bandwidths of the two instruments. The discussion in this section has been extracted from that report.

For a SeaWiFS band, it is possible to calculate the BSR, using the band's spectral response as the weighting function:

$$L_{\mathrm{B}}(\lambda_{\mathrm{B}}) = \frac{\int_{\lambda_1}^{\lambda_2} \lambda L_s(\lambda) R(\lambda) d\lambda}{\int_{\lambda_1}^{\lambda_2} R(\lambda) d\lambda}, \qquad (21)$$

where $L_B(\lambda_B)$ is the BSR for the band; λ_1 and λ_2 are the lower and upper 1% transmission points for the band, respectively; $L_s(\lambda)$ is the source spectral radiance at wavelength λ; and $R(\lambda)$ is the spectral response of the band at wavelength λ. The integration limits, λ_1 and λ_2, mark the wavelength range for the in-band response of the band. Examples of $L_s(\lambda)$ for a 12,000 K Planck function and of $R(\lambda)$ for SeaWiFS band 7 are shown in Fig. 24. The Planck function has been normalized to unity at 380 nm.

For the discussions here, the term *spectral radiance* refers to the radiant flux (in watts or photons per second) per unit wavelength. For the SeaWiFS Project, the units of spectral radiance are $\mathrm{mW\,cm^{-2}\,sr^{-1}\,\mu m^{-1}}$. The SeaWiFS instrument measures the integral of spectral radiance (Barnes 1996c). This integral is the numerator of (21). Again, for the discussions here, the integral that SeaWiFS measures is called "radiance" and does not have the term per micron ($\mu\,\mathrm{m}^{-1}$). To make SeaWiFS measurements useful, it is important to relate the measured radiance from the instrument to a reference wavelength. That wavelength connects the SeaWiFS measurement to the spectral radiance from the source at that wavelength. For the vast majority of discussions of SeaWiFS measurements in the literature, the terms radiance and spectral radiance are used interchangeably. In those presentations, radiance means the same as spectral radiance here.

In a similar manner, the BCW associated with this spectral radiance can be calculated, using $L_s(\lambda)R(\lambda)$ as the weighting function.

$$\lambda_B = \frac{\int_{\lambda_1}^{\lambda_2} \lambda L_s(\lambda) R(\lambda) d\lambda}{\int_{\lambda_1}^{\lambda_2} L_s(\lambda) R(\lambda) d\lambda}, \qquad (22)$$

where λ_B is the BCW.

Alternately, it is possible to define an effective wavelength for each band, λ_{eff}, which is the wavelength where $L_s(\lambda)$ equals $L_B(\lambda_B)$. The ECW can be applied to sources that are well behaved spectrally. In this regard, the Planck function curve in Fig. 24 is well behaved. For the source function and the band response in Fig. 24, the ECW is 765.0 nm.

For an instrument that measures with infinitely narrow bandwidths, λ_B and λ_{eff} are the same; however, for SeaWiFS the spectral bandwidths are finite. The calculated center wavelengths are different for the two methods. The center wavelength results from both calculation methods are given below. As the calculations will show, on orbit differences in the source spectral radiance at λ_{eff} and λ_B will be 0.12% or less, for each of the SeaWiFS bands.

4.3 SOURCE FUNCTIONS

Fig. 25 shows the typical SeaWiFS spectral radiances, as found in the performance specifications for the instrument (Barnes et al. 1994a). The figure also shows three Planck function curves normalized at 412 nm to the typical spectral radiance for SeaWiFS band 1. These three curves provide approximations to the Earth-exiting spectral radiances that SeaWiFS will view on orbit. Of the three, the 12,000 K Planck function is considered to have the best overall fit to the typical spectral radiances. The BCWs and ECWs are calculated below using these source spectral shapes. Because the calculation of the center wavelengths depends solely on the spectral shapes of the source functions and those of the band responses, the absolute values of the source functions are unimportant. For the calculations presented here, the Planck functions have been normalized to unity at 380 nm.

The center wavelengths are also calculated below using the spectral shape of the output of the GSFC sphere. In Barnes and Yeh (1996), each lamp setting for the sphere was considered as having an independent spectral shape. In that study, the minor differences between lamp settings were important because the results were a fundamental part of the recalibration of SeaWiFS. For the purposes of this report, the spectral shapes from the four lamp settings have been combined into one representative shape for the sphere, since for this report, the sphere's spectral shape is used only for comparisons with the Planck functions.

Finally, a constant source function of unity is used below for calculations of BCWs for each band. These BCWs can be compared with the system level center wavelengths for SeaWiFS from Table 13 of Barnes et al. (1994b). The system level center wavelengths, in turn, were calculated as the center point of the full-width at half-maximum for each band. The BCWs in this chapter differ from the system level values in Barnes et al. (1994b) by up to 0.6 nm.

4.4 CALCULATED WAVELENGTHS

The BSRs for the SeaWiFS bands were calculated, using a set of summations that approximate (21). The details of such a calculation were demonstrated in Table 20 of Barnes (1996c). The calculation of a BCW, λ_B, using (22) was demonstrated in Table 21 of Barnes (1996c).

The SeaWiFS BCWs, using the source spectral shapes described above, are listed in Table 25. The spectral shape of the GSFC sphere is given as 2,920 K—the sphere's equivalent blackbody temperature (Barnes 1996a). For SeaWiFS ocean measurements on orbit, the spectral shape of the Earth-exiting spectral radiance is expected to be close to that for a 12,000 K Planck function. For the 10,000 K; 12,000 K; and 14,000 K spectral shapes, the BCWs in Table 25 are nearly identical. For each of the bands, the center wavelengths for the 12,000 K spectral shape is less than 0.06 nm from those for the adjacent blackbody temperatures. As a result, the BCWs should remain essentially constant throughout the range of spectral shapes that SeaWiFS will encounter during its measurements of water leaving spectral radiances.

Table 25 also lists the ECW, λ_{eff}, for each SeaWiFS band and for each source spectral shape, except for the

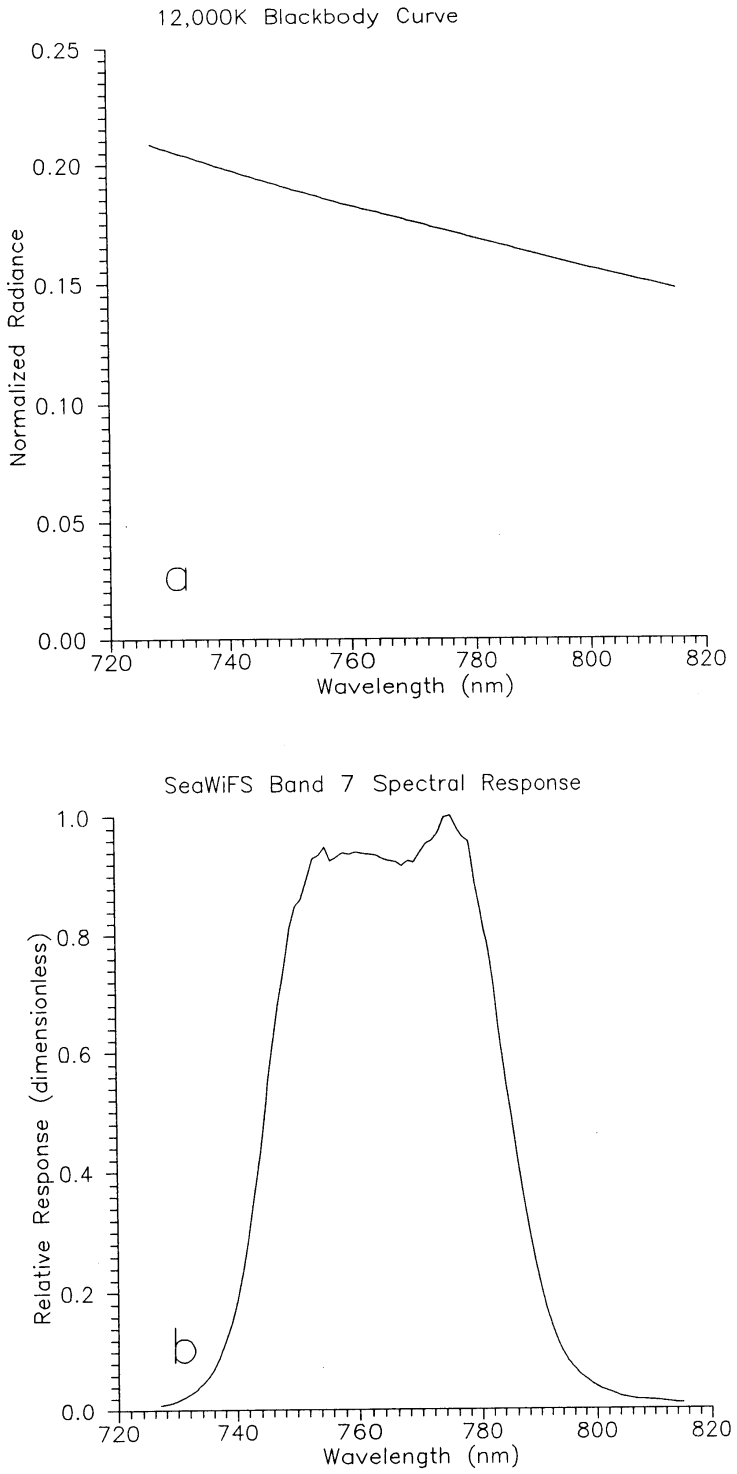

Fig. 24. A 12,000 K Planck function source curve and the relative spectral response for SeaWiFS band 7 are illustrated. The Planck function has been normalized to unity at 380 nm. The calculations of the BCWs and ECWs depend solely on the shapes of the source functions and those of the band spectral responses. **a)** The blackbody curve. **b)** The band 7 response curve.

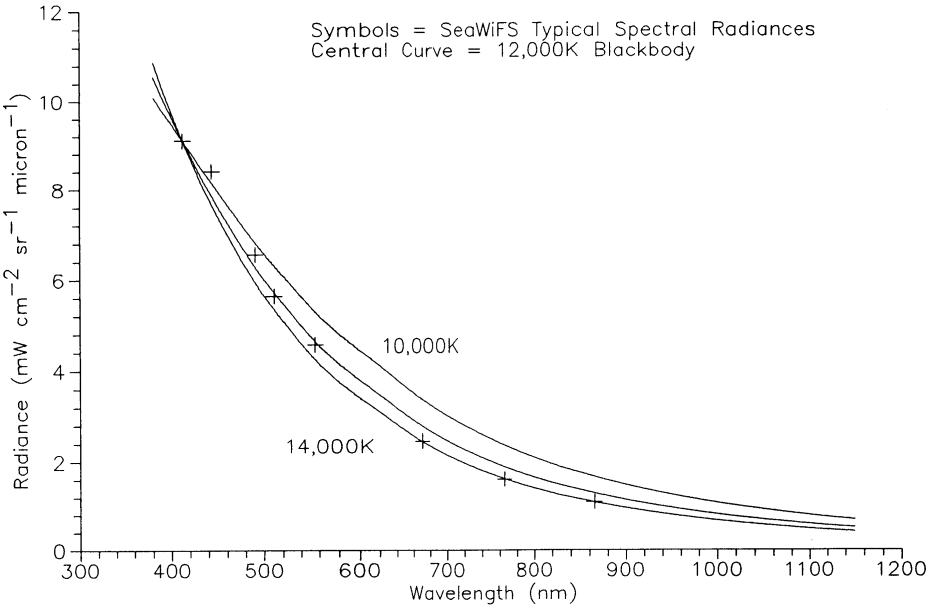

Fig. 25. Typical spectral radiances from the SeaWiFS specifications plotted with three blackbody curves are shown here.

Table 25. This table gives the calculated center wavelengths (in nanometers) for the eight SeaWiFS Bands. ECWs are given for four spectral shapes—the GSFC sphere and three Planck function curves that approximate the source spectral shape which SeaWiFS will view on orbit. The BCWs are given for the same spectral shapes and for a spectrally flat source.

Spectral Shape [K]	*BCW* (λ_B)							
	Band 1	Band 2	Band 3	Band 4	Band 5	Band 6	Band 7	Band 8
2,920 (Sphere)	414.49	444.62	491.59	510.52	555.19	668.70	765.76	866.30
Spectrally Flat	413.62	443.97	491.10	510.03	554.91	668.55	765.49	866.25
10,000	413.46	443.80	490.91	509.81	554.75	668.36	764.79	865.62
12,000	413.41	443.75	490.87	509.77	554.72	668.34	764.74	865.58
14,000	413.37	443.72	490.84	509.74	554.71	668.33	764.70	865.55
	ECWs (λ_{eff})							
2,920 (Sphere)	413.77	444.09	491.19	510.11	554.91	668.34	764.84	862.99
10,000	413.61	443.93	491.02	509.93	554.83	668.44	765.08	865.87
12,000	413.53	443.87	490.98	509.89	554.81	668.42	765.03	865.84
14,000	413.49	443.84	490.95	509.86	554.79	668.41	765.00	865.82

Table 26. The spectral radiances at the ECWs and BCWs are shown for the eight SeaWiFS bands. The source for these calculations is a 12,000 K Planck function normalized to unity at 380 nm.

Band Number	λ_{eff} [nm]	Spectral Radiance $L_s(\lambda_{\text{eff}})$	λ_{B} [nm]	Spectral Radiance $L_s(\lambda_{\text{B}})$	Ratio
1	413.53	0.857363	413.41	0.857863	1.0006
2	443.87	0.743143	443.75	0.743547	1.0005
3	490.98	0.594213	490.87	0.594521	1.0005
4	509.89	0.543435	509.77	0.543740	1.0006
5	554.81	0.440746	554.72	0.440916	1.0004
6	668.42	0.266086	668.34	0.266183	1.0004
7	765.03	0.179003	764.74	0.179215	1.0012
8	865.84	0.122143	865.58	0.122260	1.0010

spectrally flat source. The calculation of an ECW was demonstrated in Table 20 of Barnes (1996c). As with the BCWs, the ECWs in Table 25 are nearly identical for the 10,000 K; 12,000 K; and 14,000 K spectral shapes. In addition, as with the BCWs, the ECWs should remain essentially constant for SeaWiFS ocean measurements.

For the 10,000 K, 12,000 K, and 14,000 K source spectral shapes, the ECWs are shorter than the BCWs. These differences are very small. Table 26 shows the effects of these wavelengths differences in terms of differences in the spectral radiance from the source. In Table 26, the spectral radiances from a 12,000 K source are listed for each of the center wavelengths. For the SeaWiFS bands with 20 nm bandwidths (bands 1–6), the differences between the BCWs and ECWs average 0.05%. For SeaWiFS bands 7 and 8 (with 40 nm bandwidths), the differences average 0.11%. Clearly, the choice between BCWs or ECWs to represent SeaWiFS on-orbit measurements makes no appreciable difference in the results of the measurements.

For measurements of the GSFC sphere, there is a larger difference between the effective and BCWs (Table 25). Barnes (1996c) calculated differences in sphere spectral radiances for these pairs of wavelengths to be up to 1.3%. For that study, the ECWs were deemed to better represent the spectral radiance from the sphere. For measurements on orbit, the two types of center wavelengths are equivalent.

4.5 CONCLUDING REMARKS

The current center wavelengths for the SeaWiFS bands (1–8) are 412, 443, 490, 510, 555, 670, 765, and 865 nm, respectively. These are the wavelengths from the SeaWiFS specifications (Barnes et al. 1994a), and these are the wavelengths at which the instrument was calibrated in the laboratory. A more representative set of SeaWiFS wavelengths, the BCWs, are listed in Table 25. These center wavelengths are tied to the BSRs from the SeaWiFS bands. These BCWs have not been incorporated into the current calibration of SeaWiFS (Barnes et al. 1994b). It is possible, however, to derive a revised on-orbit calibration of SeaWiFS at the BCWs, using the spectral comparison of SeaWiFS and the SXR (Barnes 1996c), along with the out-of-band results from Barnes and Yeh (1996).

It is also possible to convert the SeaWiFS measured spectral radiances to wavelengths other than those in this study. This is important, because SeaWiFS's measurements will be compared with those from other satellite instruments; these other instruments will measure at wavelengths different from, but close to, SeaWiFS. OCTS, on board the Advanced Earth Observation Satellite (ADEOS-1) was launched in August 1996, and MODIS on board the Earth Observing System's morning platform (EOS-AM) is scheduled for launch in 1998. Both of these instruments have ocean color bands at wavelengths similar to SeaWiFS. If the measurements of Earth-exiting spectral radiances from each of these instruments are to be compared for uniformity, then the wavelengths at which the measurements are made must be clearly determined. For SeaWiFS, it will be possible to convert the measured spectral radiances on orbit to the spectral radiances at the wavelengths of the other instruments.

Finally, it is possible to provide a better source spectral shape than a 12,000 K Planck function for corrections to SeaWiFS measurements on orbit. This can be done by means of an atmospheric radiative transfer model, which is outside the scope of this study. Alternately, it will be possible to use initial flight data from the instrument to provide an updated set of typical spectral radiances as the basis for a better model of the source spectral shape, which will be viewed during SeaWiFS ocean color measurements.

Chapter 5

The SeaWiFS Solar Diffuser

Robert A. Barnes
Robert E. Eplee
General Sciences Corporation, Laurel, Maryland

Abstract

Measurements of the solar flux with an onboard solar diffuser will provide an important check of changes in the radiometric sensitivity of SeaWiFS over the duration of the instrument's on-orbit measurements of ocean color. Although diffuser measurements do not give an absolute determination of radiometric changes, they will identify any rapid changes that may occur in the instrument output. The diffuser was designed to produce radiance levels that approximate those for other SeaWiFS measurements. This design includes an attenuator to reduce the solar radiance levels on the diffuser, and hence, the effects of photolyzed organic compounds. The BRDF, which shows the output of the diffuser as a function of pitch and yaw angle, has been determined. This allows the removal of angular dependencies from the long-term radiometric sensitivity data. In addition, outdoor measurements have given the predicted output from SeaWiFS for initial on-orbit solar diffuser measurements.

5.1 INTRODUCTION

The SeaWiFS design requirements were based on the National Aeronautics and Space Administration (NASA) experience with the operation of the Nimbus-7 Coastal Zone Color Scanner (CZCS), since SeaWiFS is the successor instrument to CZCS. SeaWiFS is considered an improved replacement instrument for its predecessor. Among the improvements are the incorporation of lunar and solar measurements on orbit.

Lunar measurements are the single source of SeaWiFS measurements to directly monitor the long-term drift in the radiometric sensitivity (or responsivity) of the instrument (McClain et al. 1992 and Woodward et al. 1993). The sun is considered a stable, unchanging light source. The surface of the moon is also considered as unchanging over the lifetime of the SeaWiFS measurements. Geometric factors, such as the Earth-sun and Earth-moon distances, can be calculated, and differences in the lunar reflectance caused by small changes in the lunar phase angle and by lunar libration can be removed using empirically-based lunar models (Hapke 1986, Helfenstein and Veverka 1987, and Kieffer and Wildey 1996). To eliminate errors due to uncertainty in the locations of the measured pixels on the face of the moon, the lunar measurements will be used as integrated images of the entire surface of the moon (Woodward et al. 1993). With these corrections, measurements of the lunar reflectance can be used directly by SeaWiFS to detect changes in the sensitivity of the instrument, since SeaWiFS views the Earth and the moon in an identical fashion.

For solar measurements that use a diffuser to bring the solar irradiance within the SeaWiFS dynamic range, it is not possible to separate changes in the instrument sensitivity from changes in the reflectance of the diffuser plate in an a priori fashion. All that can be derived from these measurements is the product of the change in the instrument and the change in the diffuser; however, there is an assumption that can be used to tie solar diffuser measurements with lunar measurements. Basically, the change in the reflectance of the diffuser is assumed to be linear over periods of a few months. Over longer periods, from one to several years, the change may be exponential with gradually decreasing changes over time; however, this exponential change can be treated as a series of many linear segments. Experience with diffusers on previous satellite instruments (Frederick et al. 1986 and Herman et al. 1990) led to the assumption that diffuser degradation was caused by the coating of the diffuser with photolyzed organic materials that outgassed from the spacecraft. This accumulation of organic materials is generally temporally smooth and does not cause step functions in the reflectivity of the diffuser.

Using virtually simultaneous lunar- and solar-diffuser measurements, it is possible to separate changes in the sensitivity of the instrument, using lunar measurements, from changes in the reflectance of the diffuser. With the time series of diffuser measurements normalized by lunar measurements, it is possible to use the assumption of a short-term linear change in diffuser reflectivity to identify

step changes in instrument sensitivity between lunar measurements. Such step changes were found in CZCS measurements (Evans and Gordon 1994).

Determining these changes waits for the launch of SeaWiFS and the initiation of on-orbit operations. This chapter reports on the design of the diffuser and its prelaunch characterization and calibration.

5.2 DIFFUSER DESCRIPTION

Overviews of the operation of the SeaWiFS scanner were presented in Barnes and Holmes (1993) and in Barnes et al. (1994b). This section concentrates on a description of the solar diffuser, itself. Figure 26 shows the SeaWiFS instrument, the coordinate system for the instrument, and the spacecraft. The flat plate at the top of the instrument is mounted to the SeaStar spacecraft (not shown), and nadir is the $+x$ direction. Using the coordinate system in Fig. 26, SeaWiFS and SeaStar both fly in the $-y$ direction, and SeaWiFS scans west-to-east in the xz plane, or normal to the instrument's y axis. The solar diffuser (also called the solar calibrator) points in the $+y$ direction, that is, to the aft of the spacecraft. On the sunlit side of the Earth, the spacecraft moves from north to south; it has a descending equatorial crossing. As a result, the diffuser views the sun as the spacecraft passes over the Earth's South Pole.

Figure 27 is a drawing of the diffuser assembly mounted to the sensor. With the sun to the right of the drawing, sunlight passes through the attenuator, is scattered off the diffuser, and enters the instrument to the left. The diffuser plate itself is part of the diffuser housing. It is painted on the inside surface of the housing, behind the diffuser cover in Fig. 27. The figure shows the back of the diffuser cover; the back of the diffuser cover is also painted and acts as a second diffuser. The cover has a spring-loaded hinge at its bottom and is held in the vertical position by a solenoid actuator. When the one-time actuator releases the cover, the diffuser cover rotates into the page and comes to rest on the bottom of the diffuser housing, held in place by the spring on the hinge. A schematic of the diffuser assembly, as seen from above the instrument, is shown in Fig. 28. The figure shows the assembly without the diffuser cover.

The diffuser has a nominal illumination angle of 60° to avoid possible specular glints from its surface and to reduce the flux density on the diffuser plate by a factor of two. The plate and diffuser covers have coatings of YB71 paint. This paint provides a durable flat white coating with proven orbital stability, as shown in the results from the Long Duration Exposure Facility (LDEF) flown by NASA. The wavelength dependence of the reflectivity of a YB71 coated plate, as measured at SBRC, is shown in Fig. 29.

The attenuator is a flat black anodized aluminum aperture plate with holes which reduce the solar flux on the diffuser (Fig. 30). The small hole size (4.32 mm diameter) and the close spacing of the holes (6.35 mm centers) in the attenuator ensures that images of the sun partially overlap on the diffuser, providing a uniformly illuminated surface. The aperture holes were drilled in a pattern that was rotated 35° to prevent striping of the diffuser by photolyzed organic compounds over the 5-year life of the SeaWiFS mission. The spacing between the diffuser and the attenuator is such that reflections from the back of the attenuator onto the diffuser account for less than 1% of the total illumination.

The attenuator has a uniform thickness of 2.54 mm and is tilted by 30° about the x axis. This design prevents attenuator glints from reaching the diffuser. It also reduces illumination variations as the incidence angle of the sun varies over the seasons. Over each SeaWiFS orbit, the instrument rotates (pitches) about the z axis (Fig. 26). However, because of the inclination of the Earth's axis to the plane of the Earth's orbit and the inclination of the satellite's orbit about the Earth, there is also a relative motion of the solar incidence angle with respect to the instrument's xz plane over each year. This motion has a range of $\pm 5°$ about the x axis. It is the effect of this angular change that the tilted attenuator reduces (Fig. 31).

5.3 LAB MEASUREMENTS

The SeaWiFS diffuser acts to convert the input irradiance from the sun into an output radiance to be measured by the instrument. The input irradiance has units of $\mathrm{W\,cm^{-2}\,\mu\,m^{-1}}$ and the output radiance has units of $\mathrm{W\,cm^{-2}\,\mu\,m^{-1}\,sr^{-1}}$, where sr is the SI unit symbol for steradian (which is a unit of solid angle). A radiance measurement is made of a source that is large enough that the solid angle of its surface is greater than the solid angle viewed by the instrument. For example, SeaWiFS has been designed so that each radiance measurement has a solid angle equivalent to an area of 1.1×1.1 km at the Earth's surface at nadir. For SeaWiFS, the diffuser is measured as a radiance source, but the sun is an irradiance source. The solar flux is not parsed into individual units of solid angle, but is used as the flux from the entire surface area of the sun.

The ratio of the output radiance to the input irradiance is known as the BRDF, with units of inverse steradians. A perfect, 100% reflective Lambertian diffuser has a BRDF of π^{-1}, or 0.318. For SeaWiFS, the instrument gains were set to measure the ocean, which is a relatively dark light source, compared with the sun. As a result, the SeaWiFS diffuser required a smaller BRDF, corresponding to 10% of a perfect Lambertian diffuser. This requirement determined the diffuser design, with the diffuser plate tilted at an angle of 60° to the solar illumination and with the attenuator containing an array of small holes.

5.3.1 Reflectance at Normal Incidence

In order to properly test the SeaWiFS diffuser, it was illuminated with a source having an angular subtense similar

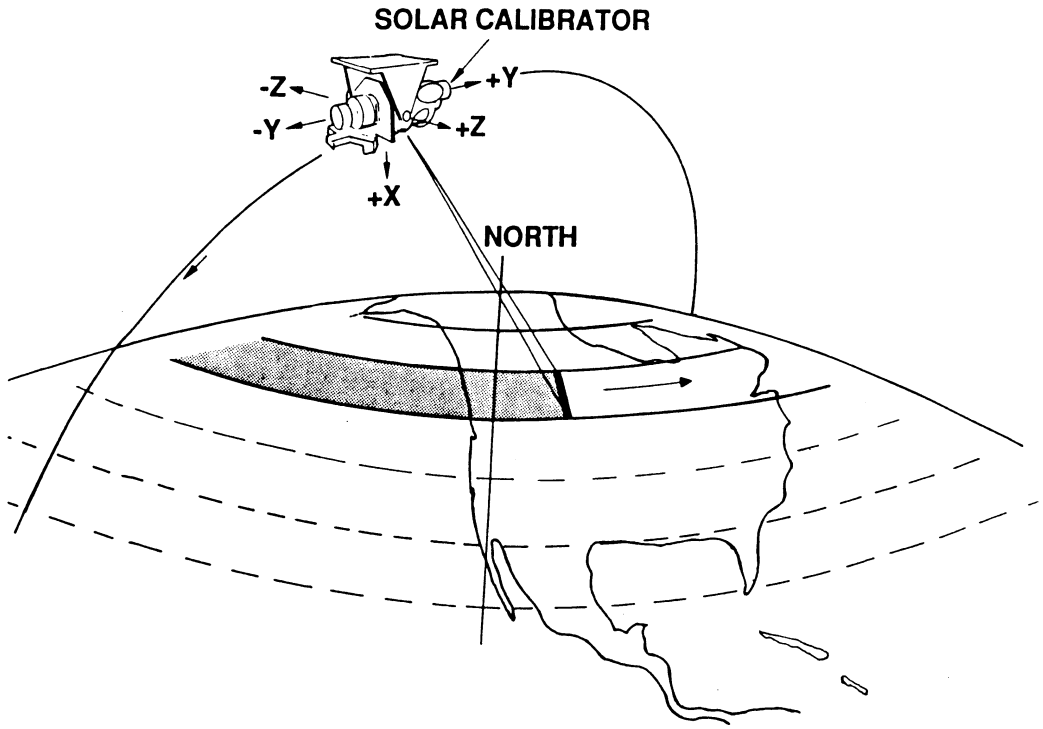

Fig. 26. The on-orbit coordinate system is shown here for SeaWiFS and for the SeaWiFS diffuser (solar calibrator). The diffuser points away from the direction of the spacecraft motion. The sun is viewed as the spacecraft passes over the South Pole.

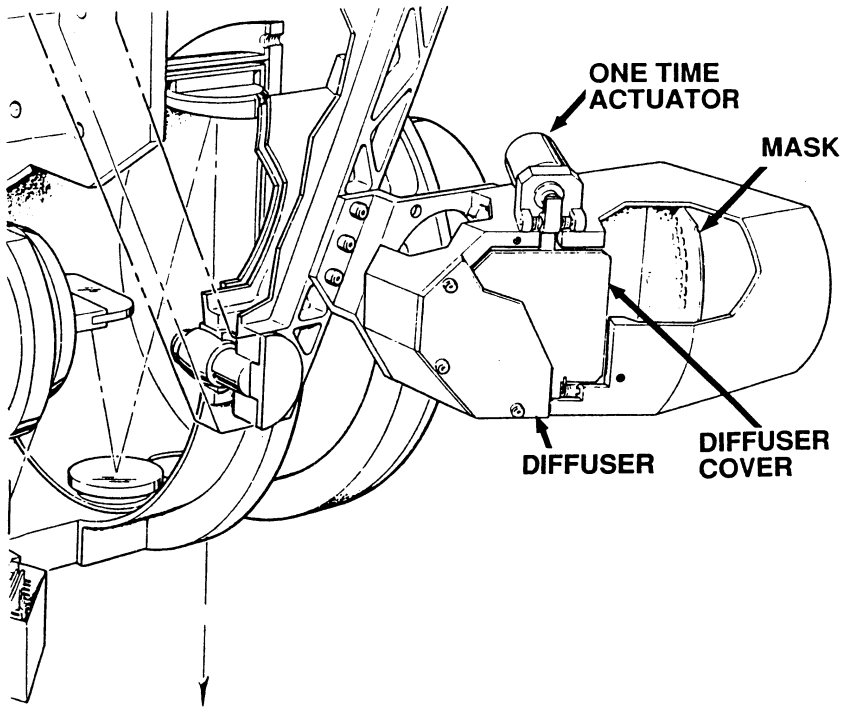

Fig. 27. This figure shows a detailed view of the diffuser assembly. The diffuser is painted on the inside of the diffuser housing, behind the diffuser cover. When the solenoid is actuated, the diffuser cover rotates into the drawing and lies on the bottom of the diffuser housing. The diffuser cover is also painted to create a second diffuser.

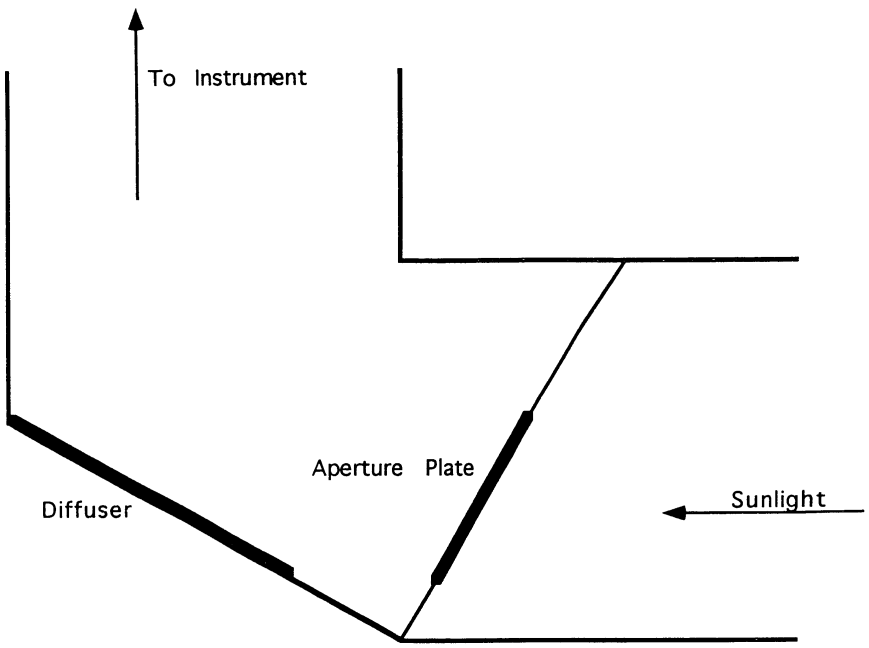

Fig. 28. This figures shows a schematic of the diffuser assembly as viewed from above. The diffuser cover is not shown.

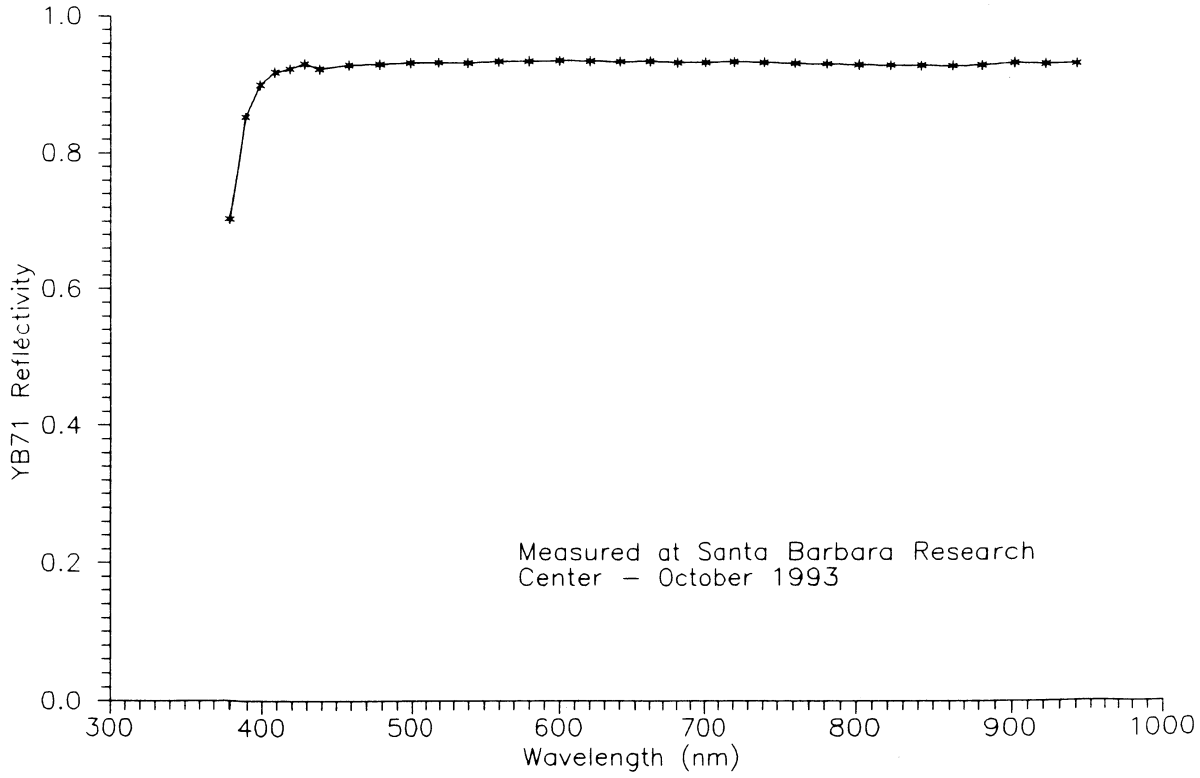

Fig. 29. Shown here is the reflectivity of YB71 paint as a function of wavelength.

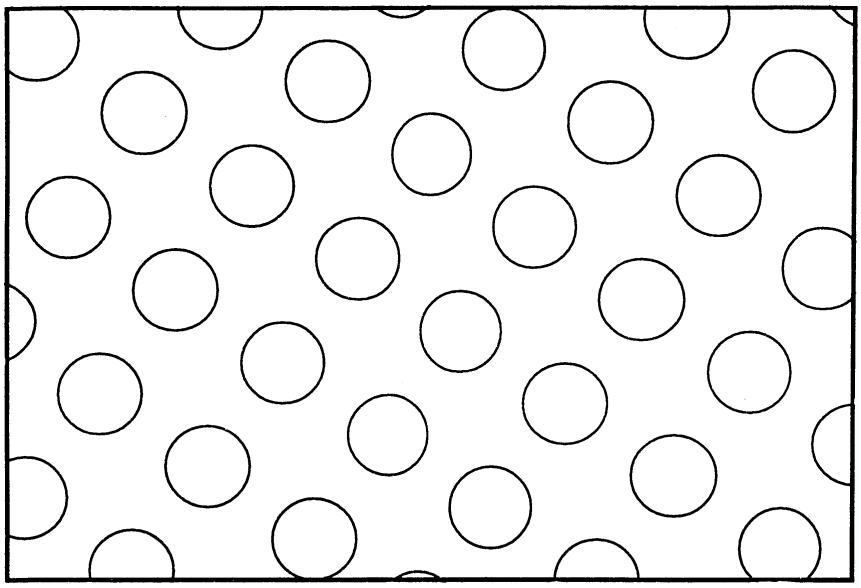

Fig. 30. The pattern of the holes in the attenuator was rotated 35° to prevent striping of the diffuser.

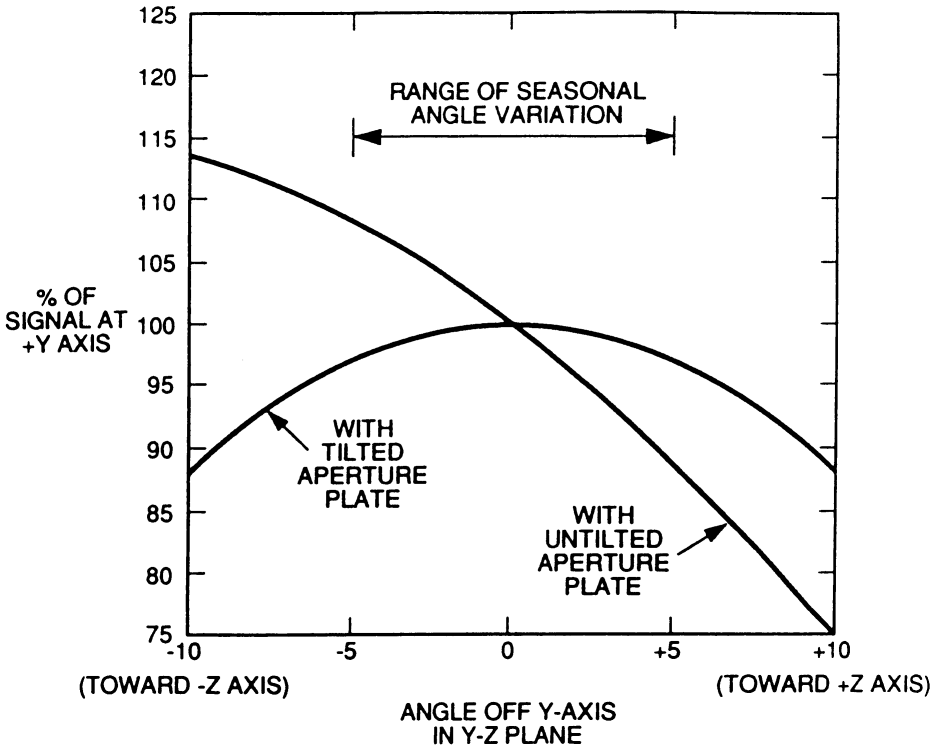

Fig. 31. This is the diffuser's response to the rotation of solar flux about the y axis. This rotation is a seasonal effect due to the inclination of the Earth's axis to the Earth-sun plane and the inclination of the satellite's orbit around the Earth. The tilted SeaWiFS attenuator greatly reduces this effect.

Table 27. The calculation of the solar diffuser reflectance is shown in this table. The data were taken using a lock-in amplifier to measure the signals from the preamplifiers. The instrument output was measured using the SeaWiFS diffuser and the amplifier output was measured using the halon diffuser. (The reflectance of the halon diffuser was $0.99/\pi\,\mathrm{sr}^{-1}$.) There are eight SeaWiFS bands, and each band has four channels.

Band	*Channel*	*Instrument Output* [μ V]	*Amplifier Output* [μ V]	*SeaWiFS Diffuser* [sr^{-1}]
1	1	65.00	773.0	
	2	65.40	778.0	
	3	66.10	769.0	
	4	68.80	804.0	
	Average	66.33	781.0	0.0268
2	1	46.00	1,640.0	
	2	145.00	1,660.0	
	3	143.00	1,620.0	
	4	143.00	1,620.0	
	Average	144.25	1,635.0	0.0279
3	1	366.00	4,270.0	
	2	364.00	4,210.0	
	3	373.00	4,230.0	
	4	374.00	4,240.0	
	Average	369.25	4,237.5	0.0275
4	1	531.00	6,020.0	
	2	523.00	5,890.0	
	3	525.00	5,920.0	
	4	536.00	5,970.0	
	Average	528.75	5,950.0	0.0281
5	1	726.00	8,420.0	
	2	712.00	8,170.0	
	3	738.00	8,410.0	
	4	716.00	8,150.0	
	Average	723.00	8,287.5	0.0276
6	1	1,120.00	12,700.0	
	2	1,090.00	12,300.0	
	3	1,130.00	12,700.0	
	4	1,120.00	12,600.0	
	Average	1,115.00	12,575.0	0.0280
7	1	2,750.00	30,800.0	
	2	2,850.00	31,700.0	
	3	2,780.00	30,500.0	
	4	2,790.00	30,600.0	
	Average	2,792.50	30,900.0	0.0285
8	1	3,420.00	36,100.0	
	2	3,640.00	38,200.0	
	3	3,520.00	36,800.0	
	4	3,400.00	35,500.0	
	Average	3,495.00	36,650.0	0.0301

Table 28. This is the normalized angular response table for band 4. The azimuth angles were measured in relation to the elevation angle with both the door deployed and the door shut.

Elevation	*Azimuth Angle with Door Deployed*												
Angle	−12.40	−10.32	−8.24	−6.17	−4.11	−2.05	0.00	2.05	4.09	6.13	8.16	10.18	12.10
−0.5	96.96	99.09	98.35	97.78	99.29	99.42	99.45	100.73	101.28	100.41	100.36	100.37	99.43
0.0	98.18	98.12	98.13	98.67	100.17	99.90	100.00	100.30	99.76	100.26	99.91	101.08	99.19
0.5	97.24	97.83	98.57	98.79	98.29	98.87	99.24	101.42	100.79	100.82	100.18	101.09	100.58
1.0	96.05	98.75	97.81	98.71	98.82	100.38	101.27	100.59	100.09	99.94	101.07	100.72	100.60
2.0	95.73	98.48	98.23	98.08	99.74	99.96	99.96	101.41	100.66	101.45	100.16	100.61	100.18
3.0	94.53	97.11	98.22	99.02	98.71	99.66	100.06	100.03	101.21	100.76	100.32	99.72	99.23
4.0	97.11	96.98	97.76	97.84	98.84	98.07	99.11	101.00	100.59	100.30	100.38	100.66	98.06
4.5	95.23	97.93	96.93	98.38	99.20	99.07	98.68	99.58	99.77	101.36	100.51	100.46	99.17
5.0	95.01	97.89	97.97	98.25	98.96	99.62	99.55	101.16	100.34	100.30	99.96	101.12	99.27
5.5	95.56	97.06	97.76	98.69	98.69	99.67	99.60	99.66	100.27	101.49	101.09	100.78	100.80
	Azimuth Angle with Door Shut												
−0.5	100.81	99.03	99.59	98.52	99.43	99.39	100.08	99.50	99.09	99.97	98.88	99.58	92.13
0.0	100.49	97.15	99.24	98.67	100.68	100.06	100.00	100.68	100.24	99.31	99.19	100.15	92.89
0.5	97.95	97.36	97.95	98.60	99.59	99.63	98.78	101.06	99.88	100.36	99.62	99.97	91.28
1.0	98.74	97.85	98.01	98.35	98.16	100.52	100.39	99.36	101.06	100.50	99.02	99.69	94.54
2.0	98.30	97.62	97.93	98.05	98.91	99.55	100.07	100.85	101.91	100.12	99.72	99.27	93.94
3.0	99.07	96.87	97.79	98.97	99.12	99.59	98.87	99.24	100.68	100.46	100.51	98.92	91.68
4.0	100.63	96.90	97.50	98.09	99.14	98.96	100.12	100.15	101.17	99.87	98.43	99.26	91.57
4.5	101.13	97.40	97.67	98.74	98.52	98.89	100.18	99.01	99.19	100.29	99.50	97.71	92.65
5.0	102.36	98.84	96.90	98.41	98.39	99.82	99.11	99.37	99.51	98.77	99.87	97.34	90.04
5.5	102.50	98.58	97.34	97.88	98.16	98.56	100.39	99.75	99.98	99.94	100.45	97.81	90.82

Table 29. This is the normalized angular response table for band 8. The azimuth angles were measured in relation to the elevation angle with both the door deployed and the door shut.

Elevation	*Azimuth Angle with Door Deployed*												
Angle	−12.40	−10.32	−8.24	−6.17	−4.11	−2.05	0.00	2.05	4.09	6.13	8.16	10.18	12.10
−0.5	76.92	86.15	91.43	95.59	97.63	99.87	99.87	99.50	97.78	94.32	89.54	83.89	73.59
0.0	78.57	86.33	91.07	94.81	97.50	99.68	100.00	99.76	97.94	94.27	89.92	83.16	73.97
0.5	80.20	86.59	91.58	95.07	97.99	99.71	100.08	99.42	97.65	94.40	89.84	83.62	74.41
1.0	80.07	86.56	91.63	95.17	98.23	99.32	99.53	99.45	97.78	94.32	89.68	83.41	73.10
2.0	80.84	86.74	91.32	94.97	97.34	99.27	99.79	99.19	96.86	93.84	89.33	83.30	72.45
3.0	78.70	86.33	91.09	95.04	97.60	99.13	99.48	99.26	96.35	93.34	88.71	83.05	72.78
4.0	76.23	86.33	90.84	94.71	96.98	99.13	99.63	98.44	96.46	93.10	88.50	82.06	71.78
4.5	74.32	84.98	90.76	94.22	96.88	98.90	99.16	98.26	96.17	92.48	87.80	82.11	70.69
5.0	72.51	83.85	90.37	93.98	96.64	98.17	99.00	98.13	96.09	92.40	87.56	81.44	69.17
5.5	70.27	82.60	89.94	93.44	96.20	98.12	98.40	98.28	95.66	92.06	87.02	80.55	67.79
	Azimuth Angle with Door Shut												
−0.5	103.62	100.01	100.02	99.80	99.96	99.63	100.10	100.09	99.76	99.53	100.09	100.23	94.30
0.0	102.42	100.74	100.42	99.87	100.20	99.76	100.00	99.54	100.18	99.87	99.64	100.49	94.71
0.5	101.21	100.35	100.05	100.07	100.01	100.00	99.95	99.53	99.84	99.53	99.70	99.58	94.52
1.0	101.66	100.14	99.66	99.93	99.51	100.13	100.37	99.93	99.65	99.64	99.88	99.80	94.25
2.0	101.05	100.71	99.71	100.55	100.55	100.08	100.02	99.93	99.94	99.49	99.60	99.28	94.53
3.0	103.44	100.23	99.82	99.79	99.96	99.86	99.91	99.28	100.89	99.86	99.62	98.81	92.37
4.0	104.52	99.96	100.16	100.03	100.33	99.70	99.60	100.22	99.86	99.51	99.19	99.51	92.71
4.5	105.30	101.12	100.13	100.33	99.81	99.62	99.94	100.16	100.16	100.69	100.61	98.78	92.93
5.0	106.00	101.80	99.98	100.44	100.38	99.87	99.45	99.45	99.46	99.46	99.57	97.76	93.24
5.5	107.47	102.65	100.41	100.44	100.59	99.66	100.20	99.24	99.62	99.52	100.06	97.79	92.45

to the sun (0.5°). The illumination source was a 1,000 W calibrated lamp placed as far as possible from the diffuser inlet (about 305 cm), yielding a divergence of 1.45° across the aperture. Determining the reflectance at normal incidence required two measurements. For the first measurement, the light from the 1,000 W lamp was measured using the SeaWiFS diffuser. For the second measurement, the entire instrument was rotated to measure the reflected light from a second diffuser as if it were viewing the Earth. In the second measurement, the light from the 1,000 W lamp was reflected off a pressed halon diffuser of known reflectance (99%). The ratio of the two measurements (SeaWiFS:halon) was used to calculate the diffuser reflectance. These calculations are given in Table 27. For the calculations, the reflectance of the pressed halon diffuser plate was $0.99/\pi$ at normal incidence.

5.3.2 BRDF

Normal incidence for the SeaWiFS diffuser lies along the $+y$ vector, that is, normal to the xz plane, facing aft (see Fig. 26). On each orbit, SeaWiFS rotates once about its z axis. For the BRDF measurements of the SeaWiFS diffuser by the manufacturer, this rotation was called "a change in elevation angle." Over the course of a year, the direction of the sun, relative to the xz plane, changes as a rotation about the x axis. For the SeaWiFS calibration, this rotation was called "a change in azimuth angle."

The BRDF for the SeaWiFS diffuser was measured for elevation and azimuth angles from the normal incidence vector ($+y$ axis). These values are shown for SeaWiFS bands 4 (Table 28) and 8 (Table 29). The values are normalized to 100% at zero azimuth and zero elevation. Those 100% values can be converted to reflectances using the corresponding SeaWiFS diffuser reflectances at normal incidence from Table 28.

5.4 FIELD MEASUREMENTS

At the instrument manufacturer's (SBRC) facility, two outdoor measurements of the solar flux using the SeaWiFS instrument and diffuser (Biggar et al. 1994 and 1995) were performed. In the interim between the two outdoor measurements, there were modifications to SeaWiFS to ameliorate the effects of instrumentally-based stray light (Barnes et al. 1995b). The experiments were made to simulate the solar flux on the diffuser on orbit using measurements on the ground.

The concept for the experiment is simple. The simulation requires only the direct solar beam, and the beam must illuminate the diffuser at the same incidence angle used during on-orbit measurements. Atmospheric effects on the direct beam in the ground measurements must be determined, and corrections for these effects must be applied to the ground results. A discussion of this correction procedure is given by Biggar et al. (1994).

The experiment after corrections for stray light in the instrument (Biggar et al. 1995) provided a set of predicted top-of-the-atmosphere digital counts from SeaWiFS. These values will be compared with digital counts from on-orbit diffuser measurements during the initial check of the instrument. In addition, the experiment after corrections for stray light in the instrument provided a comparison between the outdoor (solar radiation-based) and the indoor (integrating sphere-based) determinations of the radiometric sensitivity of SeaWiFS. In this comparison, the differences between the two methods were less than 3% for all eight SeaWiFS bands.

Glossary

ADEOS Advanced Earth Observation Satellite (Japan)

BCW Band-Weighted Center Wavelength
BRDF Bidirectional Reflectance Distribution Function
BSR Band-Weighted Spectral Radiance

CHORS Center for Hydro-Optics and Remote Sensing
CZCS Coastal Zone Solor Scanner

ECW Effective Center Wavelength
EO Electrons Out
EOS-AM Earth Observing System's morning platform

GSFC Goddard Space Flight Center
GUI Graphical User Interface

HRPT High Resolution Picture Transmission

LDEF Long Duration Exposure Facility

MODIS Moderate Resolution Imaging Spectroradiometer

NASA National Aeronautics and Space Administration
NIST National Institute of Standards and Technology
NOAA National Oceanic and Atmospheric Administration
NRT Near-Real Time

OSC Orbital Sciences Corporation
OCTS Ocean Color and Temperature Scanner

PI Photons In
PO Photons Out

RSR Relative Spectral Response

SBRC (Hughes) Santa Barbara Research Center
SeaBASS SeaWiFS Bio-Optical Archive Storage System
SeaWiFS Sea-viewing Wide Field-of-View Sensor
SIS Spherical Integrating Source
SXR SeaWiFS Transfer Radiometer

UCSB University of California at Santa Barbara Laboratory.

Symbols

$L_c(\lambda)$ Radiance corrected for oxygen A-band absorption.
L_e Earth-exiting spectral radiance integrated over the SeaWiFS spectral response.
$L_e(\lambda)$ Earth-exiting spectral radiance at a given wavelength.
$L_i(\lambda)$ Input radiance to the correction scheme for a given SeaWiFS band.
$L_o(\lambda)$ Output radiance from the correction scheme for a given SeaWiFS band.
L_s Sphere spectral radiance integrated over the SeaWiFS spectral response.
$L_s(\lambda)$ Spectral radiance from the integrating sphere at a given wavelength.
L_{typical} Typical radiances from the SeaWiFS specifications.
$L_{\text{B}}(\lambda_{\text{B}})$ Band-weighted spectral radiance for the band.

n_s Refractive index of air (dimensionless).
N_s Number density of the scattering molecules.

$R(\lambda)$ Spectral response of the band at a given wavelength
S_i Components of the spectral response for SeaWiFS band 8.

T Temperature.

W Represents the denominator in (9).
x Abscissa or longitudinal coordinate.
y Ordinate or meridional coordinate.
z Component of orbit position.

ϵ Emissivity.

λ Wavelength.
λ_{B} Band-weighted center wavelength.
λ_{eff} Effective center wavelength, that is, the wavelength where $L_s(\lambda)$ equals $L_{\text{B}}(\lambda_{\text{B}})$.
λ_m Wavelength for maximum radiance.
λ_1 Lower 1% transmission points for the band.
λ_2 Upper 1% transmission points for the band

σ Rayleigh scattering cross section per molecule.

References

Barnes, R.A., 1994: *SeaWiFS Data: Actual and Simulated.* [World Wide Web page.] From URLs: `http://seawifs.gsfc.nasa.gov/SEAWIFS/IMAGES/spectra1.dat` and `/spectra2.dat` NASA Goddard Space Flight Center, Greenbelt, Maryland.

——, 1996a: "Calculation of an equivalent blackbody temperature for the GSFC sphere." In Barnes, R.A., E-n. Yeh, and R.E. Eplee, 1996: SeaWiFS Calibration Studies, Part 1. *NASA Tech. Memo. 104566, Vol. 39,* S.B. Hooker and E.R. Firestone, Eds., NASA Goddard Space Flight Center, Greenbelt, Maryland, 5–17.

——, 1996b: "SeaWiFS center wavelengths." In Barnes, R.A., E-n. Yeh, and R.E. Eplee, 1996: SeaWiFS Calibration Topics, Part 1, *NASA Tech. Memo. 104566, Vol. 39,* S.B. Hooker and E.R. Firestone, Eds., NASA Goddard Space Flight Center, Greenbelt, Maryland, 49–53.

——, 1996c: "A comparison of the spectral response of SeaWiFS and the SeaWiFS Transfer Radiometer." In Barnes, R.A., E-n. Yeh, and R.E. Eplee, 1996: SeaWiFS Calibration Topics, Part 1, *NASA Tech. Memo. 104566, Vol. 39,* S.B. Hooker and E.R. Firestone, Eds., NASA Goddard Space Flight Center, Greenbelt, Maryland, 39–48.

——, and A.W. Holmes, 1993: Overview of the SeaWiFS ocean sensor. *SPIE,* **1,939,** 224–232.

——, W.L. Barnes, W.E. Esaias, and C.R. McClain, 1994a: Prelaunch Acceptance Report for the SeaWiFS Radiometer. *NASA Tech. Memo. 104566, Vol. 22,* S.B. Hooker and E.R. Firestone, Eds., NASA Goddard Space Flight Center, Greenbelt, Maryland, 32 pp.

——, A.W. Holmes, W.L. Barnes, W.E. Esaias, C.R. McClain, and T. Svitek, 1994b: SeaWiFS Prelaunch Radiometric Calibration and Spectral Characterization. *NASA Tech. Memo. 104566, Vol. 23,* S.B. Hooker and E.R. Firestone, Eds., NASA Goddard Space Flight Center, Greenbelt, Maryland, 55 pp.

——, W.E. Esaias, and C.R. McClain, 1995a: "A proposed on-orbit, out-of-band correction scheme for SeaWiFS." In McClain, C.R., K. Arrigo, W.E. Esaias, M. Darzi, F.S. Patt, R.H. Evans, J.W. Brown, C.W. Brown, R.A. Barnes, and L. Kumar, 1995: SeaWiFS Algorithms, Part 1, *NASA Tech. Memo. 104566, Vol. 28,* S.B. Hooker and E.R. Firestone, Eds., NASA Goddard Space Flight Center, Greenbelt, Maryland, 20–25.

——, A.W. Holmes, and W.E. Esaias, 1995b: Stray Light in the SeaWiFS Radiometer. *NASA Tech. Memo. 104566, Vol. 32,* S.B. Hooker and E.R. Firestone, Eds., NASA Goddard Space Flight Center, Greenbelt, Maryland, 76 pp.

——, and E-n. Yeh, 1996: "The effects of source spectral shape on SeaWiFS radiance measurements." In Barnes, R.A., E-n. Yeh, and R.E. Eplee, 1996: SeaWiFS Calibration Topics, Part 1. *NASA Tech. Memo. 104566, Vol. 39,* S.B. Hooker and E.R. Firestone, Eds., NASA Goddard Space Flight Center, Greenbelt, Maryland, 18–38.

Biggar, S.F., P.N. Slater, K.J. Thome, A.W. Holmes, and R.A. Barnes, 1994: "Preflight solar-based calibration of SeaWiFS." In McClain, C.R., R.S. Fraser, J.T. McLean, M. Darzi, J.K. Firestone, F.S. Patt, B.D. Schieber, R.H. Woodward, E-n. Yeh, S. Mattoo, S.F. Biggar, P.N. Slater, K.J. Thome, A.W. Holmes, R.A. Barnes, and K.J. Voss, 1994: Case Studies for SeaWiFS Calibration and Validation, Part 2, *NASA Tech. Memo. 104566, Vol. 19,* S.B. Hooker and E.R. Firestone, Eds., NASA Goddard Space Flight Center, Greenbelt, Maryland, 25–32.

——, K.J. Thome, P.N. Slater, A.W. Holmes, and R.A. Barnes, 1995: "Second SeaWiFS preflight solar-radiation-based calibration experiment." In Mueller, J.L., R.S. Fraser, S.F. Biggar, K.J. Thome, P.N. Slater, A.W. Holmes, R.A. Barnes, C.T. Weir, D.A. Siegel, D.W. Menzies, A.F. Michaels, and G. Podesta, 1995: Case Studies for SeaWiFS Calibration and Validation, Part 3, *NASA Tech. Memo. 104566, Vol. 27,* S.B. Hooker and E.R. Firestone, Eds., NASA Goddard Space Flight Center, Greenbelt, Maryland, 20–24.

Brasseur, G., and S. Solomon, 1987: *Aeronomy of the Middle Atmosphere, Second Edition.* D. Reidel Publishing Co., Boston, Massachusetts, 452 pp.

Ding, K., and H.R. Gordon, 1995: Analysis of the influence of O_2 A-band absorption on atmospheric correction of ocean-color imagery. *Appl. Opt.,* **34,** 2,068–2,080.

Evans, R.H., and H.R. Gordon, 1994: Coastal Zone Color Scanner "system calibration:" a retrospective examination. *J. Geophys. Res.,* **99,** 7,293–7,307.

Fraser, R.S., 1995: "The effect of oxygen absorption on SeaWiFS band 7 radiance." In Mueller, J.L., R.S. Fraser, S.F. Biggar, K.J. Thome, P.N. Slater, A.W. Holmes, R.A. Barnes, C.T. Weir, D.A. Siegel, D.W. Menzies, A.F. Mich aels, and G. Podesta, 1995: Case Studies for SeaWiFS Calibration and Validation, Part 3. *NASA Tech. Memo. 104566, Vol. 27,* S.B. Hooker and E.R. Firestone, Eds., NASA Goddard Space Flight Center, Greenbelt, Maryland, 16–19.

Frederick, J.E., R.P. Cebula, and D.F. Heath, 1986: Instrument characterization for detection of long-term changes in stratospheric ozone: an analysis of the SBUV/2 radiometer. *J. Atmos. Ocean. Technol.,* **3,** 472–480.

Gordon, H.R., 1995: Remote sensing of ocean color: a methodology for dealing with broad spectral bands and significant out-of-band response. *Appl. Opt.,* **34,** 8,363–8,374.

——, and M. Wang, 1994: Retrieval of water-leaving radiance and aerosol optical thickness over the oceans with SeaWiFS: a preliminary algorithm. *Appl. Opt.,* **33,** 443–452.

Hapke, B., 1986: Bidirectional reflectance spectroscopy. 4. The extinction coefficient and the opposition effect. Icarus, **67,** 264–280.

Helfenstein, P., and J. Veverka, 1987: Photometric properties of lunar terrains derived from Hapke's equation. *Icarus,* **72,** 342–357.

Herman, J.R., R.D. Hudson, and G.N. Serafino, 1990: An analysis of the 8 year trend in ozone depletion from alternate models of SBUV instrument degradation, *J. Geophys. Res.,* **95,** 7,403–7,416.

Hooker, S.B., W.E. Esaias, G.C. Feldman, W.W. Gregg, and C.R. McClain, 1992: An Overview of SeaWiFS and Ocean Color. *NASA Tech. Memo. 104566, Vol. 1,* S.B. Hooker and E.R. Firestone, Eds., NASA Goddard Space Flight Center, Greenbelt, Maryland, 24 pp., plus color plates.

Johnson, B.C., S.S. Bruce, E.A. Early, J.M. Houston, T.R. O'Brian, A. Thompson, S.B. Hooker, and J.L. Mueller, 1996: The Fourth SeaWiFS Intercomparison Round-Robin Experiment, *NASA Tech. Memo. 104566, Vol. 37,* S.B. Hooker and E.R. Firestone, Eds., NASA Goddard Space Flight Center, Greenbelt, Maryland, 65 pp.

Kieffer, H.H., and R.L. Wildey, 1996: Establishing the moon as a spectral radiance standard. *J. Atmos. Oceanic Technol.,* **13,** 360–375.

McClain, C.R., W.E. Esaias, W. Barnes, B. Guenther, D. Endres, S. Hooker, G. Mitchell, and R. Barnes, 1992: Calibration and Validation Plan for SeaWiFS, *NASA Tech. Memo. 104566, Vol. 3,* S.B. Hooker and E.R. Firestone, Eds., NASA Goddard Space Flight Center, Greenbelt, Maryland, 43 pp.

McClain, C.R., R.S. Fraser, and E-n. Yeh, 1994:" SeaWiFS pressure and oxygen absorption study." In McClain, C.R., K.R. Arrigo, J. Comiso, R. Fraser, M. Darzi, J.K. Firestone, B. Schieber, E-n. Yeh, and C.W. Sullivan, 1994: Case Studies for SeaWiFS Calibration and Validation, Part 1, *NASA Tech. Memo. 104566, Vol. 13,* S.B. Hooker and E.R. Firestone, Eds., NASA Goddard Space Flight Center, Greenbelt, Maryland, 15–20.

Penndorf, R., 1957: Tables of the refractive index for standard air and the Rayleigh scattering coefficient for the spectral region between 0.2 and 20.2 μm and their application to atmospheric optics. *J. Opt. Soc. Am.,* **47,** 176–182.

Walker, J.H., R.D. Saunders, and A.T. Hattenburg, 1987: Spectral Radiance Calibrations. *NBS Special Publication 250-1,* National Institute of Standards and Technology (formerly National Bureau of Standards), Washington, D.C., 68 pp.

Woodward, R.H., R.A. Barnes, C.R. McClain, W.E. Esaias, W.L. Barnes, and A.T. Mecherikunnel, 1993: Modeling of the SeaWiFS Solar and Lunar Observations, *NASA Tech. Memo. 104566, Vol. 10,* S.B. Hooker and E.R. Firestone, Eds., NASA Goddard Space Flight Center, Greenbelt, Maryland, 26 pp.

Wyatt, C.L., 1978: *Radiometric Calibration: Theory and Methods.* Academic Press, New York, 220 pp.

The SeaWiFS Technical Report Series

Vol. 1

Hooker, S.B., W.E. Esaias, G.C. Feldman, W.W. Gregg, and C.R. McClain, 1992: An Overview of SeaWiFS and Ocean Color. *NASA Tech. Memo. 104566, Vol. 1,* S.B. Hooker and E.R. Firestone, Eds., NASA Goddard Space Flight Center, Greenbelt, Maryland, 24 pp., plus color plates.

Vol. 2

Gregg, W.W., 1992: Analysis of Orbit Selection for SeaWiFS: Ascending vs. Descending Node. *NASA Tech. Memo. 104566, Vol. 2,* S.B. Hooker and E.R. Firestone, Eds., NASA Goddard Space Flight Center, Greenbelt, Maryland, 16 pp.

Vol. 3

McClain, C.R., W.E. Esaias, W. Barnes, B. Guenther, D. Endres, S.B. Hooker, G. Mitchell, and R. Barnes, 1992: Calibration and Validation Plan for SeaWiFS. *NASA Tech. Memo. 104566, Vol. 3,* S.B. Hooker and E.R. Firestone, Eds., NASA Goddard Space Flight Center, Greenbelt, Maryland, 41 pp.

Vol. 4

McClain, C.R., E. Yeh, and G. Fu, 1992: An Analysis of GAC Sampling Algorithms: A Case Study. *NASA Tech. Memo. 104566, Vol. 4,* S.B. Hooker and E.R. Firestone, Eds., NASA Goddard Space Flight Center, Greenbelt, Maryland, 22 pp., plus color plates.

Vol. 5

Mueller, J.L., and R.W. Austin, 1992: Ocean Optics Protocols for SeaWiFS Validation. *NASA Tech. Memo. 104566, Vol. 5,* S.B. Hooker and E.R. Firestone, Eds., NASA Goddard Space Flight Center, Greenbelt, Maryland, 43 pp.

Vol. 6

Firestone, E.R., and S.B. Hooker, 1992: SeaWiFS Technical Report Series Cumulative Index: Volumes 1–5. *NASA Tech. Memo. 104566, Vol. 6,* S.B. Hooker and E.R. Firestone, Eds., NASA Goddard Space Flight Center, Greenbelt, Maryland, 9 pp.

Vol. 7

Darzi, M., 1992: Cloud Screening for Polar Orbiting Visible and IR Satellite Sensors. *NASA Tech. Memo. 104566, Vol. 7,* S.B. Hooker and E.R. Firestone, Eds., NASA Goddard Space Flight Center, Greenbelt, Maryland, 7 pp.

Vol. 8

Hooker, S.B., W.E. Esaias, and L.A. Rexrode, 1993: Proceedings of the First SeaWiFS Science Team Meeting. *NASA Tech. Memo. 104566, Vol. 8,* S.B. Hooker and E.R. Firestone, Eds., NASA Goddard Space Flight Center, Greenbelt, Maryland, 61 pp.

Vol. 9

Gregg, W.W., F.C. Chen, A.L. Mezaache, J.D. Chen, J.A. Whiting, 1993: The Simulated SeaWiFS Data Set, Version 1. *NASA Tech. Memo. 104566, Vol. 9,* S.B. Hooker, E.R. Firestone, and A.W. Indest, Eds., NASA Goddard Space Flight Center, Greenbelt, Maryland, 17 pp.

Vol. 10

Woodward, R.H., R.A. Barnes, C.R. McClain, W.E. Esaias, W.L. Barnes, and A.T. Mecherikunnel, 1993: Modeling of the SeaWiFS Solar and Lunar Observations. *NASA Tech. Memo. 104566, Vol. 10,* S.B. Hooker and E.R. Firestone, Eds., NASA Goddard Space Flight Center, Greenbelt, Maryland, 26 pp.

Vol. 11

Patt, F.S., C.M. Hoisington, W.W. Gregg, and P.L. Coronado, 1993: Analysis of Selected Orbit Propagation Models for the SeaWiFS Mission. *NASA Tech. Memo. 104566, Vol. 11,* S.B. Hooker, E.R. Firestone, and A.W. Indest, Eds., NASA Goddard Space Flight Center, Greenbelt, Maryland, 16 pp.

Vol. 12

Firestone, E.R., and S.B. Hooker, 1993: SeaWiFS Technical Report Series Cumulative Index: Volumes 1–11. *NASA Tech. Memo. 104566, Vol. 12,* S.B. Hooker and E.R. Firestone, Eds., NASA Goddard Space Flight Center, Greenbelt, Maryland, 28 pp.

Vol. 13

McClain, C.R., K.R. Arrigo, J. Comiso, R. Fraser, M. Darzi, J.K. Firestone, B. Schieber, E-n. Yeh, and C.W. Sullivan, 1994: Case Studies for SeaWiFS Calibration and Validation, Part 1. *NASA Tech. Memo. 104566, Vol. 13,* S.B. Hooker and E.R. Firestone, Eds., NASA Goddard Space Flight Center, Greenbelt, Maryland, 52 pp., plus color plates.

Vol. 14

Mueller, J.L., 1993: The First SeaWiFS Intercalibration Round-Robin Experiment, SIRREX-1, July 1992. *NASA Tech. Memo. 104566, Vol. 14,* S.B. Hooker and E.R. Firestone, Eds., NASA Goddard Space Flight Center, Greenbelt, Maryland, 60 pp.

Vol. 15

Gregg, W.W., F.S. Patt, and R.H. Woodward, 1994: The Simulated SeaWiFS Data Set, Version 2. *NASA Tech. Memo. 104566, Vol. 15,* S.B. Hooker and E.R. Firestone, Eds., NASA Goddard Space Flight Center, Greenbelt, Maryland, 42 pp., plus color plates.

Vol. 16

Mueller, J.L., B.C. Johnson, C.L. Cromer, J.W. Cooper, J.T. McLean, S.B. Hooker, and T.L. Westphal, 1994: The Second SeaWiFS Intercalibration Round-Robin Experiment, SIRREX-2, June 1993. *NASA Tech. Memo. 104566, Vol. 16,* S.B. Hooker and E.R. Firestone, Eds., NASA Goddard Space Flight Center, Greenbelt, Maryland, 121 pp.

Vol. 17

Abbott, M.R., O.B. Brown, H.R. Gordon, K.L. Carder, R.E. Evans, F.E. Muller-Karger, and W.E. Esaias, 1994: Ocean Color in the 21st Century: A Strategy for a 20-Year Time Series. *NASA Tech. Memo. 104566, Vol. 17,* S.B. Hooker and E.R. Firestone, Eds., NASA Goddard Space Flight Center, Greenbelt, Maryland, 20 pp.

Vol. 18

Firestone, E.R., and S.B. Hooker, 1995: SeaWiFS Technical Report Series Cumulative Index: Volumes 1–17. *NASA Tech. Memo. 104566, Vol. 18,* S.B. Hooker and E.R. Firestone, Eds., NASA Goddard Space Flight Center, Greenbelt, Maryland, 47 pp.

Vol. 19

McClain, C.R., R.S. Fraser, J.T. McLean, M. Darzi, J.K. Firestone, F.S. Patt, B.D. Schieber, R.H. Woodward, E-n. Yeh, S. Mattoo, S.F. Biggar, P.N. Slater, K.J. Thome, A.W. Holmes, R.A. Barnes, and K.J. Voss, 1994: Case Studies for SeaWiFS Calibration and Validation, Part 2. *NASA Tech. Memo. 104566, Vol. 19,* S.B. Hooker, E.R. Firestone, and J.G. Acker, Eds., NASA Goddard Space Flight Center, Greenbelt, Maryland, 73 pp.

Vol. 20

Hooker, S.B., C.R. McClain, J.K. Firestone, T.L. Westphal, E-n. Yeh, and Y. Ge, 1994: The SeaWiFS Bio-Optical Archive and Storage System (SeaBASS), Part 1. *NASA Tech. Memo. 104566, Vol. 20,* S.B. Hooker and E.R. Firestone, Eds., NASA Goddard Space Flight Center, Greenbelt, Maryland, 40 pp.

Vol. 21

Acker, J.G., 1994: The Heritage of SeaWiFS: A Retrospective on the CZCS NIMBUS Experiment Team (NET) Program. *NASA Tech. Memo. 104566, Vol. 21,* S.B. Hooker and E.R. Firestone, Eds., NASA Goddard Space Flight Center, Greenbelt, Maryland, 43 pp.

Vol. 22

Barnes, R.A., W.L. Barnes, W.E. Esaias, and C.R. McClain, 1994: Prelaunch Acceptance Report for the SeaWiFS Radiometer. *NASA Tech. Memo. 104566, Vol. 22,* S.B. Hooker, E.R. Firestone, and J.G. Acker, Eds., NASA Goddard Space Flight Center, Greenbelt, Maryland, 32 pp.

Vol. 23

Barnes, R.A., A.W. Holmes, W.L. Barnes, W.E. Esaias, C.R. McClain, and T. Svitek, 1994: SeaWiFS Prelaunch Radiometric Calibration and Spectral Characterization. *NASA Tech. Memo. 104566, Vol. 23,* S.B. Hooker, E.R. Firestone, and J.G. Acker, Eds., NASA Goddard Space Flight Center, Greenbelt, Maryland, 55 pp.

Vol. 24

Firestone, E.R., and S.B. Hooker, 1995: SeaWiFS Technical Report Series Cumulative Index: Volumes 1–23. *NASA Tech. Memo. 104566, Vol. 24,* S.B. Hooker and E.R. Firestone, Eds., NASA Goddard Space Flight Center, Greenbelt, Maryland, 36 pp.

Vol. 25

Mueller, J.L., and R.W. Austin, 1995: Ocean Optics Protocols for SeaWiFS Validation, Revision 1. *NASA Tech. Memo. 104566, Vol. 25,* S.B. Hooker, E.R. Firestone, and J.G. Acker, Eds., NASA Goddard Space Flight Center, Greenbelt, Maryland, 66 pp.

Vol. 26

Siegel, D.A., M.C. O'Brien, J.C. Sorensen, D.A. Konnoff, E.A. Brody, J.L. Mueller, C.O. Davis, W.J. Rhea, and S.B. Hooker, 1995: Results of the SeaWiFS Data Analysis Round-Robin (DARR-94), July 1994. *NASA Tech. Memo. 104566, Vol. 26,* S.B. Hooker and E.R. Firestone, Eds., NASA Goddard Space Flight Center, Greenbelt, Maryland, 58 pp.

Vol. 27

Mueller, J.L., R.S. Fraser, S.F. Biggar, K.J. Thome, P.N. Slater, A.W. Holmes, R.A. Barnes, C.T. Weir, D.A. Siegel, D.W. Menzies, A.F. Michaels, and G. Podesta, 1995: Case Studies for SeaWiFS Calibration and Validation, Part 3. *NASA Tech. Memo. 104566, Vol. 27,* S.B. Hooker, E.R. Firestone, and J.G. Acker, Eds., NASA Goddard Space Flight Center, Greenbelt, Maryland, 46 pp.

Vol. 28

McClain, C.R., K.R. Arrigo, W.E. Esaias, M. Darzi, F.S. Patt, R.H. Evans, J.W. Brown, C.W. Brown, R.A. Barnes, and L. Kumar, 1995: SeaWiFS Algorithms, Part 1. *NASA Tech. Memo. 104566, Vol. 28,* S.B. Hooker, E.R. Firestone, and J.G. Acker, Eds., NASA Goddard Space Flight Center, Greenbelt, Maryland, 38 pp., plus color plates.

Vol. 29

Aiken, J., G.F. Moore, C.C. Trees, S.B. Hooker, and D.K. Clark, 1995: The SeaWiFS CZCS-Type Pigment Algorithm. *NASA Tech. Memo. 104566, Vol. 29,* S.B. Hooker and E.R. Firestone, Eds., NASA Goddard Space Flight Center, Greenbelt, Maryland, 34 pp.

Vol. 30

Firestone, E.R., and S.B. Hooker, 1996: SeaWiFS Technical Report Series Cumulative Index: Volumes 1–29. *NASA Tech. Memo. 104566, Vol. 30,* S.B. Hooker and E.R. Firestone, Eds., NASA Goddard Space Flight Center, Greenbelt, Maryland, 43 pp.

Vol. 31

Barnes, R.A., A.W. Holmes, and W.E. Esaias, 1995: Stray Light in the SeaWiFS Radiometer. *NASA Tech. Memo. 104566, Vol. 31,* S.B. Hooker, E.R. Firestone, and J.G. Acker, Eds., NASA Goddard Space Flight Center, Greenbelt, Maryland, 76 pp.

Vol. 32

Campbell, J.W., J.M. Blaisdell, and M. Darzi, 1995: Level-3 SeaWiFS Data Products: Spatial and Temporal Binning Algorithms. *NASA Tech. Memo. 104566, Vol. 32,* S.B. Hooker, E.R. Firestone, and J.G. Acker, Eds., NASA Goddard Space Flight Center, Greenbelt, Maryland, 73 pp., plus color plates.

Vol. 33

Moore, G.F., and S.B. Hooker, 1996: Proceedings of the First SeaWiFS Exploitation Initiative (SEI) Team Meeting. *NASA Tech. Memo. 104566, Vol. 33,* S.B. Hooker and E.R. Firestone, Eds., NASA Goddard Space Flight Center, Greenbelt, Maryland, 53 pp.

Vol. 34

Mueller, J.L., B.C. Johnson, C.L. Cromer, S.B. Hooker, J.T. McLean, and S.F. Biggar, 1996: The Third SeaWiFS Intercalibration Round-Robin Experiment (SIRREX-3), 19–30 September 1994. *NASA Tech. Memo. 104566, Vol. 34,* S.B. Hooker, E.R. Firestone, and J.G. Acker, Eds., NASA Goddard Space Flight Center, Greenbelt, Maryland, 78 pp.

Vol. 35

Robins, D.B., A.J. Bale, G.F. Moore, N.W. Rees, S.B. Hooker, C.P. Gallienne, A.G. Westbrook, E. Marañón, W.H. Spooner, and S.R. Laney, 1996: BAOPW-1 Cruise Report and Preliminary Results. *NASA Tech. Memo. 104566, Vol. 35,* S.B. Hooker and E.R. Firestone, Eds., NASA Goddard Space Flight Center, Greenbelt, Maryland, 87 pp.

Vol. 36

Firestone, E.R., and S.B. Hooker, 1996: SeaWiFS Technical Report Series Cumulative Index: Volumes 1–35. *NASA Tech. Memo. 104566, Vol. 36,* S.B. Hooker and E.R. Firestone, Eds., NASA Goddard Space Flight Center, Greenbelt, Maryland, (in press).

Vol. 37

Johnson, B.C., S.S. Bruce, E.A. Early, J.M. Houston, T.R. O'Brian, A. Thompson, S.B. Hooker, and J.L. Mueller, 1996: The Fourth SeaWiFS Intercalibration Round-Robin Experiment (SIRREX-4), May 1995. *NASA Tech. Memo. 104566, Vol. 37,* S.B. Hooker and E.R. Firestone, Eds., NASA Goddard Space Flight Center, Greenbelt, Maryland, 65 pp.

Vol. 38

McClain, C.R., M. Darzi, R.A. Barnes, R.E. Eplee, J.K. Firestone, F.S. Patt, W.D. Robinson, B.D. Schieber, R.H. Woodward, and E-n. Yeh, 1996: SeaWiFS Calibration and Validation Quality Control Procedures. *NASA Tech. Memo. 104566, Vol. 38,* S.B. Hooker and E.R. Firestone, Eds., NASA Goddard Space Flight Center, Greenbelt, Maryland, 68 pp.

Vol. 39

Barnes, R.A., E-n. Yeh, and R.E. Eplee, 1996: SeaWiFS Calibration Topics, Part 1. *NASA Tech. Memo. 104566, Vol. 39,* S.B. Hooker and E.R. Firestone, Eds., NASA Goddard Space Flight Center, Greenbelt, Maryland, 66 pp.

REPORT DOCUMENTATION PAGE

Form Approved
OMB No. 0704-0188

1. AGENCY USE ONLY *(Leave blank)*	2. REPORT DATE	3. REPORT TYPE AND DATES COVERED
	October 1996	Technical Memorandum

4. TITLE AND SUBTITLE
SeaWiFS Technical Report Series
Volume 39–SeaWiFS Calibration Topics, Part 1

5. FUNDING NUMBERS
Code 970.2

6. AUTHOR(S)
Robert A. Barnes, Eueng-nan Yeh, and Robert E. Eplee

Series Editors: Stanford B. Hooker and Elaine R. Firestone

7. PERFORMING ORGANIZATION NAME(S) AND ADDRESS(ES)
Laboratory for Hydrospheric Processes
Goddard Space Flight Center
Greenbelt, Maryland 20771

8. PERFORMING ORGANIZATION REPORT NUMBER
97B00004

9. SPONSORING/MONITORING AGENCY NAME(S) AND ADDRESS(ES)
National Aeronautics and Space Administration
Washington, D.C. 20546–0001

10. SPONSORING/MONITORING AGENCY REPORT NUMBER
TM–104566, Vol. 39

11. SUPPLEMENTARY NOTES
Elaine R. Firestone, Robert A. Barnes, Eueng-nan Yeh, and Robert E. Eplee: General Sciences Corporation, Laurel, Maryland

12a. DISTRIBUTION/AVAILABILITY STATEMENT
Unclassified–Unlimited
Subject Category 48
Report is available from the Center for AeroSpace Information (CASI),
7121 Standard Drive, Hanover, MD 21076–1320; (301)621-0390

12b. DISTRIBUTION CODE

13. ABSTRACT *(Maximum 200 words)*

For Earth-observing satellite instruments, it was standard to consider each instrument band to have a spectral response that is infinitely narrow, i.e., to have a response from a single wavelength. The SeaWiFS bands, however, have nominal spectral bandwidths of 20 and 40 nm. These bandwidths affect the SeaWiFS measurements on orbit. The effects are also linked to the manner in which the instrument was calibrated and to the spectral shape of the radiance that SeaWiFS views. Currently, SeaWiFS is calibrated such that the digital counts from each instrument band are linked to the Earth-exiting radiance at an individual center wavelength. Before launch, SeaWiFS will be recalibrated so that the digital counts from each band will be linked to the Earth-exiting radiance integrated over the spectral response of that band. In this technical memorandum, the effects of the instrument calibration and the source spectral shape on SeaWiFS measurements, including the in-band and out-of-band responses, and the center wavelengths are discussed.

14. SUBJECT TERMS
SeaWiFS, Oceanography, Calibration, Validation, Blackbody Temperature
Spectral Shape, Radiance Measurements, Spectral Responses, Center Wavelengths,
Solar Diffuser

15. NUMBER OF PAGES
66

16. PRICE CODE

17. SECURITY CLASSIFICATION OF REPORT	18. SECURITY CLASSIFICATION OF THIS PAGE	19. SECURITY CLASSIFICATION OF ABSTRACT	20. LIMITATION OF ABSTRACT
Unclassified	Unclassified	Unclassified	Unlimited